Improving XBeach non-hydrostatic model predictions of the swash morphodynamics of intermediate-reflective beaches

MSc Thesis

C.E. Jongedijk

Technische Universiteit Delft

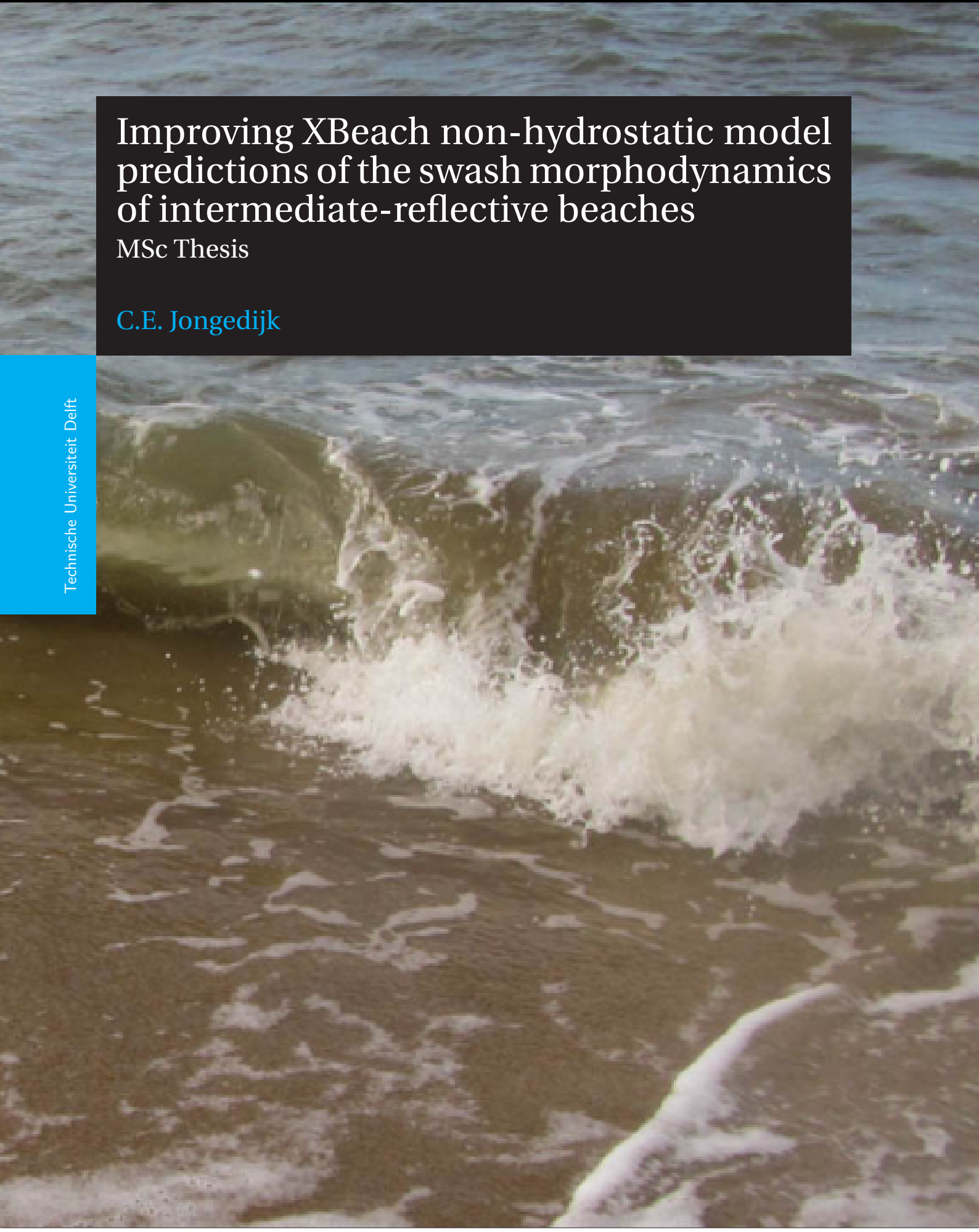

TU Delft Delft University of Technology

Challenge the future

IMPROVING XBEACH NON-HYDROSTATIC MODEL PREDICTIONS OF THE SWASH MORPHODYNAMICS OF INTERMEDIATE-REFLECTIVE BEACHES

MSc THESIS

by

C.E. Jongedijk

Delft University of Technology Faculty of Civil Engineering
Department of Hydraulic Engineering
Section Environmental Fluid Mechanics

To be defended the 12th of October 2017.

Daily Supervisor:	Dr.Ir. R.T. McCall	TU Delft/Deltares
Thesis committee:	Prof.Dr.Ir. A.J.H.M. Reniers	TU Delft (Chair)
	Dr.Ir. M. de Schipper	TU Delft
	Dr.Ir. J.J. van der Werf	Deltares

Cover image: Swash Bore (Image from: `http://queenslandcoast.blogspot.com`)

TU Delft Delft University of Technology

Deltares Enabling Delta Life

ABSTRACT

A very common observation is the episodic erosion of beaches during storms and the slow recovery (accretion) afterwards (Yates et al. 2009). Morphodynamic models parameterize physical processes in order to relate the fluid motions (hydrodynamics) to the bed level changes (morphodynamics) over a wide range of spatial and temporal scales. Despite recovery of the beach profile being a slow process, accretion mechanisms in the swash zone are complex to represent by a numerical model due to the shallow, rapidly varying flows and high concentration gradients (Brocchini & Baldock 2008). The swash zone on most beaches is readily accessible, but this accessibility does not translate into a broad knowledge of the underlying physical processes (Chardón-Maldonado et al. 2015). This research focused on assessing the representation of physical processes in the swash zone of intermediate-reflective beaches during erosive and accretive conditions in the non-hydrostatic version of the XBeach model (XBeach). This is a depth-averaged phase resolving model, mainly used for calculations of storm impact (hours-days) on sandy and gravel beaches. Based on conclusions in literature, relevant physical processes that contribute to accretion were determined. Using a simple planar beach bathymetry, the sediment transport formulations in XBeach and the individual influence of groundwater effects, bed slope effects, sediment response time and wave breaking induced turbulence were assessed. The results showed that for both accretive and erosive wave conditions, XBeach predicts erosion in the swash zone. Groundwater infiltration and wave breaking induced turbulence are likely to enhance onshore transport significantly Reniers et al. (2013), Turner & Masselink (1998).

To verify the findings of the planar beach modeling approach, in the second part of this thesis the morphodynamical predictions of XBeach were compared to the dataset collected during the Bardex II experiment. Bardex II was performed in 2012 in the Delta Flume in the Netherlands and the dataset contains observations of a series of experiments focusing on the effect of varying wave, sea level and beach groundwater conditions on a sandy beach (D_{50}=0.42 mm)(Masselink et al. 2013). Stored data and published results were used for comparison with the morphodynamical prediction performance of XBeach. Two timescales have been analyzed, the total morphological response of the beach on a timescale of 100 minutes and the intra-swash sediment transport processes on a timescale of 10 seconds. Two experiments from the series have been reproduced. The first, experiment A4, has an almost stable, slightly erosive morphological response throughout the swash zone. The second, experiment A8, shows accretion in the upper swash and a stable profile in the rest of the swash zone. XBeach erroneously (over)predicted erosion above the mean sea level (MSL) for both A4 and A8 conditions. This conclusion was related to the results of the intra-swash sediment transport assessment. The modeled velocity in both uprush and backwash were higher than the Bardex II measured velocity and XBeach extremely underpredicted uprush sediment concentrations suggesting that turbulence induced by the bore is not enough taken into account. Over-predicted backwash sediment concentrations for both accretive and erosive conditions suggested that groundwater infiltration was not strong enough. However, enhancing wave breaking induced turbulence and groundwater infiltration did not lead to an improvement of the predictions of sediment concentrations in the swash.

The sediment transport formulations of XBeach were developed using a long wave resolving (short wave averaging) model, and widely validated and calibrated on field and experimental data (Soulsby 1997, van Rijn et al. 2007, Van Thiel De Vries 2009). Therefore, in the last part of this thesis two possible improvements of the two sediment formulations of XBeach (van Thiel-van Rijn and Soulsby-van Rijn) when applying them in a short wave resolving model are assessed using a 1D sediment transport model. The decomposition of the velocity signal in a mean and a fluctuating part improved mainly the predictions using Soulsby-van Rijn where the separate calibration of turbulent kinetic energy resulted in better predictions for both transport formulations. This analysis was performed only at one point on the cross-shore domain (slightly above MSL). Although the results for this position were promising, comparison of modeled sediment transport with Bardex II observations at different positions throughout the upper and lower swash zone is needed to give a full validation of the proposed adaptations to the transport formulations.

ACKNOWLEDGMENTS

During the last 8 months, Deltares has not only been 'Enabling Delta Life' but also pretty much my personal life. Therefore I owe an acknowledgment to the facilitating staff, in the person of Radha for silently organizing Deltares' students life while not so silently sharing silly jokes with the 'student corner'. I would like to thank anyone who was in that corner in the period that I was hosted at Deltares. You guys gave me a great time and the possibility of complaining about Matlab figures and sharing Visual Studio shortcuts made my project time a lot more bearable. The student lunch was a moment of relief and relaxation and I will definitely miss the excitement about the delicious Thursday's 'Roti Kip'. Although I spent my thesis time mostly at Deltares, I owe a big thanks to my professor Ad Reniers. He suggested the research topic in January 2017 when I came to his office demanding something challenging and fundamental. I enjoyed his incredible speed of thinking which I had to keep up with in every progress meeting and even more during our discussions in the desolated civil engineering faculty during summer about the mismatch between data and model. I would like to thank Jebbe for sharing his experimental experience and his criticism of my research methodology and results. Thanks to Matthieu for all the questions during the progress meetings, they made me look critical at my own results. I would like to thank Robert, my daily supervisor for the patience while I was learning XBeach, the flexibility of supervision during the process and the impatience in the end when it came to produce always more results which in the final weeks of the project led to a complete new chapter! This new chapter and equally the existing ones, implied that my family, friends and Dicken did not get the attention they deserved the last few months. Please bear with me one more week because when I start my PhD I will make up for the lost social quality time... promised...

C.E. Jongedijk
Delft, October 2017

CONTENTS

GLOSSARY

variable	description	unit
A_{sb}	Bed load coefficient	-
A_{ss}	Suspended sediment coefficient	-
C_b	Depth-averaged bed load concentration	$\frac{m^3}{m^3}$
C_s	Depth-averaged suspended sediment concentration	$\frac{m^3}{m^3}$
Cb_{eq}	Depth-averaged equilibrium bed load concentration	$\frac{m^3}{m^3}$
Cs_{eq}	Depth-averaged equilibrium suspended sediment concentration	$\frac{m^3}{m^3}$
D_{10}	D10 grain size	m
D_{50}	D50 grain size	m
D_{90}	D90 grain size	m
D_*	Dimensionless sediment diameter	
D_c	Sediment diffusion coefficient	
D_r	Roller energy dissipation	$\frac{W}{m^2}$
H_{m0}	Wave height, zero order moment	m
H_{rms}	Root mean squared wave height	m
H	Wave height	m
K_x	hydraulic conductivity XBeach (=Ky =Kz)	$\frac{m}{s}$
K	hydraulic conductivity	$\frac{m}{s}$
S_b	Bed load transport (Subg)	$\frac{m^2}{s}$
S_s	Suspended sediment transport (Susg)	$\frac{m^2}{s}$
T_p	Peak wave period	s
T_{rep}	Representative wave period	s
$T_{s,min}$	Threshold value for sediment response time	s
T_{swash}	Swash period	s
T_s	Sediment response time	s
T	Wave period	s
Δ	relative density	-
α_1	factor	
α_2	factor	
α_Ψ	angle between velocity vector and x-axis	
$\bar{u}$	flow part of the velocity	$\frac{m}{s}$
β	factor in critical slope for bore turbulence	
β	ratio between velocity due to waves and currents	
δ	wave height enhancement factor	
ν	kinematic viscosity	$\frac{m^2}{s}$
ρ_s	density sediment	$\frac{km}{m^3}$
ρ_w	density water	$\frac{km}{m^3}$
τ_x	cross shore shear stress	$\frac{kg}{m^2}$
τ_y	alongshore shear stress	
θ	Shields parameter	
$\tilde{u}$	flow part of the velocity	$\frac{m}{s}$
dt	calculation time step	s
f_{swash}	Swash frequency	Hz
f_s	Depth averaging correction factor f_s for w_s	
g	gravitational acceleration	m s$^-$2

variable	description	unit
h_{min}	preset minimal water depth cutoff	m
h_{old}	Local water depth previous time step	m
h_{roller}	roller thickness	m
h	Local water depth	m
k_b	turbulent kinetic energy bottom	$\frac{J}{kg}$
k_{gain}	calibration factor for turbulent kinetic energy k_{turb}	
k_{source}	source term for turbulent kinetic energy k_{turb}	
k_s	wave averaged turbulent energy	
$k_{turbulence}$	turbulent kinetic energy at water surface	$\frac{J}{kg}$
k_{turb}	Short wave breaking induced turbulent kinetic energy	$\frac{J}{kg}$
k	Wave number	
p	porosity	
q_x	Total sediment transport rate	$m^2\ s^{-1}$
t	Time	s
u^E	Eulerian velocity	m/s
u^L	Lagrangian velocity	m/s
$u_{cr,c}$	critical velocity for sediment to move due to waves	$\frac{m}{s}$
$u_{cr,w}$	critical velocity for sediment to move due to currents	$\frac{m}{s}$
u_{cr}	critical velocity for sediment to move	$\frac{m}{s}$
u_{meas}	measured velocity	$\frac{m}{s}$
u_{mod}	modeled velocity	$\frac{m}{s}$
$u_{rms,2}$	Adapted orbital velocity	$\frac{m}{s}$
u	cross-shore velocity	$\frac{m}{s}$
u	alongshore velocity	$\frac{m}{s}$
w_s	Fall velocity	$m\ s^{-1}$
x	Cross shore position	m
x	Alongshore direction	m
z_b	Bed level	m
z_s	Surface level	m

List of Figures

List of Tables

1

INTRODUCTION

The main goal of this thesis is to improve XBeach non-hydrostatic model predictions of swash morphodynamics on intermediate reflective beaches. In this introduction a brief motivation for this goal and research questions which needs to be answered to achieve the main goal are presented. The last section contains a summary of the research questions and an outline of the thesis.

1.1. SWASH MORPHODYNAMICS

Nearshore Characterisation A very common observation is the episodic erosion of beaches during storms and the slow recovery (accretion) afterwards. Morphodynamic processes, the physical processes relating the fluid motions (hydrodynamics) to movement of sediments are responsible for this erosion and accretion. To predict the morphological response of a beach, the morphodynamic processes on the nearshore have to be understood. The nearshore is the region between the beach and the edge of the offshore (usually considered from a depth larger than 20 m) and can be characterized in several zones as shown in Figure 1.1.

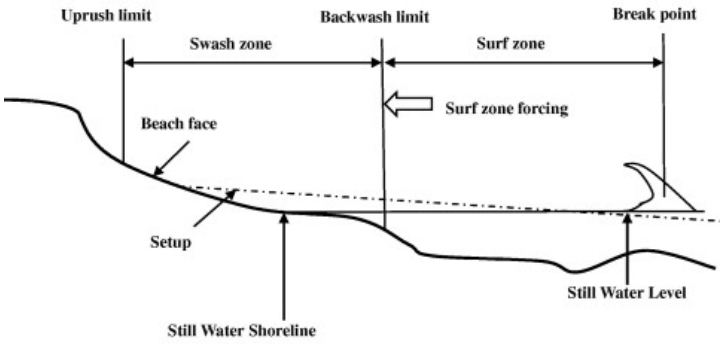

Figure 1.1: Near shore characterisation, image from Bakhtyar et al. (2009)

Intermediate-reflective Beaches For all regions of the nearshore, the same physical processes are present. Water reacts instantaneously to changes, forcing the hydrodynamic processes to adapt immediately to for example a changed bed level. The morphodynamic processes need time to adapt to changed waves, tides and currents and therefore are almost always lagging behind the hydrodynamic conditions, hardly ever reaching an equilibrium state. The contribution of several morphodynamic processes and the speed of morphological response to changed hydrodynamic conditions depends on the beach type, the sediment type and the fluctuations in hydrodynamic conditions (Butt et al. (2004)). The beach types have been classified in three categories by Wright & Short (1984): reflective, intermediate, and dissipative beaches. These three types have been visualized in Figure 1.2 where also can be seen that intermediate-reflective beaches due to the combination of long and short wave breaking know the most dynamic swash zone.

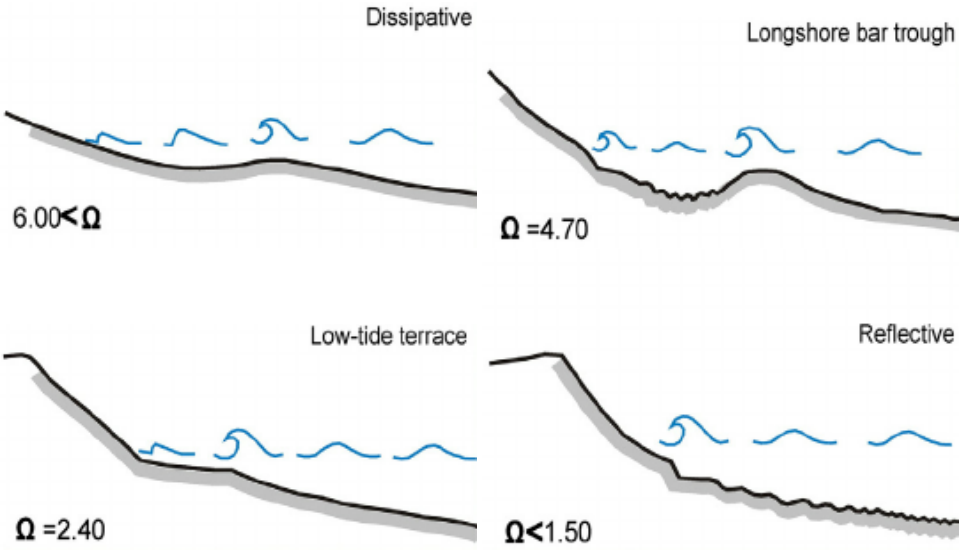

Figure 1.2: Characterization of beach types. Dissipative, reflective and two different types of intermediate-reflective beaches. Ω is an dimensionless parameter of the ratio between wave steepness and grain size. Image from Hughes et al. (2014)

Sediment transport Mechanisms Three mechanisms of sediment transport can be classified. If the flow velocities are low, only on the bed the sand grains will move (bed load transport) as shown in the left panel of Figure 1.3. If velocities get higher, the whole upper layer of the sediment starts moving as one saturated sheet. This is called sheet flow (shown in the middle panel of Figure 1.3). When the velocities are high enough, the sand particle will be fully lifted by the hydrodynamic force and will move through the domain in suspension. This is called suspended sediment transport and is sketched in the right panel of Figure 1.3.

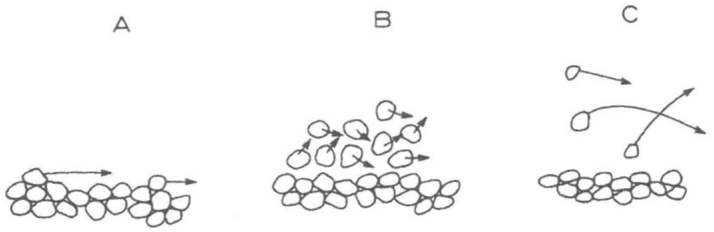

Figure 1.3: Different modes of sediment transport, A Bed load, B sheet flow, C Suspended load, image from Bosboom & Stive (2013)

The swash zone, defined between the uprush and backwash limit i.e. the alternating wet/dry zone of the beach is the most dynamic zone of the nearshore. The intermittent flows are rapidly varying and high values and gradients for the sediment concentration are present. Because of the shallow water and high flow velocities close to the bed, all types of sediment transport are expected to play a role Butt (1999). The widely varying range of length scales in swash processes, from the smallest turbulence scales to processes that take place on a 100 m length scale like longshore bar systems (as sketched in Figure 1.2), are all relevant when determining the different swash morphodynamic processes. Intermediate-reflective beaches have a very dynamic swash zone. This leads to the first research question of this thesis: *What are the relevant physical processes for the morphodynamics in the swash zone on intermediate-reflective beaches?*

1.2. MODELING SWASH MORPHODYNAMICS

Modeling Challenges Many processes in the swash zone are generally considered complex to model and experimental results are not yet correctly reproduced by models (Brocchini & Baldock (2008), Briganti et al. (2016)). For these reasons, most coastal morphodynamic models do not explicitly resolve morphodynamic processes in the swash zone. So far, especially in areas with little swash dynamics, Roelvink et al. (2009) showed that this model strategy works quite well. However, for areas where the complex swash dynamics add significantly to the sediment transport (for example for more reflective beaches), this approach does not

yet represent the observed results. Measuring swash processes intuitively should be easy because the swash zone is very reachable (closest to shore) but in practice can be difficult because measuring and maintenance of measurement instruments is complicated. This is because the flow is very shallow, the flow has high velocities, flow reversal timing is complex and gradients are high due to rapidly varying flow and sediment concentrations. Turbulence is acknowledged as important for energy considerations but hard to measure due to continuous emergence and submergence of instruments. There are different modes of transport dominant in different swash regions (sheet flow, bed load and suspended). Therefore, being able to correctly represent swash processes in a numerical model is important for the understanding of the contribution of individual processes and for the prediction of storm impact on beaches and recovery afterwards. The resolution and amount of processes incorporated depends on the type and application of the model used. A division can be made in their contribution to either onshore, or offshore directed transport and to which transport mechanism (see Figure 1.3) they contribute.

Temporal and Spatial Scales On the small scales, Briganti et al. (2016) found that turbulence originating from the bore and boundary layer play a role. On the intermediate scale, Brocchini & Baldock (2008) found that it is hard to determine a representative swash event, and simplifications made for larger coastal systems (neglecting short waves) usually include surf zone, but neglect the swash zone transport. On the large scale, Brocchini & Baldock (2008) and Chardón-Maldonado et al. (2015) found that the position of the instantaneous shoreline is the largest challenge due to a mismatch between measured and modeled run-up. Also 2D and 3D effects are becoming significantly more important which makes depth averaged modeling less favorable. On dissipative beaches swash is initiated by infra gravity movement, the more reflective a beach, the more the swash motions are initiated by short waves.

The surf-beat version of XBeach does not resolve short waves and therefore does not calculate swash on short wave dominated beaches correctly. The non-hydrostatic module of XBeach uses the inclusion of a non-hydrostatic pressure correction term to resolve short waves and is therefore promising to calculate the swash correctly. Very advanced modeling techniques (e.g. full 3D flow resolving approaches) are helpful in understanding processes on a very short timescale, though very unhelpful in engineering practice due to their high computational cost. This leads to the second research question of this thesis: *How are the relevant processes represented by XBeach non-hydrostatic?*

1.3. BARDEX II

The Bardex II experiment was performed in 2012 in the Delta Flume and resulted in a large dataset of observations of morphodynamical processes on a sandbar (Masselink et al. 2013). The complete Bardex experiment includes experiments A-E with different goals for every experiment. In this thesis, the morphodynamical predictions of XBeach are compared with observations during one erosive experiment (A4) and one accretive experiment (A8). The other experiments will not be described here but can be found in Masselink et al. (2016). Measuring in a controlled environment with on one hand a simplified beach and conditions, but on the other hand access to measurement devices and control over forcing conditions allows for very detailed comparison between the modeled results and measured reality. Having determined relevant processes from literature (mainly from field measurements) and understood the implementation of the processes in the non-hydrostatic extension of XBeach, the comparison with measurements therefore introduces the third research question of this thesis: *How do the numerical results perform compared to the experimental results from Bardex II (erosive and accretive) and do we need new processes/improvements of current physics?*

1.4. IMPROVEMENT OF PREDICTIONS WITH XBEACH

The morphodynamic predictions will be made in the reference frame of the non-hydrostatic extension to XBeach. XBeach is a process-based depth averaged, phase resolving model. The non-hydrostatic extension, as developed by Smit et al. (2014), is necessary in the framework of intermediate reflective beaches since it makes the model capable of solving non-linear waves, wave-current interaction and wave breaking in the surf zone. Therefore the additions or changes that are made to the model should respect, and co-act with the existing functionality of the model in other regions (mainly the surf zone dynamics). The answer on the first three research questions will lead to conclusions about the current performance of the non-hydrostatic version of XBeach. The last research question of this thesis is:*How can predictions be improved for swash morphodynamics of intermediate-reflective beaches?*

This research is performed as part of the CoMIDAS (Coastal Modeling, Intelligent Defense and Adaptation based on Scientific understanding) project. The aim of this project is to develop a modeling framework for coastal erosion studies along the South Korean East Coast (Deltares (2017)). The South Korean East coast is a complex coastal system both due to its natural conditions (e.g. crescentic sandbars, typhoons) and human interventions (e.g. ports, groins and offshore breakwaters). The East coast suffers from coastal erosion, leading to significant impacts for the local infrastructure. Currently, the processes driving the coastal erosion are not well understood and the modeling tools to calculate and predict these processes seem insufficient. This is mainly because the South Korean East coast is an intermediate reflective beach where the complex swash processes are expected to influence the sediment transport significantly.

1.5. RESEARCH OBJECTIVE, RESEARCH QUESTIONS AND THESIS OUTLINE

Objective The main objective of this study is to:

- **Determine relevant processes in the swash zone in order to improve XBeach non-hydrostatic model predictions of swash morphodynamics on intermediate reflective beaches**

Research questions The research questions that are answered in this thesis are:

- RQ[1]: What are the relevant physical processes for the morphodynamics in the swash zone on intermediate-reflective beaches?
- RQ[2]: How are the relevant processes represented by XBeach non-hydrostatic?
- RQ[3]: How do the numerical results perform compared to the experimental results from Bardex II (erosive and accretive) and do we need new processes/improvements of current physics?
- RQ[4]: How can we improve predictions of swash morphodynamics on intermediate-reflective beaches?

.

Approach A literature study gave answer on [RQ1]. With the conclusions of the literature study a qualitative modeling study on a planar beach was be set-up in order to gain insight in the sediment transport formulations of XBeach. The influence on the swash morphodynamics of the relevant physical processes are individually assessed with a focus on whether the behavior was expected/understood, where in the swash zone or cycle the influence of the process was the strongest/significant and whether the process had a significant influence on the total morphological change of the planar beach. After that the performance of XBeach was compared to the measured morphodynamics of the Bardex II experiment in order to answer [RQ3]. The total morphological response was compared as well as the intra-swash sediment transport processes. In the last part of the thesis [RQ4] was answered assessing two different modifications of the current sediment transport formulations in XBeach.

Outline Thesis In this chapter a short introduction was given to swash morphodynamics and the research goal and research questions were given. Chapter 2 will summarize the results of a literature study and address the physics and implementation in XBeach of four relevant processes. The results of a qualitative modeling study on a planar beach can be found in Chapter 4 where in Chapter 5 the performance of XBeach is compared to measurements of two Bardex II experiments. Chapter 6 presents the results of modified sediment transport formulations. The methodology for all modeling cases will be explained in Chapter 3 and all results will be discussed in Chapter 7. The conclusions, leading to the answers on the research questions, and outlook to further research are presented in Chapter 8.

2

THEORY

Introduction This chapter focuses on the relevant physical processes in the swash in literature and in XBeach. In the first section, an overview of the individual swash cycle and interactions between swash cycles is given. After that the current parameterizations in XBeach for a 1DH calculation of morphodynamical processes are given. The second section of this chapter contains the physics behind, and implementation in XBeach of, four processes that are expected to influence the morphodynamics in the swash.

2.1. SWASH MORPHODYNAMICS

2.1.1. PHYSICS OF SWASH MORPHODYNAMICS

One swash cycle To systematically study morphodynamics, comparison to single swash event is useful. Gross bed level changes during swash events are large while net changes for example over one tidal cycle are small and in the order of the bed level change of one event (Blenkinsopp et al. 2011). A general swash event can be described, if neglecting bottom friction and flow infiltration/exfiltration. First an incident wave breaks, and starts dissipating energy due to induced turbulence. The wave height decreases and the wavefront rotates to shore parallel due to change in water depth. When the bore reaches the shoreline, the bore front and the water behind the front rapidly accelerate and the bore collapses. Swash can be characterized in four phases, schematically shown in Figure 2.1:

- High onshore accelerating velocity when bore passes, strong offshore velocity close to bed, high vertical mixing.
- Slow onshore accelerating due to push from bore, potential groundwater infiltration.
- Maximum landward point, offshore acceleration due to gravity, very thin layer of water
- deceleration of offshore flow due to collision with next bore, retrogressive bore might develop inshore causing exfiltration.

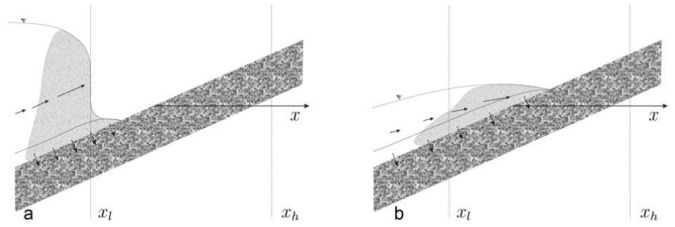

(a) Runup phase of a swash event. Bore collapse (left), Runup (right)

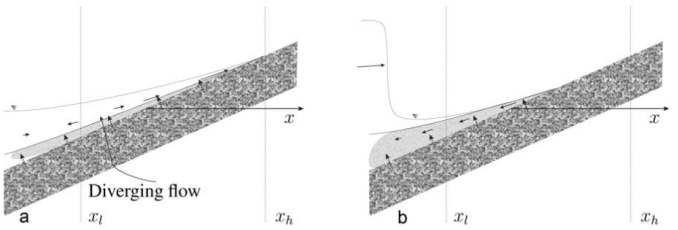

(b) Run-down phase of a swash event. rundown(left), subsequent incoming wave (right).

Figure 2.1: Schematic swash cycle: Solid arrows indicate depth-averaged velocity, dashed arrows at the bed indicate infiltration and exfiltration, the solid line near the bed indicates the top of the boundary layer, while the shaded area in the wave body indicates the region of highest sediment concentration and greatest shear stress. Figure from Brocchini & Baldock (2008).

Whether flow reversal correlates with maximum water level is dependent on the beach type and foreshore location. The duration of the uprush is shorter than the duration of the downwash with similar or slightly stronger velocities resulting in predominantly negative velocity skewness in the swash zone. Measured peak uprush shear stress was twice the measured peak downwash shear stress. Without a satisfactory physical explanation, generally agreed is the empirical friction factor for uprush to be larger than for backwash but the value (because of the lack of physical evidence) is still under debate (Brocchini & Baldock (2008)). From the Bardex II experiment, friction factors estimated from the logarithmic profile were of the same order of magnitude for the uprush and the backwash, but with a strong variability related to the boundary layer growth during the backwash (Ruju et al. (2016)). An analytical solution (variation of the original analytical solution of Shen & Meyer (1963)) to the flow velocity in the swash cycle is proposed by Baldock & Hughes (2006), where the solution based on a method of adapted characteristics meet the observations relatively well. This is mainly because of better represented water levels and run up distances. This analytical solution is shown in Figure 2.2 where the different flow regions (a) and acceleration (b) resulting from this solution are shown. Sediment transport processes during one representative swash cycle are summarized by Masselink & Puleo (2006) and shown in the schematic Figure 2.3. During uprush, positive swash velocity causes the water to flow on the beach, where under the incoming bore a lot of turbulence is generated. Because of the pressure increase under a rising water level, water infiltrates in the ground. At flow reversal, all sediment has settled. In the backwash, bed induced turbulence is generated and because of the falling water level, groundwater exfiltrates back into the swash.

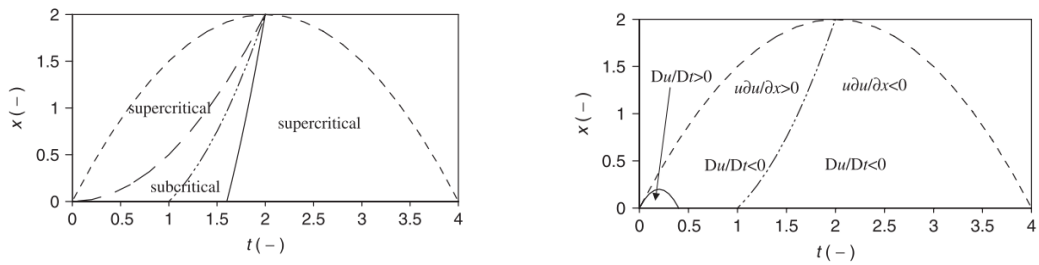

Figure 2.2: Results of the adapted analytic solution as first proposed by Shen & Meyer (1963). a) Flow regions derived from the analytical (characteristics) swash solution. — = shoreline position, long dash u = c(uprush), -.- u=0, solid line u=c(backwash) and b) Regions of different flow acceleration derived from the swash solution of Peregrine and Williams (2001). The local or Eulerian acceleration, $\partial u/\partial t$ is always negative. — = shoreline position, — . — $u\partial u/\partial t = 0$, —— $Du/Dt = 0$. Figure adapted from Baldock & Hughes (2006).

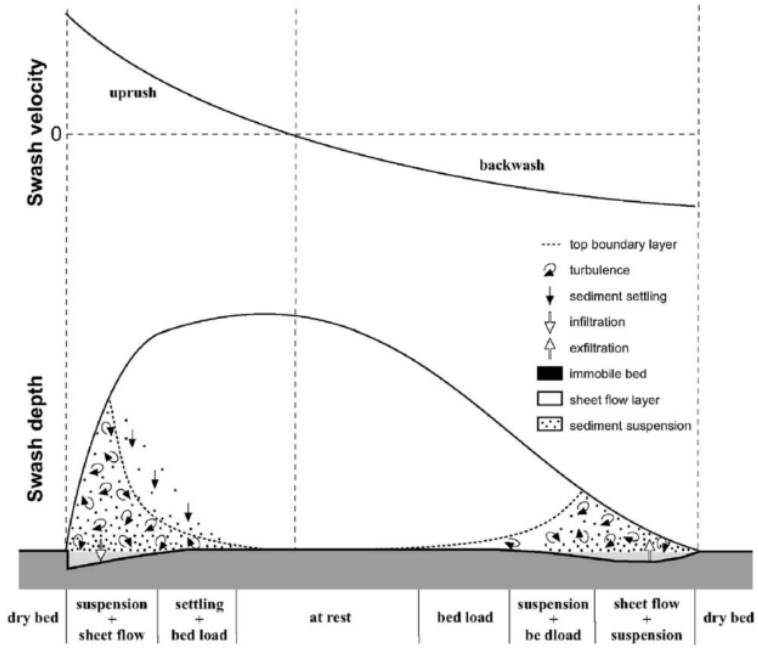

Figure 2.3: Schematic of sediment transport processes during a swash cycle, image from Masselink & Puleo (2006)

Multiple swash cycles The morphodynamics and hydrodynamics of the beach face can not be seen isolated from those in the surf zone. Masselink & Puleo (2006) studied the interactions between the different regions in the nearshore (as shown in Figure 1.1). Figure 2.4 shows their results in the form of a schematic framework for the surf-swash interactions. These interactions are dependent on the time scales of swash motions which range from seconds (steep or reflective beaches, calm conditions) to minutes (mild sloped or dissipative beaches, energetic conditions). For steep beaches or beaches with low tidal range, the swash zone is very defined because there is very little interaction with the surf zone. On beaches with a high tidal range and/or very mildly sloped, there is a lot of interaction between swash, surf and shoaling waves. As discussed in Chapter 1, Masselink & Puleo (2006) states that feedback between morphology and hydrodynamics is essential component of the swash zone and has two scales: swash-surf interactions (global) and interactions within the swash zone (local).

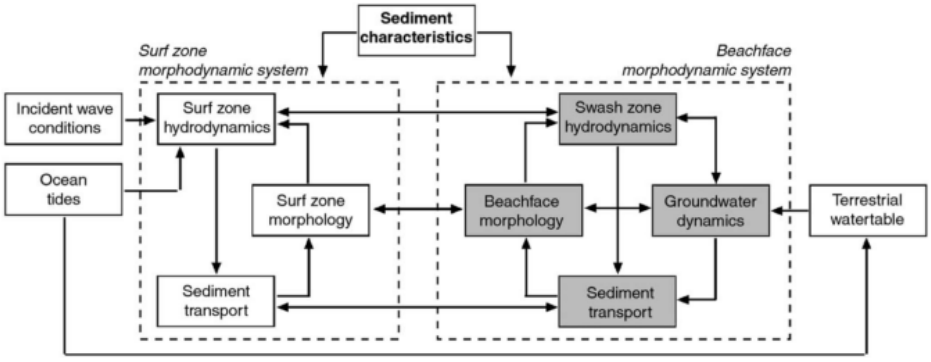

Figure 2.4: Framework for surf-swash interactions. Image from Masselink & Puleo (2006)

Brocchini & Baldock (2008) studied the cause of swash zone sediment concentrations. They found that in swash zone, final dissipation of short wave energy occurs, while most of the low frequency wave energy is generally reflected back seaward. Short wave-short wave and short wave-long waves interactions can create more low frequency waves (LFW) which can transport large amounts of sediment that have been stirred up by wind waves. Induced by these two waves, two types of swash can be distinguished: High frequency swash ($f_{swash} > 0.05$Hz) from bore collapse and standing, low frequency swash ($f_{swash} < 0.05$Hz). Masselink & Puleo (2006) determined which type of swash occurs depending on the beach type and the incident wave

conditions, and that this can be predicted using a surf similarity parameter based on breaker height, incident wave period and beach gradient. Low frequency swash dominates mainly on mildly sloped beaches. If assuming that waves show monochromatic behavior, the maximum swash amplitude is in that case limited by interaction with preceding and following uprush and backwash. Since the swash amplitude therefore not depends on bore height variation we call the swash saturated. Brocchini & Baldock (2008) defined the natural swash period as T_{swash} where the amount of swash-swash interactions can be represented by the ratio between T_{swash} and T_{rep}. If that ratio is small there is no interaction, and if it is large there is a lot of interaction. Brocchini & Baldock (2008)

Chardón-Maldonado et al. (2015) Describes three different events when taking into account that there are multiple swash events instead of one representative that can flow with the natural period without interaction. As is shown in Figure 2.5 during swash overtake onshore transport is enhanced, during weak backwash bore interaction also onshore transport is enhanced, but during very strong backwash bore interaction the bore can not fully propagate on the beach resulting in enhanced offshore transport. Independent on the beach type, Brocchini & Baldock (2008) found that during storm events stronger correlation between low frequency waves and short wave result in offshore transport enhancement where during recovery, alongshore bars induce more breaking and therefore onshore transport enhancement.

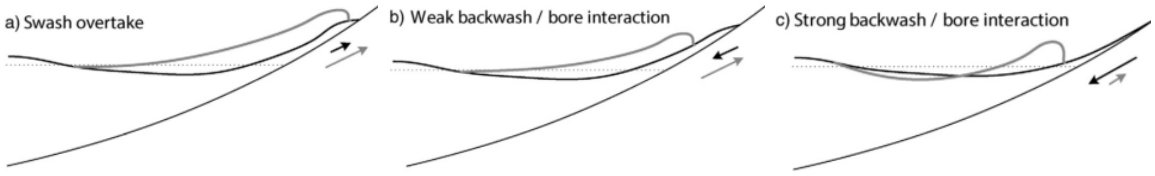

Figure 2.5: Schematic of interactions in the swash zone: a)swash overtake where a bore initializes a new swash event before the preceding swash event has experienced backwash; b)weak backwash/bore interaction where the bore propagates shore ward largely unimpeded by the preceding backwash; c) strong backwash/bore interaction where a rapid backwash flow collides with an ensuing bore possibly slowing the bore or causing a hydraulic jump. The thin black curve is the foreshore. The dotted line is the still water level. The thick black curve is the initial swash event. The thick gray curve is the ensuing bore motion. Arrows indicate the direction and scale of expected sediment flux. Image from Chardón-Maldonado et al. (2015)

2.1.2. SWASH MORPHODYNAMICS IN XBEACH NON-HYDROSTATIC

This section contains the governing equations of XBeach for the calculation of the morphodynamics. For the hydrodynamics is referred to Roelvink et al. (2015) and will not be further discussed in detail since the focus of this thesis is on the sediment transport processes.
Sediment is transported in bed load or in suspended load (See Figure 1.3). The default sediment transport formulation in XBeach is the van Thiel-van Rijn method based on Van Thiel De Vries (2009) and van Rijn et al. (2007) and given in Equation 2.2 and 2.1 for bed load and suspended load respectively.

$$Cs_{eq} = \frac{A_{ss}}{h}\left(\sqrt{u^2 + 0.64u_{rms,2}} - u_{cr}\right)^{2.4} \tag{2.1}$$

$$Cb_{eq} = \frac{A_{sb}}{h}\left(\sqrt{u^2 + 0.64u_{rms,2}} - u_{cr}\right)^{1.5} \tag{2.2}$$

The van Thiel-van Rijn method calculates the equilibrium concentration on the bed and in suspension when the velocity is higher then the critical velocity u_{cr} which is a threshold velocity above which sediment is mobile. The terms under the square root is a combined velocity term representing the force on the sediment where $\bar{u}$ is the flow part of the velocity and $u_{rms,2}$ is the turbulence and the orbital velocity combined (more details in Section 2.2.4). The terms A_{ss} and A_{sb} are dependent on sediment properties and given by Equations 2.3 and 2.4 with D_* the dimensionless diameter of sediment depending on Δ, D_{50}, g and the kinematic viscosity ν.

$$A_{ss} = 0.015h\frac{(D_{50}/h)^{1.2}}{(\Delta g D_{50})^{0.75}} \tag{2.3}$$

$$A_{sb} = 0.012D_{50}\frac{(D_*)^{-0.6}}{(\Delta g D_{50})^{1.2}} \tag{2.4}$$

The threshold velocity for motion (Equation 2.8) is based on Komar & Miller (1975) and consists of a contribution due to waves and a contribution due to currents (Equation 2.5). The factor β is the ratio between the mean flow and the combined orbital velocity and turbulence term $u_{rms,2}$ and decides whether waves or currents dominate.

$$u_{cr,c} = 0.19 {D_{50}}^{0.1} \log 10 \left(\frac{4h}{D_{90}} \right) \tag{2.5}$$

$$u_{cr,w} = 0.24 \left(\Delta g \right)^{2/3} \left(D_{50} T_{rep} \right)^{0.33} \tag{2.6}$$

$$\beta = \frac{|u|}{|u| + u_{rms,2}} \tag{2.7}$$

$$u_{cr} = \beta u_{cr,c} + \left(1 - \beta \right) u_{cr,w} \tag{2.8}$$

The above equations leading to the equilibrium concentrations only hold for sediment with a D_{50} under 0.0005m.The depth averaged advection-diffusion equation (Equation 2.9, Galappatti & Vreughenhil (1985)) is used to calculate the suspended sediment concentration in the water column based on the difference between the actual concentration and the equilibrium concentration. These equations includes advection and introduces a time lag due to the sediment response time (see Section 2.2.2).

$$\frac{\partial hC_s}{\partial t} + \frac{\partial hC_s u}{\partial x} + \frac{\partial}{\partial x} \left[D_c h \frac{\partial C_s}{\partial x} \right] = \frac{hCs_{eq} - hC_s}{T_s} \tag{2.9}$$

After the introduced time lag and including advection, the suspended and bed load sediment transport are calculated by multiplying the concentrations with the local velocity (Equation 2.10 and 2.11 for suspended and bed load transport respectively).

$$S_s = (C_s uh - \text{diffusion}) \tag{2.10}$$

$$S_b = (C_b uh) \tag{2.11}$$

The final step in the morphodynamical calculation is to calculate the rate of bed level change due to the total sediment transport, $\frac{\partial z_b}{\partial t}$. The XBeach user can choose to not perform a so called 'bed-update' and Equation 2.12 will then be skipped.

$$\frac{\partial z_b}{\partial t} + \frac{1}{1-p} \left(\frac{\partial q_x}{\partial x} \right) = 0 \tag{2.12}$$

where z_b is the rate of change of the bed level, $\frac{\partial q_x}{\partial x}$ the total transport gradient, p the porosity. The total transport q_x is the sum of suspended and bed load transport:

$$q_x = S_s + S_b \tag{2.13}$$

Summary In this section first the general physics of swash morphodynamics is explained. In the next section four processes that influence the swash morphodynamics are further elaborated on. The general sediment transport formulation that XBeach uses to calculate a bed level change due to hydrodynamic forcing was explained in this section, but the specific implementation of the four processes will be discussed with each process in the next section.

2.2. PROCESSES INFLUENCING SEDIMENT TRANSPORT IN THE SWASH

Introduction Several physical processes have been shortly addressed in the explanation of the swash cycle in Section 2.1.1. Four processes that influence sediment transport in the swash will be elaborated on further in this section. In the literature study, the focus was on processes that could lead to beach recovery (accretion) or prevent overprediction of erosion (see Chapter 1). The four processes are bed slope effects, sediment response time, exchange with groundwater and bore induced turbulence. The physics behind and implementation in the above described sediment transport formulations in XBeach will be described in the next four subsections.

2.2.1. BED SLOPE EFFECTS

Gravity stimulates transport during backwash and inhibits transport during uprush, the steeper the profile the more significant these offshore enhancing effects. To get representative numerical results compared to observations, the calibration factor for uprush needs to be twice the factor for downwash (both for energetics and shear stress model, (Brocchini & Baldock 2008)) implying that processes are not well represented. As Walstra et al. (2007) describes, most transport formulas are only valid for nearly horizontal beds. Based on experiments, the bed slope effect can work on the sediment transport in three ways: change the local near bed velocity, change the threshold for motion and/or change of sediment direction once in motion. Also In XBeach, a sediment particle feels the bed locally as being horizontal. Several processes as avalanching and the gravity enhanced rolling down over rolling up of sand particles are compensated for by scaling the sediment transport values with the bed slope effects after the calculation of the transport rates.

Bed slope effects in XBeach There are two different theories of bed slope effects already implemented in XBeach. The bed slope effect magnitude is implemented in two modules, SOULSBY and ROELVINK. Both of them have an option BED and TOTAL which means that for total, the bed and suspended transport are affected and for bed only the bed load transport is. The ROELVINK module is a 2D improvement on the 1D formulation but for 1D, both of them are equal and therefore only ROELVINK is in the scope of this thesis.

For the TOTAL modules, after the calculation of the suspended transport S_s and bed load transport S_b with Equation 2.13, both of them are corrected with a bed slope effect factor:

$$S_{sslope} = q_x - 1.6hC_s u\frac{\partial z_b}{\partial x} \tag{2.14}$$

$$S_{bslope} = S_b - 1.6hC_b u\frac{\partial z_b}{\partial x} \tag{2.15}$$

Where for the BED module, only the bed load transport is adapted according to Equation 2.15 and the suspended transport remains untouched.

2.2.2. SEDIMENT RESPONSE TIME

The advection-diffusion equation of Galappatti & Vreughenhil (1985) contains a source/sink term on the right hand side of Equation 2.9 based on the equilibrium sediment concentration and the sediment response time T_s. The stirring up and even more the settling of the sediment particles back to the bed is not an instantaneous process and takes time. A small value for T_s means nearly instantaneous sediment response, a long response time means that the sediment response is lagging more behind the hydrodynamic forcing. For large T_s the sediment concentration lags behind the oscillation of the flow. When the highest sediment concentration is not in phase with the highest velocity (regardless whether this occurs during maximum uprush or maximum downwash velocities) the sediment flux due to advection will be lower than for a (nearly) instantaneous sediment response. Another effect of this lag is that sediment during flow reversal still remains in the water column and is transported in opposite direction afterwards, as measured by Dohmen-Janssen et al. (2002). She observed that due to asymmetric flow there is more sediment stirred up during uprush, and that the slower the sediment response time, the bigger the lag between concentration and flow velocity, and the higher the concentrations moved offshore after reversal. This resulted in net offshore transport over one swash cycle. Others, like Alsina et al. (2009), found that all suspended sediment settles after completion of the swash uprush and that all the sediment that is transported in the downwash is also entrained during this downwash. His results, as shown in Figure 2.6, indicate that there is no such reversal of suspended sediment.

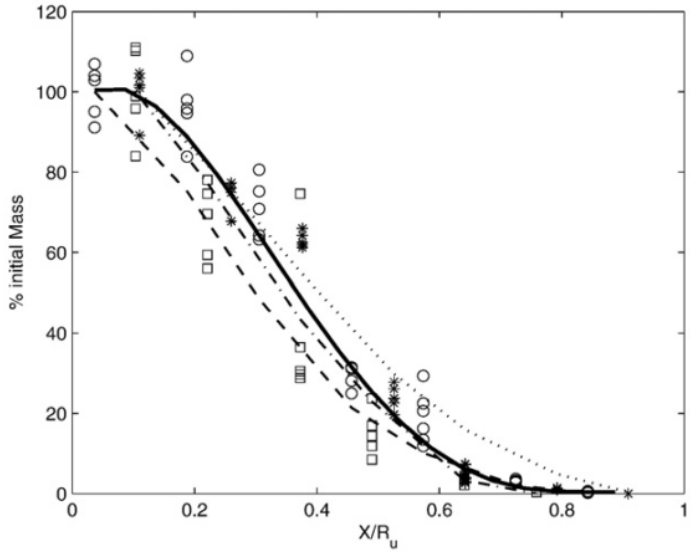

Figure 2.6: Cross-shore distribution of modeled (lines) and measured (symbols) sediment mass in the swash zone. The x-coordinate is made dimensionless with the horizontal run-up length; Different lines represent separate tests. Measured data are shown as the mean value and standard deviation represented by the error bars. Figure from Alsina et al. (2009).

Sediment response time in Bardex II From the Data storage report (Masselink et al. (n.d.)), a sediment fall velocity of 0.046m/s is assumed. After each test, the sediment fall velocity of samples that were taken of part of the beach profile (between x=80 and x= 110 m) was determined. The mean sediment fall velocity of the barrier sediment, computed by taking into account all sediment samples, was 0.046m/s. Masselink et al. (2016) found that the fall velocities varied considerably in time and space (see Figure 2.7). Starting with very equal distribution of sediment, throughout the tests sediment redistribution took place causing the mid-lower swash zone and inner surf zone to become coarser (ws=0.06 - 0.08 m/s) and the barrier crest region to become finer (ws=0.03 -0.04 m/s).

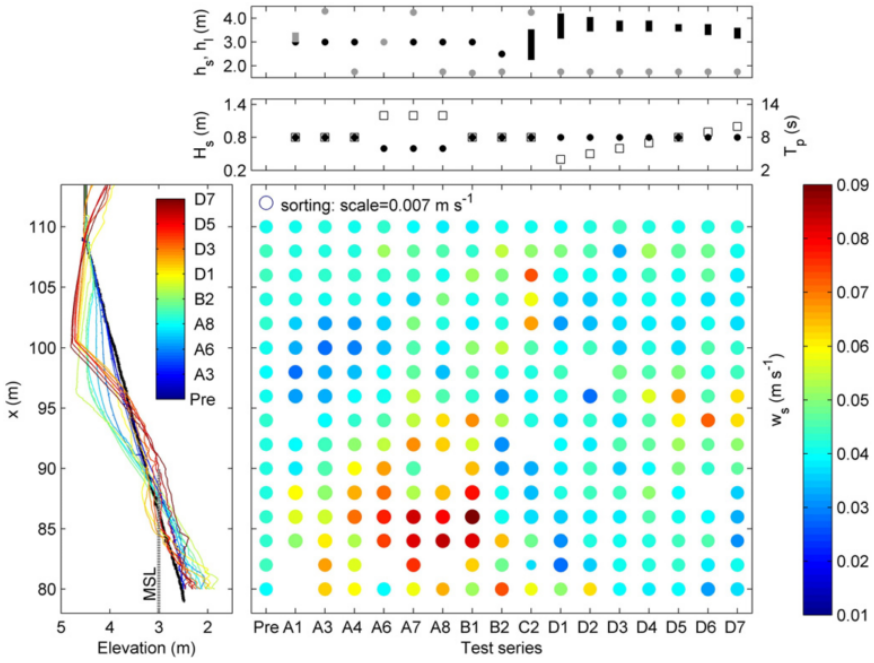

Figure 2.7: Time series of sea level hs (black symbols) and lagoon level hl (gray symbols), and significant wave height Hs (black circles) and peak wave period Tp (white squares) during the experiment (top two panels); beach profiles after each of test (left panel); and spatial and temporal variability in the sediment fall velocity (color of the symbol) and sorting (size of the symbol). Figure from Masselink et al. (2016)

Sediment response time in XBeach The settling time scale is a parameter dependent on the water depth h and the sediment fall velocity w_s and is calculated with Equation 2.16. A large value of T_s means slow response where a very small value, $T_{s,min}$, is nearly instantaneous sediment response. f_s is a compensation factor for depth averaging. To avoid the denominator to become zero when the water depth decreases to zero, a minimum value for T_s is set, default $T_{s,min} = 0.5$

$$T_s = max\left(f_s \frac{h}{w_s}, T_{s,min}\right) \tag{2.16}$$

$$w_s = \alpha_1 \sqrt{\Delta g D_{50}} + \alpha_2 \frac{\Delta g {D_{50}}^2}{\nu} \tag{2.17}$$

where α_1, α_2 are sediment type related factors, Δ the relative density, D_{50} the grain diameter, g the gravitational acceleration and ν the kinematic viscosity.

As derived according to Equation 2.16 and Equation 2.17, the sediment response time and fall velocity influence the sedimentation during the swash. The parameter T_s is calculated from the fall velocity an is not separately variable in XBeach, there is a set minimum T_{smin} on the parameter, described by Equation 2.16 which can be varied in order to see the effect of T_s on erosion/accretion.

2.2.3. GROUNDWATER

Turner & Masselink (1998) describes the effect of interactions between the beach groundwater table and swash motion on sediment transport processes on the upper beach and, therefore, beach stability. These interactions are strongly controlled by the elevation of the beach groundwater table relative to sea level, and it is often considered that a low water table promotes beach stability, while a high water table has a destabilizing effect on the beach. They found that sediment transport rates are proportional to the Shields parameter, θ, which is defined as

$$\theta = \frac{\tau}{\rho_w (s-1) g D} \tag{2.18}$$

with τ the bed shear stress, ρ_w the fluid density, ρ_s the density of the sediment material, D the sediment particle size and s the relative density ($\frac{\rho_s}{\rho_w}$). The nominator in Equation 2.18 acts as a destabilizing (force) term where the denominator acts as a stabilizing (weight) term. So changing either the effective weight of the particles or the stress acting on it will affect the sediment transport rate. Two mechanisms caused by groundwater flow will be described, first a mechanism that affects the effective weight of the sediment particles and then a mechanism that affects the force on the sediment particles.

The vertical seepage force causes the sediment particles to be lifted (decreasing the effective weight) if it is upwards directed (out of the bed) and therefore enhances the mobility. If it is directed downwards (into the bed) it is increases the effective weight causing restricted mobility. The seepage force, S_{bed}, is given by

$$S_{bed} = \rho_w g \frac{\partial h}{\partial z} \tag{2.19}$$

with h the hydraulic head, which can be rewritten forcing Darcy's law

$$w = -K \frac{\partial h}{\partial z} \tag{2.20}$$

with w the vertical flow velocity (upward positive) and K the hydraulic conductivity, into

$$S_{bed} = -\rho_w g \frac{w}{K} \tag{2.21}$$

The seepage force as described in Equations 2.19 and 2.21 holds only for particles fully inside a permeable bed. Seepage force that works on the sediment particles on the surface is a factor a smaller: $S_{surface} = a S_{bed}$ and therefore Equation 2.22 turns into:

$$S_{bed} = -a \rho_w g \frac{w}{K} \tag{2.22}$$

The weight W_w, of a surfacial sediment particle is therefore

$$S_{bed} = \left(\rho_s - \rho w\right) g - a \rho_w g \frac{w}{K} \tag{2.23}$$

so whenever $\frac{w}{k} \geq \frac{(s-1)}{a}$, the effective weight of a surface sediment particle is 'negative' and the bed is fluidized. Recalling Equation 2.18, where the shields parameter is inversely related to the sediment weight, the sediment transport due to infiltration/exfiltration only is given by:

$$\frac{Q_{w/K}}{Q_0} = \left(\frac{1}{W_w/W0}\right)^{3/2} \tag{2.24}$$

where the subscript 0 stands for no vertical flow. For physically reasonable values the relative sediment weight and transport are indicated in Figure 2.8. Qualitatively, when the flow is upward sediment transport is enhanced, when the flow is downward, sediment transport is reduced.

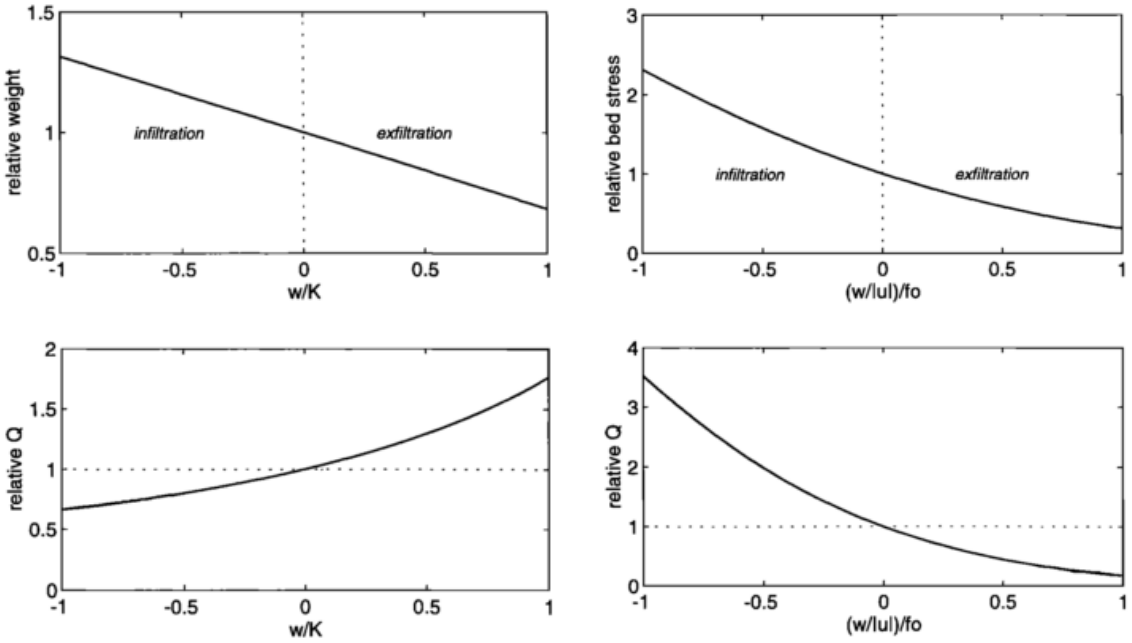

Figure 2.8: Secondary groundwater effects. The relative weight of the sediment grains during uprush and backwash(left) and the change in relative bed stress during uprush and backwash(right)

An downward flow (infiltration), besides the effects described on the relative weight, also results in streamlines closer to the bed, and an upward flow (exfiltration) results in streamlines further away from the bed. This results in a thinning (for infiltration) and thickening (exfiltration) of the boundary layer velocity profile, which in its turn affects the bed shear stress. The bed stress with vertical flow related to the bed stress without vertical flow is

$$\frac{\tau_w}{\tau_0} = \frac{\Theta}{e^{\Theta} - 1} \tag{2.25}$$

where $\Theta = c\frac{w}{u}/f_0$, f_0 a friction factor, c is a constant. Similar to Equation 2.24, for the bed shear stress influence on the transport rates:

$$\frac{Q_{w/u}}{Q_0} = \left(\frac{\tau_w}{\tau_0}\right)^{3/2} \tag{2.26}$$

and again, Figure 2.8 shows the relative bed stress and resulting relative sediment transport rates again for physically reasonable range of $(w/|u|)/f_0$. Upward flow (exfiltration) now results in a reduction of the sediment transport rate while downward flow (infiltration) results in increased sediment transport rate.

In the uprush, altered bed stress dominate, in the downwash altered bed stress effects are still dominating although a stronger compensating effect of the altered effective weight is making it less pronounced. The new relative shields parameter shows distinct asymmetry, indicating that the addition of infiltration and exfiltration processes to the sediment transport are most significant during beginning (first half) of wave uprush, in deeper swash regions, and the end of downwash. Turner & Masselink (1998) shows that combining seepage and boundary layer transport leads to 40% increasing transport during the lower swash uprush, 10% increasing transport in the mid swash uprush and 5% increasing transport in the upper swash uprush. Offshore

increasing transport rates only occur in the lower backwash swash with 5-10%. Turner & Masselink (1998). In these results gravity and suspended sediment processes have not been taking into account, also the effects of accelerating, decelerating flow and very thin flow depths on the boundary layer profile might influence the results.

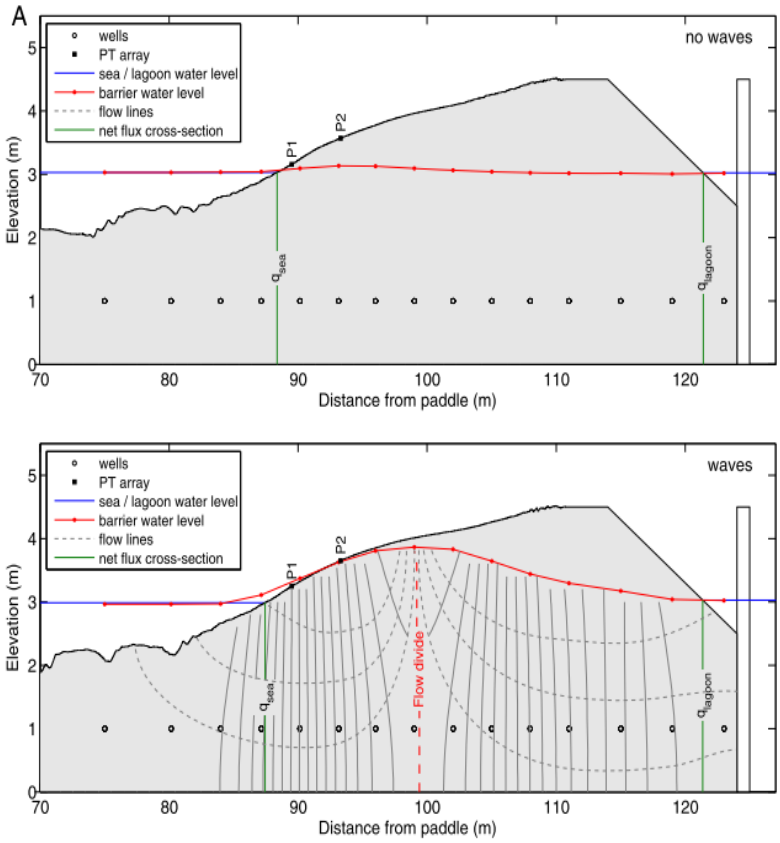

Figure 2.9: Barrier water table and equipotential lines without waves (top panel) and with waves (lower panel). Hydraulic heads are averaged over a 300 s, and contour lines are spaced at 5 cm head intervals (note that the vertical dimension is exaggerated). Image from Turner et al. (2016).

Groundwater flow measured in Bardex II It was observed that the groundwater level, flow paths, and fluxes within the beach face region of the barrier were predominantly controlled by the action of waves at the beach face, regardless of the overall seaward- or landward-directed barrier-scale hydraulic gradients Turner et al. (2016). The groundwater table before and after the wave series are shown in Figure 2.9. Instantaneous reaction of the groundwater dynamics on uprush and backwash are measured with two buried pressure sensors at different depths. The results of this and the calculated vertical in/exfiltration velocity w as calculated with formula 2.20 are shown in Figure 2.11. In the swash zone infiltration occurs in the upper swash where exfiltration happens in the lower swash, resulting in a flow circulation cell beneath the swash zone as shown in Figure 2.10.

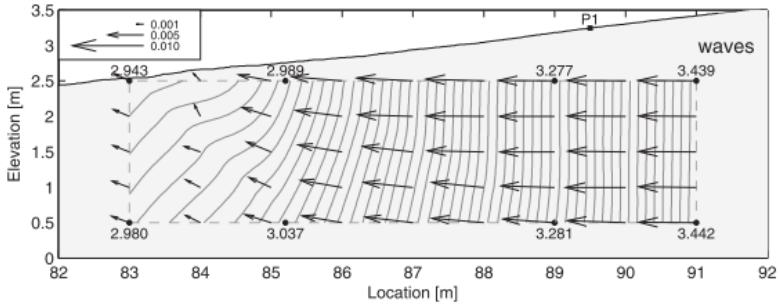

Figure 2.10: 300s time averaged hydraulic head distribution and flow under the swash zone. Image from Turner et al. (2016).

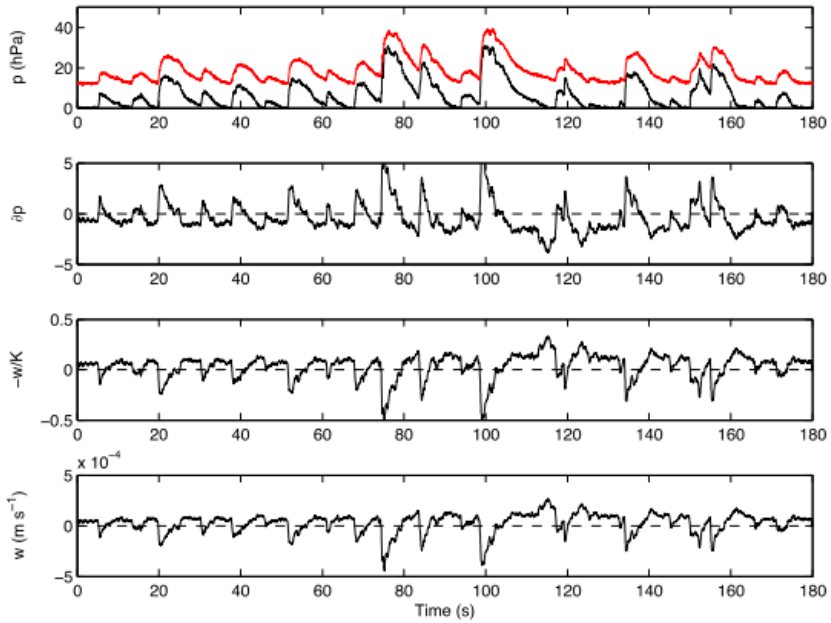

Figure 2.11: Summary of instantaneous swash infiltration-exfiltration for steady state wave conditions. negative values imply infiltration positive exfiltration. Figure from Turner et al. (2016).

2.2.4. WAVE BREAKING INDUCED TURBULENCE

Turbulence in the swash zone has four components: the energy flux is onshore directed, the uprush turbulence is bore-induced, the backwash turbulence is dominated by growing boundary layer and the Kolmogorov length scale increases towards the bed (dissipation dominant near surface) (Masselink & Puleo (2006)). Moreover, the bore advects turbulence into the seabed from the surface containing large amounts of sediment. This results in a uniform sediment distribution over the water depth for shallow flows.

Brocchini & Baldock (2008) studied the effects of turbulence on boundary layer and found that penetration of turbulence would increase stress which therefore increases the friction factor C_f. A trade off has to be made between computational expensive nonlinear shallow water equations (NSE) solving strategies or empirical relations where physical evidence is lacking and not enough processes can be included potentially. Reniers et al. (2013) studied the bore induced turbulence for an event of 10 days and therefore used critical steepness ($m_c r$) to calculate breaking induced turbulence. The fraction of turbulence that reached the bed was then included in the Shields shear stress term, Θ. The bed slope is implemented as a correction factor on the bed load transport S_b in Nielsen transport equation (Nielsen & Callaghan (2003)). The studied beach was relatively steep (1:7.5, linear profile). A result of this parametrization of bore generated turbulence is shown in Figure 2.12.

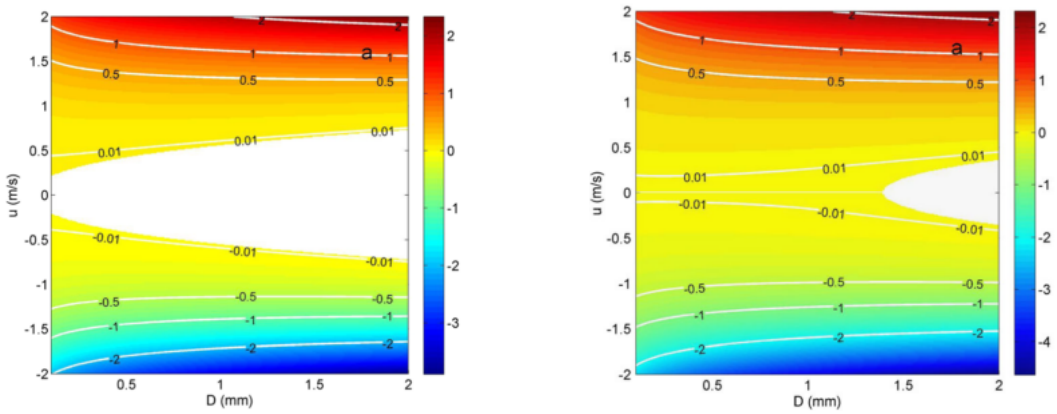

Figure 2.12: (a) Bed load sediment transport at 1m water depth as function of the cross-shore velocity and grain size diameter without wave breaking turbulence. No sediment particle motion is indicated by the white area. Color bars and contour lines represent sediment transport in m2/h. (b) Bed load sediment transport as function of the free stream velocity and grain size diameter at 1m water depth with 0.4 m2/s2 wave breaking turbulence added. Image from Reniers et al. (2013)

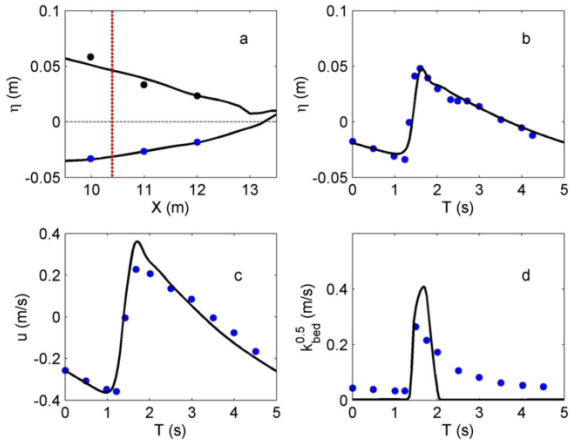

Figure 2.13: (a) Computed surface elevation envelope (solid line) compared with observations (dots). (b) Model (black line) comparison with the intra-wave surface elevation (dots) at X= 10.3 (indicated by the vertical red dashed line in Figure A1a. (c)Comparison of model (black line) and observed (dots) velocities at X= 10.3 m. (d) Comparison of model (black line) and observed (dots) turbulent near-bed kinetic energy at X= 10.3m, image from Reniers et al. (2013)

Bakhtyar et al. (2009) showed that a challenge for depth-averaged models is to represent wave breaking correctly. The velocity differences between water surface and bed level, due to the complex depth dependent hydrodynamic processes that follow from the breaking, make depth averaging complex. Correct simulation of the flow and turbulence fields around the wave breaking needs more investigating of governing hydrodynamic equations. In the Bardex experiment, Ruju et al. (2016) showed that vertical turbulence structure in the surf zone evolved from bottom-dominated (due to bed shear stress) to surface-dominated (due to wave breaking/bore generation) with an increase in the fraction of breaking waves to 50 %. In the swash zone, the turbulence was predominantly bottom-induced during the backwash and showed a homogeneous turbulence profile during uprush.

Bore induced turbulence in XBeach The turbulence options are described in subroutine waveturb which is called if $lwt = 1$, and/or if the wave averaged or bore averaged parameter settings are defined (Roelvink et al. (2015), p23).
The roller thickness increase or decay is calculated with the critical slope of the wave:

$$\frac{dz_s}{dt}_{cr} = \beta\sqrt{gh} \tag{2.27}$$

$$\text{increase}\,(h_{roller}) = dt\frac{dz_s}{dt} - \frac{dz_s}{dt}_{cr} \tag{2.28}$$

and after this calculation the control steps: $0 < h_{roller} < h$ and roller thickness of zero on dry points are executed. A source term for the turbulent kinetic energy is then calculated with Equation 2.29

$$k_{source} = g h_{roller} \beta \sqrt{gh} \tag{2.29}$$

Without turbulence advection (turbadv=none), the wave averaged turbulent energy k_{turb} is calculated with

$$k_{turb} = \left(\frac{D_r}{\rho_w} \right)^{2/3} \tag{2.30}$$

where this turbulent kinetic energy is used as an extra term to the orbital velocity $\tilde{u}$ in the calculation of sediment transport:

$$u_{rms,2} = \tilde{u} + 1.45 k_{turb} \tag{2.31}$$

The turbulence decay as described by Reniers et al. (2013) and implemented in the XBeach surf-beat model, is not implemented in the XBeach non-hydrostatic extension yet.

2.3. SUMMARY

In this chapter the findings from a literature study on the swash morphodynamics and relevant conclusions from the observations in the swash of the Bardex II experiment are summarized. Towards answering research question [RQ1] -What are relevant physical processes for the morphodynamics in the swash zone on intermediate-reflective beaches?- four processes have been determined:

- **Bed slope effects**. The bed slope effects on (relatively steep, <1:10) intermediate reflective beaches was determined as a process that could overpredict erosion.
- **Sediment response time**. The minimum sediment response time threshold to secure numerical stability in Equation 2.9 in the XBeach sediment transport formulation is high compared to the sediment response time (via fall velocity) as observed in Bardex II. The error introduced by this threshold can lead to wrong predictions of the suspended sediment concentrations or transport.
- **Groundwater**. The infiltration during uprush leads to a loss of water. The water level and velocity during the backwash afterwards are lower. This leads to a reduction in offshore transport implying that onshore transport is enhanced if groundwater effects are taken into account.
- **Turbulence**. The turbulent bore is a powerful mechanism to bring sediment into suspension. The parametrization based on Reniers et al. (2013) is implemented in XBeach surf-beat, but not yet implemented in the non-hydrostatic version of XBeach.

In Chapter 3, a modeling approach will be presented to assess the morphodynamical formulations in XBeach as described in Section 2.1.2 and the implementation and influence of the four processes described in Section 2.2 on the morphodynamical predictions of the swash zone.

3

METHODOLOGY

This thesis contains three main parts in order to answer the 4 research questions. For the first part (see Section 3.1) a simple planar bathymetry is used to study the sediment transport formulations of XBeach and the influence of the four processes described in Section 2.1.2. In the second part, the experimental results of Bardex II were used to compare the results of XBeach. The second part consists of two steps: a comparison to the total morphological response (Section 3.2.2) and an intra-swash analysis of sediment transport (Section 3.2.3). Based on the findings from the qualitative modeling on the planar beach and the comparison with measurements of the Bardex II experiment, the third part of this thesis uses a 1D Matlab sediment model which is described in Section 3.3. This model was used to test several modifications to the transport formulations as used by XBeach.

3.1. PLANAR BEACH

3.1.1. INTRODUCTION

To test the implementation of the four processes (Groundwater, Bed slope effects, sediment response time and turbulence) as described in Chapter 2 a simple steep planar beach is studied. This is mainly to exclude the influence of e.g. offshore bars or other complex geometries on the transport formulations. The bathymetry is shown in Figure 3.1. In the first subsection the reference case is described, in the subsections after that the approach for the four different processes is given.

3.1.2. REFERENCE CASE

The reference case was chosen to show the behavior of the sediment transport formulations in XBeach with inclusion of the least possible processes that could influence it. This is preferred over the default settings to prevent interaction or double counting any of the influences caused by the four processes of interest that will be studied as separately as possible. This means that the reference case is not the default XBeach settings but a simplified version. The settings that differ from the default settings of XBeach are listed in Table 3.1.

Table 3.1: Model set up reference case

Processes		
	Reference case	default
nonh	1	0
swave	0	1
gwflow	0	0
Tsmin	0.5	0.5
lwt	0	0
bedslpeffmag	NONE	ROELVINK_TOTAL
Hydrodynamics		
	Reference Case	
H(monochromatic) / H_{m0}(spectrum)	0.8 m	
T(monochromatic) / T_p(spectrum)	12 s	
D_{50}	0.000424 m	

Two different swash morphological time scales were analyzed for the reference case. The first case focuses on the details of the intra-swash sediment transport processes to gain knowledge about the absolute transports (rather than the net transport) and the position (in time and space) where several processes influence the sediment transport during one swash cycle. The second case focuses on the morphological change due to many swash cycles (net sediment transport).

For the first case, only a few (monochromatic) waves are forced in order to analyze the intra-swash sediment transport. First the maximum run-up of one swash event is determined and then the time window is set from $-1/2T_{swash}$ to $+1/2T_{swash}$ around the maximum run-up, see Figure 3.1. The model was set up in such way, that morphodynamical changes to the bed were only allowed after the start of the time window to avoid influence of the bed level change of earlier events. The wave height and period were chosen similar to the planned conditions in the accretive Bardex II experiment (see Section 3.2.2).

In the second modeling case, a longer timescale with a smaller output frequency - to control the computational time - is used in order to study the morphological response of the shoreface to a series of waves. Approximately 1000 waves are forced to obtain a morphological equilibrium in the profile. Two wave forcing conditions are used to analyze the cumulative sediment transport. A JONSWAP spectrum with $H_{m0} = 0.8m$ and respectively $T_p = 8s$ and $T_p = 12s$ is used. These are again similar wave conditions as measured in the accretive and erosive Bardex II experiment (see Section 3.2.2). These conditions are chosen to allow comparison with the Bardex II observations.

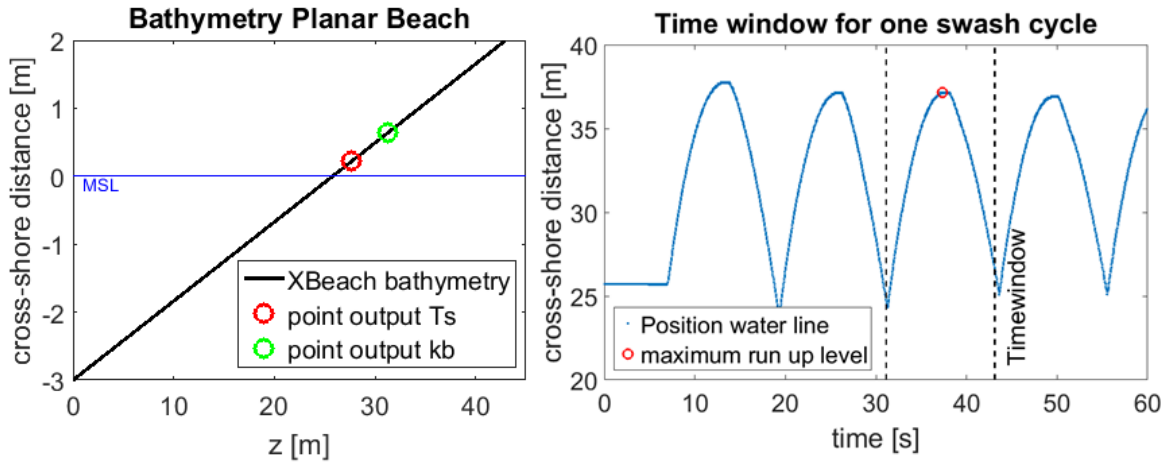

Figure 3.1: Left: Planar beach bathymetry used for reference case and analysis of processes; Right: Determination of the time window for one swash cycle, from the maximum run-up (red dot) a perod of 1/2 T_{swash} to left and right is taken.

The results of both the short and the long time scales are presented in Section 4.2. This reference case

is not 'the best we can do'. It serves purely as a reference frame for the analysis of the influence of the four processes of which the methodology will be explained in the next sections.

3.1.3. PROCESS 1: GROUNDWATER

Only one of the three effects of groundwater in/exfiltration as described in Section 2.2.3 is implemented in XBeach. Therefore only the primary effect, the infiltration and exfiltration of water into the bed (reducing the backwash volume and therefore velocity), is taken into account in the effects of groundwater on swash zone morphodynamics. According to Equation 2.20, the rate of exchange of groundwater is related to the hydraulic conductivity K. Therefore, to test the influence of the primary groundwater effect on the morphodynamics, the hydraulic conductivity was varied. To avoid the boundaries of the model domain to influence the groundwater flow in the swash zone, the domain of the model has been extended (compared to the reference case) to -3 m (depth of impermeable layer) and 87m (horizontal position landward boundary), while the shoreface characteristics (steepness of the profile, mean sea level, forcing) are kept the same as for the reference case.

Table 3.2: Model set up groundwater

Groundwater	
gwflow	1
gwnonh	1
gw0 (initial groundwater table=MSL)	0 m
aquibot (impermeable layer)	-3m
hydraulic conductivity (K)	0.01, 0.0003, 0.00005 m/s

The equilibrium groundwater table on a beach forced by waves needs sufficient time to develop after the wave action has started (the measured Bardex II equilibrium groundwater table is shown in Figure 2.9 in Section 2.2.3). Also in the model a period is included where wave forcing is switched on and the groundwater table can reach equilibrium. Therefore for the groundwater modeling cases, first the beach is forced with a long time series of waves. The development of the groundwater table is highly dependent on the value of the hydraulic conductivity K. The groundwater table development is shown in Figure 3.2 for a conductivity of $K = 0.00005$ m/s. In here it is assumed that the seepage velocity further onshore in the soil is small (i.e. the in/exfiltration processes are of much faster time scales then groundwater table development) compared to the infiltration/exfiltration velocity every wave. Therefore in this modeling study only the near-beach part of the groundwater table has to be in equilibrium. For the smallest value of the hydraulic conductivity (least permeable) this time is around 2500s of wave forcing.

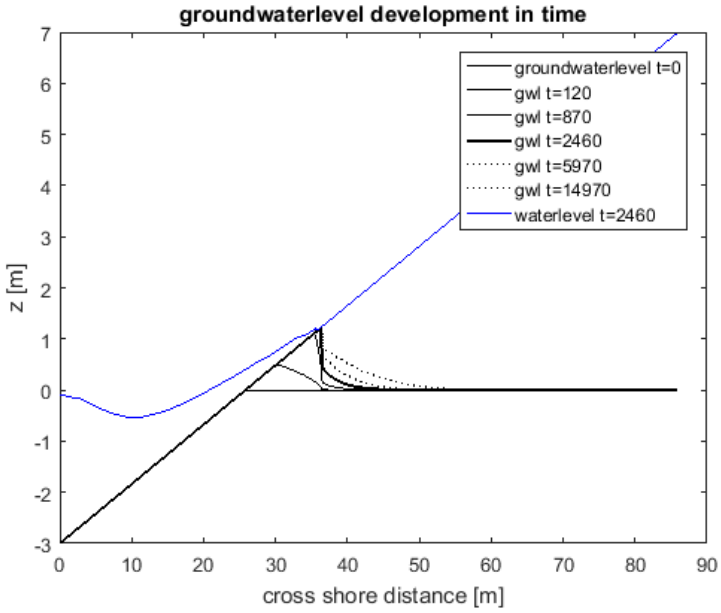

Figure 3.2: Crosssection of the groundwater table development with K_x=0.00005. Different lines represent different time since start of wave forcing.

3.1.4. PROCESS 2: SEDIMENT RESPONSE TIME

The sediment response time is a parameter dependent on the fall velocity which introduces a time lag between local velocity and sediment concentrations in the 1D advection diffusion equation (Equation 2.9). Because the sediment response time is in the denominator of Equation 2.9, a minimum response time has to be set in order to avoid the denominator to become (close to) zero which will imply steep gradients and/or numerical instability. As Equation 2.16 shows, the minimum sediment response time $T_{s,min}$ is introduced for small water depths. Swash water depths are small and therefore in parts of the swash domain the sediment response time is not calculated with the fall velocity but is set to $T_{s,min}$. The effect of the value of $T_{s,min}$ on the sediment transport and morphology was tested in four modeling cases which are described in Table 3.3. A high value means that $T_{s,min}$ is used for deeper water and a very low value means that T_s is calculated with the fall velocity for most of the domain. The results of these four cases can be found in Section 4.4.

Table 3.3: Four modeling cases for the sediment response time

Case	$T_{s,min}$ (s)
Reference case	0.5
Case 1	0.01
Case 2	0.1
Case 3	10

3.1.5. PROCESS 3: BED SLOPE EFFECTS

Bed slope effects enhance offshore transport and therefore they contribute to the erosion of the beach. The steeper the beach, the more influence the bed slope effects have on the sediment transport, as described in Section 2.2.1. Although intuitively only the bed load transport is affected by the steepness of the bed, in practice there are many processes accounted for in the bed slope correction and therefore the XBeach default is set to ROELVINK_TOTAL (the XBeach setting for bed slope effects on both suspended and bed load transport). In this study three different scenarios are modeled to assess the influence of the bed slope effects on the total transport and on the bed load transport separately. These scenarios are compared to the reference case where no bed slope effects are taken into account. An overview of the modeling cases is given in Table 3.4.

Table 3.4: Three modeling cases for the bed slope effects

Case	XBeach bed slope effect setting	Affected transport mechanism
Reference case	NONE	none
Case 1	ROELVINK_BED	bed load transport
Case 2	ROELVINK_TOTAL	bed load and suspended transport

3.1.6. PROCESS 4: TURBULENCE INDUCED BY WAVE BREAKING

As described in Section 2.2.4, sediment is stirred up by the wave breaking induced turbulence. In XBeach, this turbulence is added to the orbital velocity and together they form the $u_{rms,2}$ term in Equations 2.2 and 2.1. The parametrization of this bore induced turbulence is based on hydrodynamical parameters available in the surf-beat model. The surf-beat model uses a short wave energy balance for the wave breaking process and calculation of turbulence. However, since the non-hydrostatic version of XBeach is short wave resolving, parameters like $\tilde{u}$ and D_r are zero (because of the absence of the short wave energy balance). If turbulence advection is not taken into account (which is the default), this results in a calculation of zero turbulent kinetic energy k_{turb} (k_{turb} in XBeach). To be able to test the influence of turbulence on the sediment transport and morphology the XBeach source code is adapted in the following way:

In Equation 2.30 the turbulent source term (Equation 2.29) is added leading to Equation 3.1.

$$k_{turb} = \left(\frac{D_r}{\rho_w} + k_{source}\right)^{2/3} \tag{3.1}$$

The parameter β (default value = 0.1), representing the critical wave steepness before breaking occurs, is present in Equation 2.27 where a larger value leads to less turbulent kinetic energy. However, β is also present in the turbulence source term k_{source} where a larger value leads to more turbulent kinetic energy. This opposite influence that β has on the turbulent kinetic energy makes it impossible to use as an turbulent enhancing factor. Therefore a new turbulence calibration factor k_{gain} has been added to the XBeach source code. This is done by changing the expression for the turbulent kinetic energy k_{turb} (Equation 2.30) to Equation 3.2.

$$k_{turb} = k_{gain} g \beta \sqrt{gh} \tag{3.2}$$

With these two modifications to the source code, the effect of the turbulence induced by wave breaking on the morphodynamics of the planar beach was studied. The turbulence in XBeach is included by switching on the long wave turbulence (lwt=1).

The XBeach modeling cases as used for the result are shown in Table 3.5. The results of the modifications in the source code and the results of the assessment of the influence of enhanced turbulent kinetic energy on the morphodynamics of the planar beach are presented in Section 4.6.

Table 3.5: Turbulence model set up

Case	lwt	k_{gain}
Reference case	0	-
Case 1	1	1
Case 1	1	2
Case 1	1	10
Case 1	1	100

3.1.7. SUMMARY PLANAR BEACH

This section presented a modeling framework to assess the sediment transport formulations in XBeach. First a reference case is set-up, after which the influence of bed slope effects, the minimum sediment response time, groundwater effects and the wave breaking induced turbulence are assessed in separate modeling cases. The results of the reference case and four processes cases are presented in Section 4.

3.2. COMPARISON TO OBSERVATIONS FROM BARDEX II

3.2.1. INTRODUCTION

Observations of swash morphodynamical processes during the Bardex II experiment were used in two ways to assess the performance of XBeach. In the first part the observed morphological response of an erosive and an accretive experiment were compared to the modeled morphological response using the default settings of XBeach. This gave an insight in the current performance of the morphodynamical predictions of XBeach non-hydrostatic on intermediate reflective beaches. In the second part, observations of the intra-wave hydrodynamics and sediment transport processes in two sub-experiments, one erosive and one accretive, were compared to the results obtained with XBeach.

3.2.2. BARDEX II TOTAL MORPHOLOGICAL RESPONSE

Bathymetry During experiments A4 and A8 of Bardex II, respectively erosive and accretive wave steering signals were made for a water depth of 3m. Both A4 and A8 consists of five consecutive wave forcing time series resulting in sub experiments A4_01 to A4_05 and A8_01 to A8_05. The measured bathymetries before the first sub experiment and after the last sub experiment (the total morphological response of experiment A4 and A8) are shown in Figure 3.3. The initial measured bathymetry of experiment A4 and A8 are used to create the bathymetry for the XBeach model. The bottom of the flume and the toe of the bar were made of concrete, therefore they form an impermeable layer in the XBeach model. To complete the XBeach bathymetry, the CAD drawing of the planned profile as shown in Figure 3.4 is used for the part from the end of the concrete toe to the beginning of the profiler measurements and for the part from the end of the profiler measurements to the landward lagoon boundary. The result is shown in Figure 3.5.

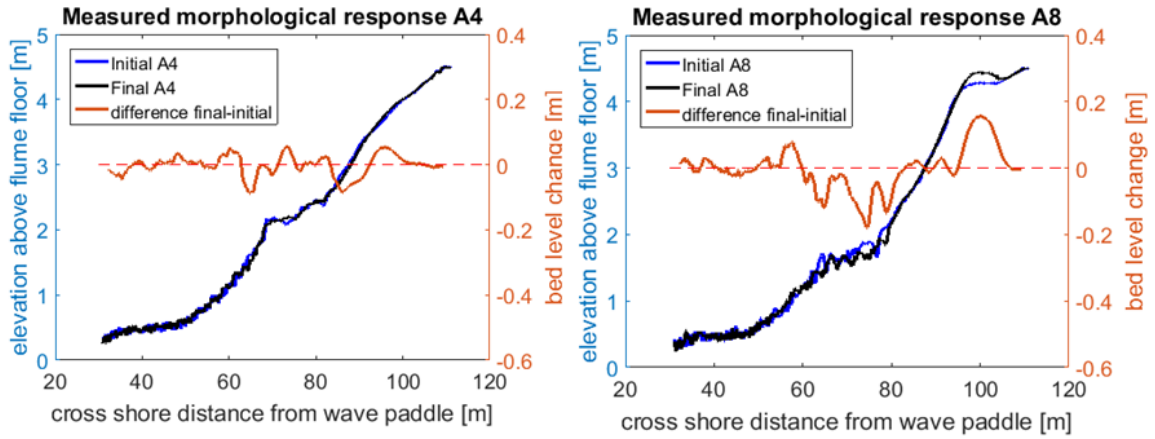

Figure 3.3: Morphological response as obtained by the profiler (bathymetry measuring instrument) during erosive (A4) and accretive (A8) wave conditions.

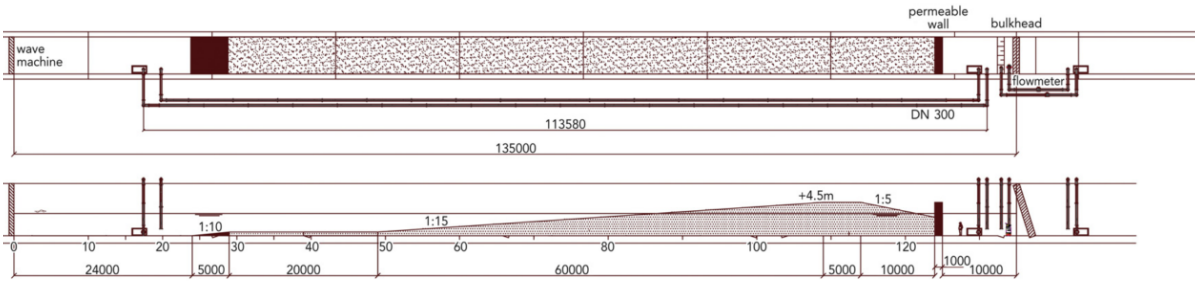

Figure 3.4: CAD drawing of experimental set-up in the Delta Flume during Bardex II experiment, showing plan view and longitudinal section of the flume, distances in mm. Figure from Masselink et al. (2016)

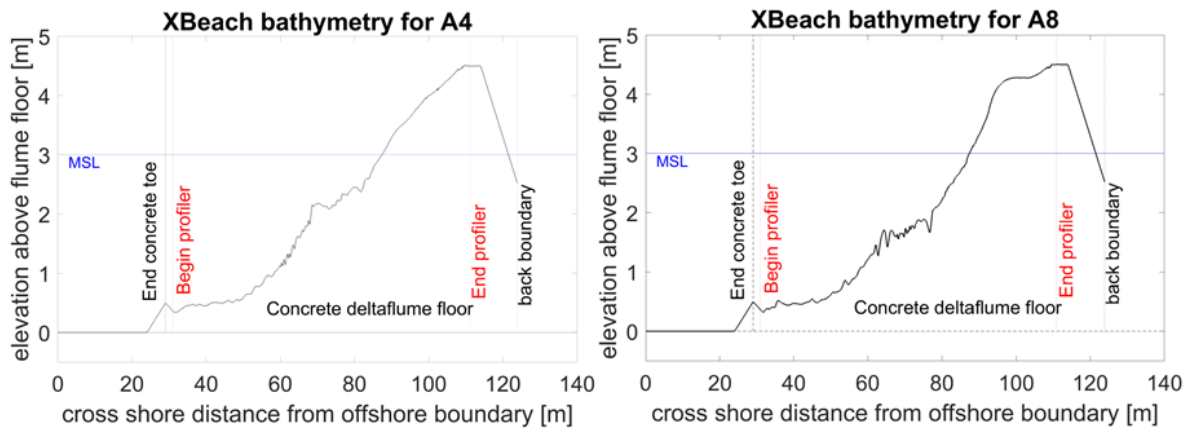

Figure 3.5: Bathymetry (black solid line) used for experiments A4 (left) and A8 (right) with mean sea level (blue line), concrete toe and floor (impermeable layers, black dotted lines) and beginning and ending point of the profiler (red dotted lines)

Wave forcing The Bardex II experiment is forced with a JONSWAP wave steering signal of which the planned wave conditions are given in Table 3.6. A pressure sensor measured the wave conditions for each sub experiment at cross-shore position x=36.2 m. The pressure data were corrected for depth attenuation using linear theory and a frequency cut-off based on the peak frequency and the water depth, but the signal was not separated into the incoming and outgoing signal. Significant wave height was determined as four times the standard deviation of the time series Masselink et al. (n.d.). The measured conditions are given in Table 3.7. A JONSWAP spectrum was created by XBeach at the offshore boundary using these measured spectral values of the five sub-experiments of A4 and A8.

Table 3.6: Planned wave conditions for Bardex II experiment A4 and A8 with sea and lagoon water levels h_s and h_l, respectively. JONSWAP spectrum wave characteristics are defined by significant wave height H_s and peak wave period T_p. Table adapted from Masselink et al. (2013)

Test	H_s**(m)**	T_p**(s)**	h_s**(m)**	h_l**(m)**	T_{test}**(min)**
Test series A: Beach response to varying wave conditions and different lagoon levels; no tide					
A4	0.8	8	3	1.75	200
A8	0.6	12	3	1.75	200

Table 3.7: Measured wave conditions for all sub experiments of A4 and A8 from Bardex II, with sea and lagoon water levels h_s and h_l, respectively. Jonswap spectrum wave characteristics are defined by significant wave height H_s and peak wave period T_p. Data from Masselink et al. (n.d.)

Test	**Start time**	**Stop time**	H_s**(m)**	T_p**(s)**	h_s**(m)**	h_l**(m)**
Test series A4: Erosive experiment; no tide						
A4_01	10:14:10	10:41:09	0.87	8.00	2.98	1.75
A4_02	11:20:03	11:48:23	0.88	8.00	2.97	1.74
A4_03	12:13:20	12:41:29	0.86	7.88	3.01	1.73
A4_04	13:07:18	13:35:22	0.87	7.88	3.00	1.73
A4_05	14:07:53	15:05:29	0.84	8.39	3.00	1.73
Test series A8: Accretive experiment; no tide						
A8_01	09:03:35	09:32:18	0.78	12.80	2.98	1.75
A8_02	10:08:00	10:36:46	0.77	13.13	2.95	1.76
A8_03	11:06:25	11:35:03	0.76	12.80	2.99	1.76
A8_04	12:01:20	12:29:55	0.74	12.80	2.99	1.77
A8_05	14:37:40	14:55:18	0.75	12.80	2.96	1.75

Model set-up The focus of this XBeach model set-up is to compare the modeled with the measured morphological response of the beach. In the previous section a reference case is described for the planar beach

(see Section 3.1). This reference case does not include groundwater effects, bore induced turbulence and bed slope effects. The reference case is the first case that will be also run with the bathymetry as shown in Figure 3.5. The second case that was studied is a XBeach default case. Groundwater effects were taken into account using the measured hydraulic conductivity from Bardex II. The bed slope effects are taken into account using the XBeach default option: ROELVINK_TOTAL (see 4.5). The turbulence is taken into account (see 3.1) by using the first modification of the turbulence formulations as described in Section 3.1 but turbulence is not extra enhanced (k_{gain}=1). These two cases are summarized in Table 3.8.

3.2.3. BARDEX II INTRA-SWASH ANALYSIS

Bathymetry A shorter model domain is used for the intra-swash analysis. The bathymetry for the XBeach model was based on the measured profiles of sub-experiments A4_03 and A8_03. As can be seen in Figure 3.6, during the two sub-experiments the measured morphological response is small. Therefore morphological changes in the model are not taken into account for the intra-swash analysis (XBeach parameter morphology=0). The offshore boundary for the model domain was at a 72.5 m cross shore position. From there the measured bathymetry is followed until the crest of the bar (the end point of the profiler instrument). From the crest of the bar to te lagoon landward boundary the bathymetry is similar to the morphodynamical set-up. The total model domain for the intra-swash analysis is shown in Figure 3.7.

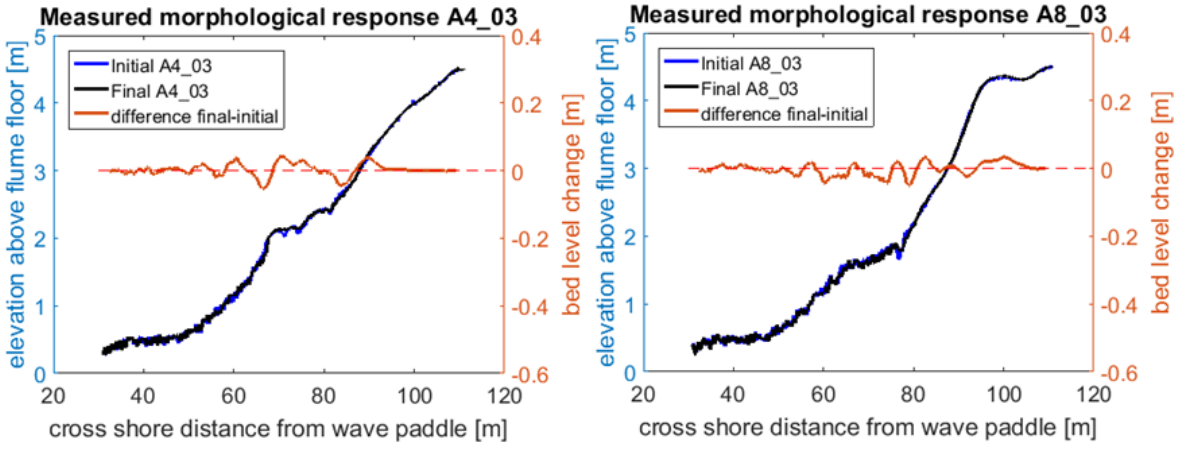

Figure 3.6: Morphological response as obtained by the profiler of erosive sub-experiment (A4_03) and accretive sub-experiment (A8_03) wave conditions.

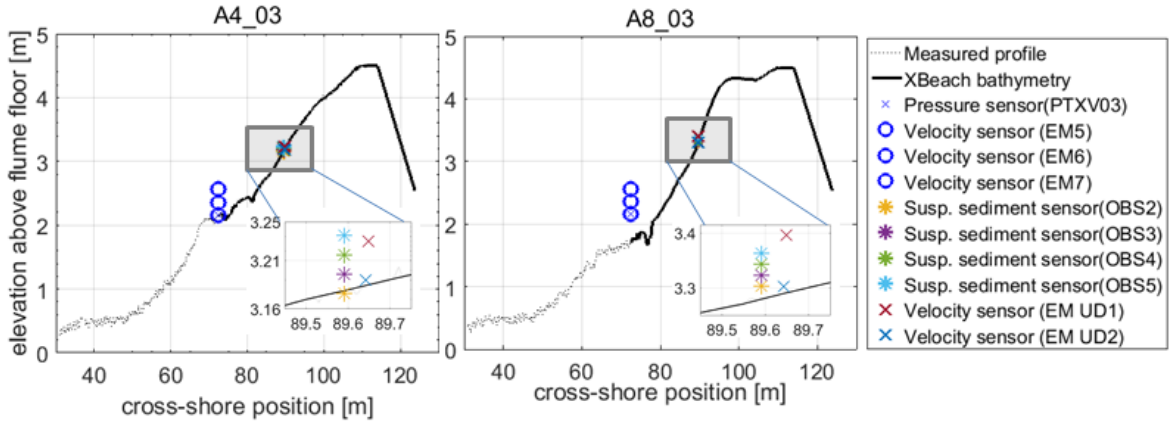

Figure 3.7: Overview of measurement instrument position and the bathymetry (solid black line) based on the measured initial bathymetry (dotted black line) of A4_03 (left) and A8_03 (right). The model domain stretches from the blue circles (where boundary conditions time series are measured) to the lagoon landward boundary. The enlarged box shows the cross shore position and elevation above the bed of the sensors used for the intra-swash analysis of velocity and sediment concentrations.

Wave forcing To allow for detailed comparison of the model results with the measured values, the wave forcing of the model should be the same as the forcing of the Bardex II sub-experiments on a scale of single waves. When the observed wave time series are used to force XBeach, a one to one comparison between the hydrodynamics (uprush/downwash velocities, run up etc.) of modeled and measured swash events can be made. Therefore, instead of forcing with spectral values (T_p, H_{m0}) which were used as forcing for the comparison of the morphological changes, for the intra-swash analysis measured wave time series were used to force XBeach. It is more work-intensive to prepare the measured time series of water level and velocity as a boundary condition, therefore only one sub-experiment of both A4 and A8, A4_03 and A8_03 are used as representative cases for the whole A4 and A8 experiment respectively. The time series of pressure sensor PTXV03 (blue cross in Figure 3.7) was transformed to a water level time series, see Figure 3.8 and velocity time series (from EM5,EM6 and EM7, blue circles in Figure 3.7) were used to determine a time series of depth average velocity. The depth average velocity is determined from the three EM sensors. The velocities measured at different elevations above the bed are very similar as can be seen in Figure 3.9. Therefore the depth averaged velocity is taken as the mean value of the three measurements.

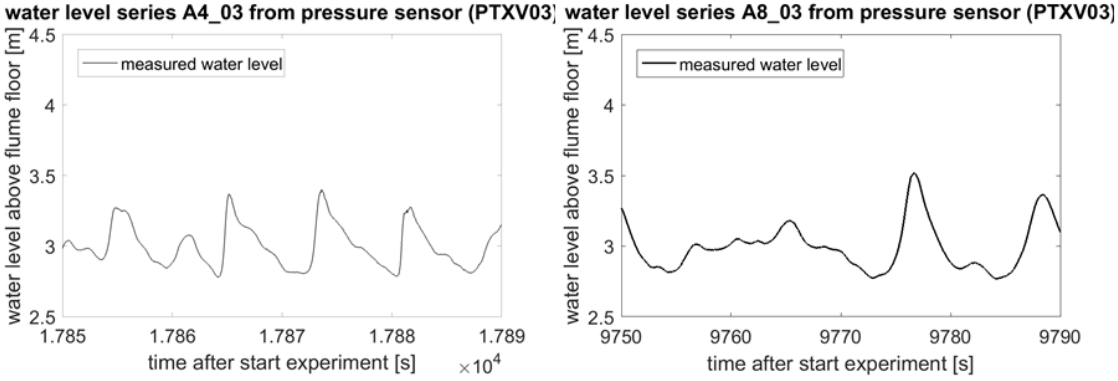

Figure 3.8: Water level obtained with the pressure from sensor PTXV03 (see Figure 3.7 for position of sensor).

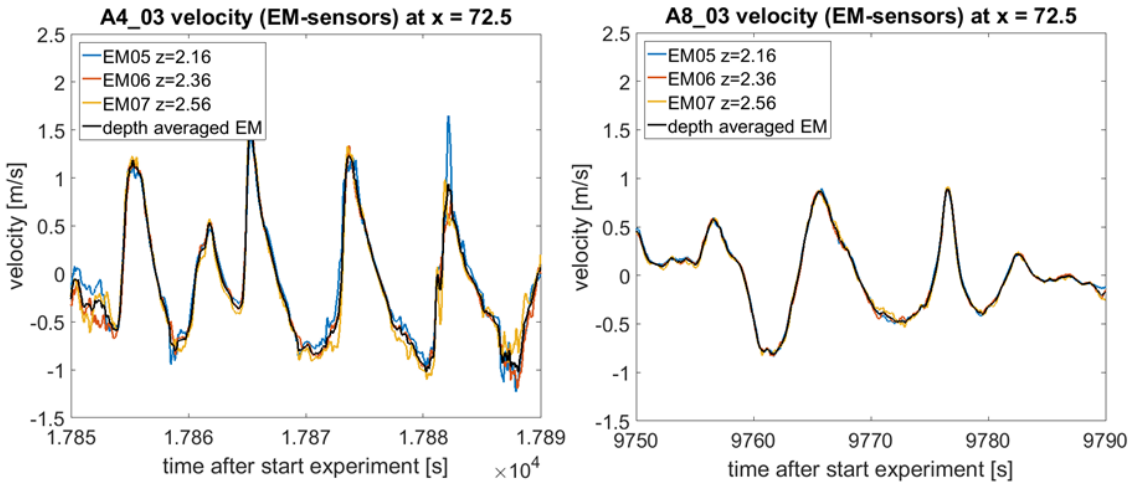

Figure 3.9: Colored lines show the velocity from the three EM sensors at different elevation above the bed and black line shows the depth average velocity (see Figure 3.7 for position of sensors).

The velocity and water level sensors measured both incoming and outgoing wave signals. Only the incoming waves should be used in the forcing time series at the XBeach offshore model boundary. Therefore the signal was decomposed into an incoming and outgoing water level time series and velocity time series according to Guza et al. (1985). The result of the decomposition for A4_03 and A8_03 for the same fragment of the time series as Figure 3.9 and 3.8 is shown in Figure 3.10. The incoming velocity and water level series resulting from the decomposed measured time series at x = 72.5 m are used as forcing for XBeach.

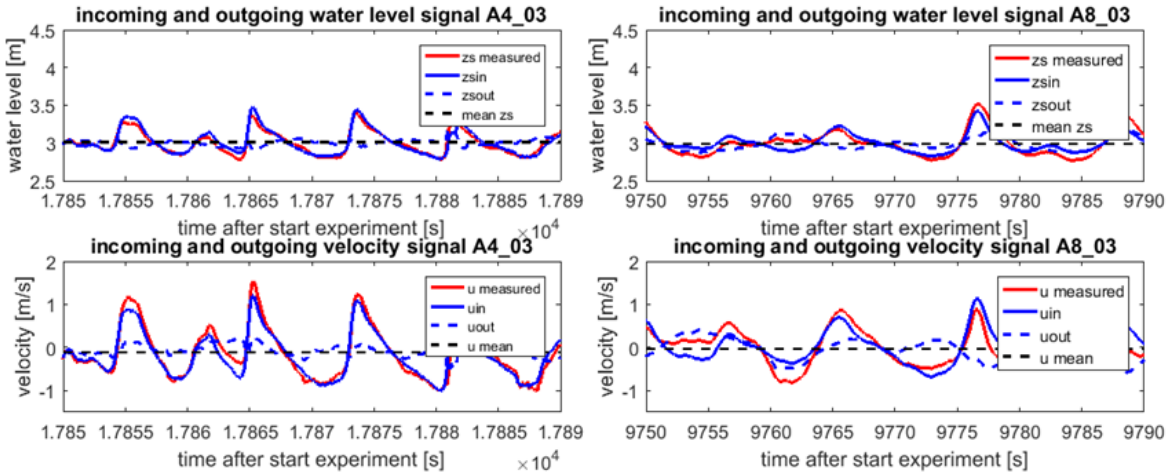

Figure 3.10: Incoming and outgoing waves split according to Guza theory for experiment A4(left) and A8(right).

Model set-up The modeled velocity, water levels and sediment concentrations were compared to the observations of Bardex II. The observations were made at cross shore position x=89.6m (see the enlarged box in Figure 3.7). The three model cases that are compared are the XBeach default case, one case with enhanced groundwater infiltration (by means of a higher hydraulic conductivity K) and one case with enhanced wave breaking induced turbulence (by means of k_{gain}). An overview of the settings is given in Table 3.6.

3.2.4. SUMMARY BARDEX II

The model set up and measurements used to compare observations from experiment A4 and A8 from Bardex II to the results of XBeach non-hydrostatic are explained in this section. In Section 5, the results of the com-

parison between the observed and modeled morphological response and the results of the intra-swash analysis are presented.

Table 3.8: Measured Bardex II sediment properties used for the XBeach Model setup for the morphological response and intra-swash comparison to Bardex II experiment A4 and A8.

Measured sediment properties Bardex II	
D_{50}	0.424 mm
D_{90}	0.903 mm
Hydraulic conductivity (K)	0.0008 m/s

Morphological response					
JONSWAP spectrum of measured T_p and H_{m0}					
Case	Morph. changes	$T_{s,min}$	Groundwater effects (Hydraulic conductivity K)	Bed slope effects	Turbulence (k_{gain})
Reference case	on	0.5 s	off	NONE	off
XBeach default	on	0.5 s	on (K=0.0008 m/s)	ROELVINK_TOTAL	on (k_{gain}=1)

Intra-swash analysis					
Measured time series surface elevation and water level at x=72.5 m					
Case	Morph. changes	$T_{s,min}$	Groundwater effects (Hydraulic conductivity K)	Bed slope effects	Turbulence (k_{gain} value)
XBeach default	off	0.5 s	on (K=0.0008 m/s)	ROELVINK_TOTAL	on (k_{gain}=1)
Enhanced groundwater	off	0.5 s	on (K=0.01 m/s)	ROELVINK_TOTAL	on (k_{gain}=1)
Enhanced turbulence	off	0.5 s	on (K=0.0008 m/s)	ROELVINK_TOTAL	on (k_{gain}=50)

3.3. MATLAB MODEL

3.3.1. INTRODUCTION

In the last part of the thesis a 1D sediment transport model in Matlab was used to study different modifications to the two sediment transport formulations (see Section 2.1.2). This point-model calculates the equilibrium sediment concentrations with the same transport formulations as XBeach, with a time series of local water depth and cross-shore velocity as input parameters and suspended sediment transport as output. Sediment advection and bed level change can not be calculated with this model, since only one point in the cross-shore domain is assessed and the bed level change is the result of spatial gradient of sediment transport. The time lag due to the sediment response time is included in the Matlab model. This analysis consists of three parts for both of the in XBeach available transport formulations (Van Thiel-Van Rijn and Soulsby-Van Rijn), see Section 2.1.2. The first part is the comparison between using measured (in Bardex experiment A8) and modeled water depth and velocity time series as input for the sediment transport formulations. In the second part, the decomposition of the velocity in a mean and a fluctuating part in the sediment transport formulations was studied. In the last part, the influence of the possibility of separate calibration of turbulent kinetic energy in the transport formulation is assessed.

3.3.2. MEASURED VERSUS MODELED HYDRODYNAMICAL FORCING

The approach of the Matlab model is to first test the effect of substitution of the modeled time series of water depth and cross shore velocity (used by XBeach locally as input for the sediment transport formulations) with the Bardex II measured time series at the same cross-shore location. For this, the sediment concentrations calculated with the measured velocity time series are compared with the sediment concentrations calculated with the modeled velocity time series at x=89.6m. Section 5.3 describes the determination of the measured

depth average velocity and water level for Bardex II experiment A8. The modeled and measured time series were synchronized using the arrival of the bore. The measurements of velocity and water level have gaps in the time series at the dry intervals of the sensor. The water level sensor is positioned approximately 6 cm above the bed. Therefore when the water depth is smaller than 6 cm, no velocity will be measured and therefore no sediment transport will be calculated. To obtain a fair comparison with XBeach, the modeled time series were also only taken into account at intervals where the water level was above the threshold level of 6 cm. Figure 3.11 shows the results of applying the threshold water depth.

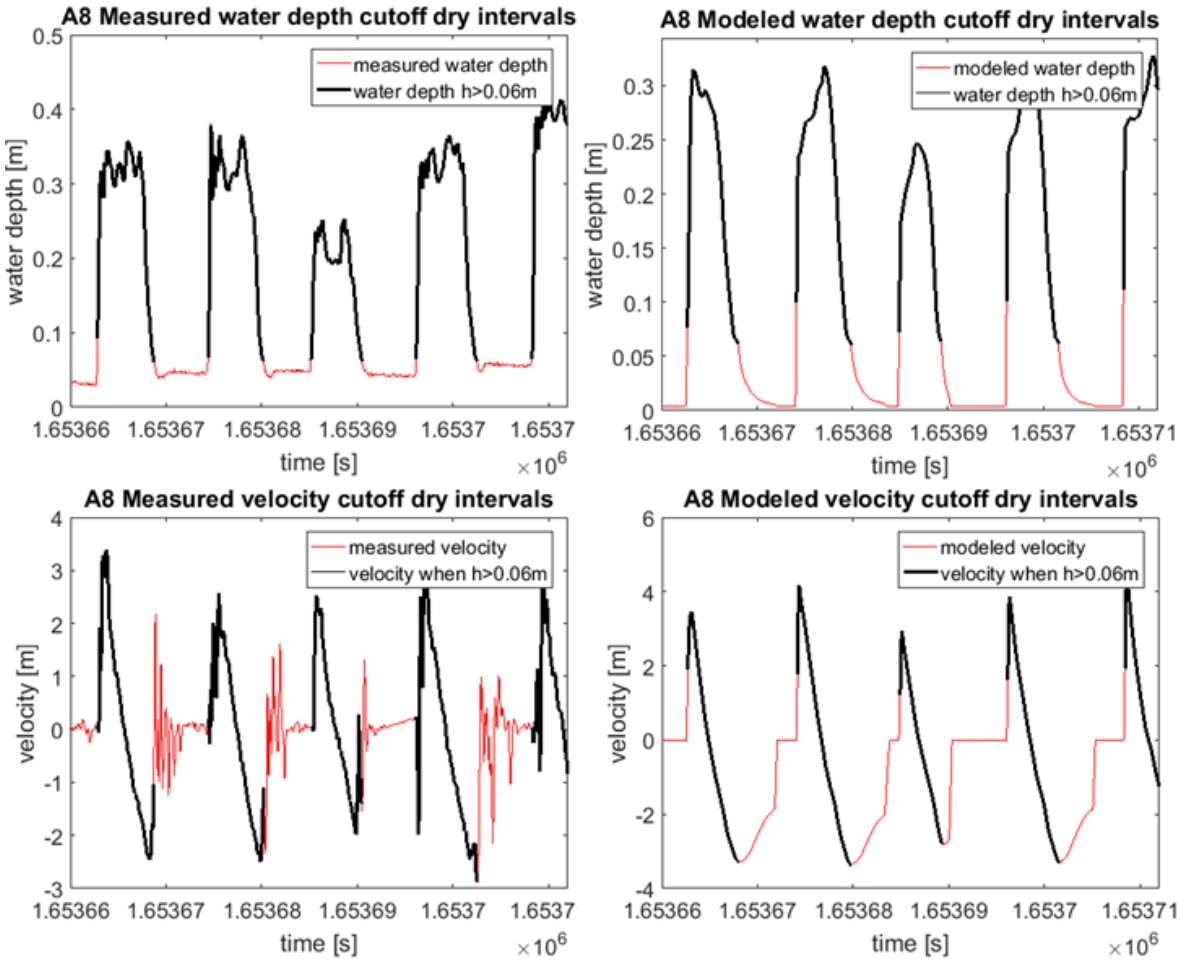

Figure 3.11: Measured and modeled water depth and velocity time series (red) and after applying cutoff depth (black)

3.3.3. DECOMPOSITION OF MEAN AND FLUCTUATING PART OF VELOCITY IN TRANSPORT FORMULATIONS

The XBeach sediment transport formulations (see Equation 2.1) originate from the surf-beat version of XBeach and are based on the division of the velocity in a flow part (u) and a fluctuating part ($u_{rms,2}$). As described in Equation 2.31 $u_{rms,2}$ contains the orbital velocity and the turbulent kinetic energy at the bottom. In the non-hydrostatic extension of XBeach, the short waves are resolved and the velocity u now is the total depth averaged velocity under long and short waves together. The orbital velocity $\tilde{u}$ is zero over the whole domain due to the absence of a wave energy balance leaving $u_{rms,2}$ only with the turbulence term. The effect of this is that the velocity term in the transport equation have been switched around as Figure 3.12 shows for the bed load transport term in Soulsby-van Rijn (but the same principle holds for suspended transport and van Thiel-van Rijn).

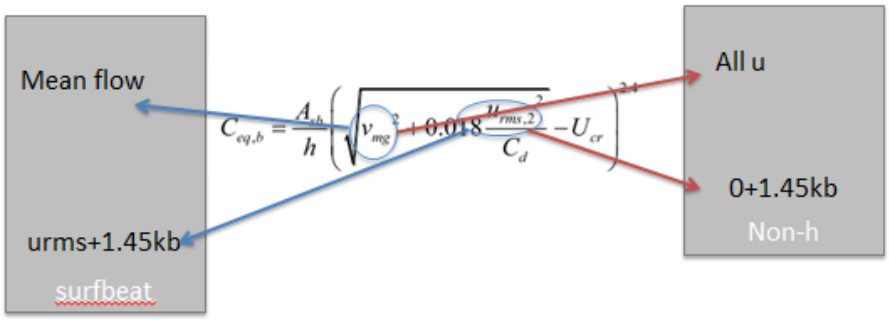

Figure 3.12: Difference of origin of velocity terms used in Equation 2.1 for the surf-beat (left box) and non-hydrostatic (left box) version of XBeach.

Two steps were performed to test the decomposition in the non-hydrostatic version. First the non-hydrostatic velocity was considered to be the fluctuation part, resulting in Equation 3.3 for van Thiel-van Rijn.

$$C_{eqs} = \frac{Ass}{h}\left(\sqrt{0 + 0.64\left(u^2 + 1.45k_{turb}\right)} - u_{cr}\right)^{2.4} \tag{3.3}$$

In the second step the velocity is averaged over 25 seconds, to allow for the calculation of a mean flow and a fluctuation part. The resulting mean flow is subtracted from the non-hydrostatic velocity for the fluctuation part, see Equation 3.4.

$$u = \bar{u} + \tilde{u} \tag{3.4}$$

$$C_{eqs} = \frac{Ass}{h}\left(\sqrt{\bar{u}^2 + 0.64\left(\tilde{u}^2 + 1.45k_{bed}\right)} - u_{cr}\right)^{2.4} \tag{3.5}$$

With this two new equations the sediment concentrations and following transports were calculated with the Matlab model.

3.3.4. SEPARATE CALIBRATION OF TURBULENT KINETIC ENERGY

The turbulent kinetic energy at the bed k_{turb} is an important source of onshore sediment transport. In the current transport formulations, both for van Thiel-van Rijn as Soulsby-van Rijn k_{turb} is calibrated together with the fluctuating part of the velocity. To study the effect of enhanced turbulent kinetic energy a separate calibration term was introduced in the transport formulations, see Equation 3.6 for van Thiel-van Rijn (similar for Soulsby-van Rijn).

$$C_{eqs} = \frac{Ass}{h}\left(\sqrt{\bar{u}^2 + 0.64\tilde{u}^2 + k_{gain}k_{turb}} - u_{cr}\right)^{2.4} \tag{3.6}$$

3.3.5. SUMMARY MATLAB MODEL

With the 1D sediment transport Matlab model improvements of the transport formulation will be tested for both the van Thiel-van Rijn as the Soulsby-van Rijn sediment equations. The measured hydrodynamics is used to force the model, the velocity is decomposed into a flow and fluctuating part and the turbulent kinetic energy is calibrated separately. The results of the Matlab model of this three cases are presented in Chapter 6.

4

RESULTS PLANAR BEACH

4.1. INTRODUCTION

In Chapter 2 all the equations are given used to calculate the bed level change caused by wave action on the beach. The key parameters, local velocity and water depth, are influenced by several physical processes. Besides these processes, sediment properties like the grain size and the hydraulic conductivity influence the transport. At last, there are calibration factors and numerical stabilizing factors that should not influence the physics significantly but especially in the extremely shallow water of the swash could start to play a significant role. These three types of influences are studied and the processes and model set-up for these is discussed in Chapter 3. The modeling framework consists of two model set-ups. A planar beach will be used to study the very detailed influence of different parameters and processes for one swash cycle and also the morphological change after a time series of wave impact, excluding the effect of complex geometries in the results.

The results of the modeling set-up as presented in Section 3.1 will be presented and discussed in this section. The calculations XBeach non-hydrostatic performs to determine the bed level change due to sediment transport which is calculated from the sediment concentrations are explained in Section 2.1.2. The results of these computations without the influence of the processes described in Section 2.2 will be presented in Section 4.2 which will then be used as a reference case in the analysis of the sediment response time (Section 4.4), the effect of groundwater infiltration (Section 4.3), bed slope effects (Section 4.5) and the influence of bore induced turbulence on the sediment transport (Section 4.6).

4.2. REFERENCE CASE

Introduction To have a reference for the analysis of different swash processes case will be studied, where the physical processes that were assessed later are excluded from the model set-up. Although some of the processes like bed-slope effects, turbulence, or groundwater effects are proven to (or likely to) give more realistic results, they are not taken into account in the reference case. Therefore this scenario should not be seen as 'the best we can do now' but as a tool in the analysis of the effect of the addition of different physical processes.

Total morphological response The final measure of morphodynamics is the bed level change. To investigate the effect of a longer duration forcing the linear beach is exposed to a JONSWAP spectrum consisting of approximately 1000 waves with T_{rep} = 12 of which the results is shown in Figure 4.1. The Bardex II beach was observed to be accretive under 12s waves with a beach profile of similar steepness.

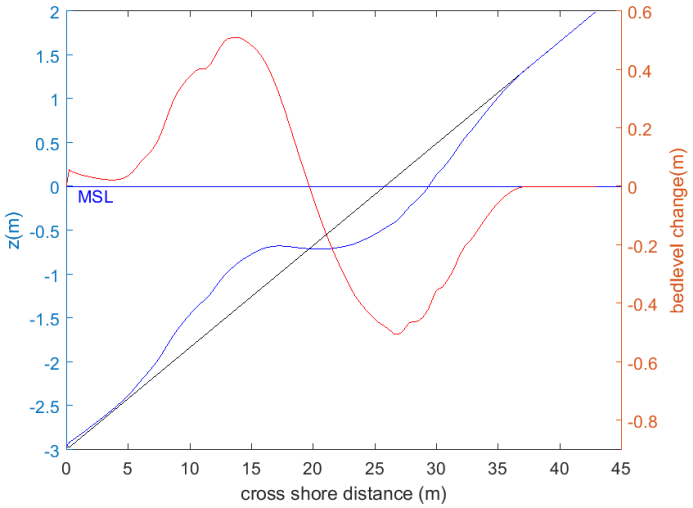

Figure 4.1: Initial (black) and final (blue) profiles and bed level change (red) after 1000 waves with $H_{m0} = 0.8$ and $T_{rep} = 12$

As Figure 4.1 shows, the morphological response of the reference case is to erode in the upper swash and to deposit this sediment further offshore. Around the water line the beach is steepening. In the next paragraph, more details of the sediment transport ar discussed.

Intra-swash analysis The details of the modeling set up for intra-swash analysis can be found in Chapter 3. In Figure 4.3, the bed level change over one swash cycle (determined according to Figure 3.1) is shown. The total transport shows similar behavior as the response to 1000 waves, erosion in upper swash and deposition in de lower swash. Two visualizations of the sediment transport processes will be used to analyze the results of the reference case, and later to compare with the results of the different added processes. First, the cross section of the profile gives information about the morphological change after one swash cycle, as schematically visualized in the left panel of Figure 4.2. However, when analyzing where spatially in the swash and at which moment during the cycle the transport and bed level changes apply, a '1D' x,t diagram as in the right panel of Figure 4.2 will be used. The x,t diagram allows for detailed intra wave analysis of the swash processes.

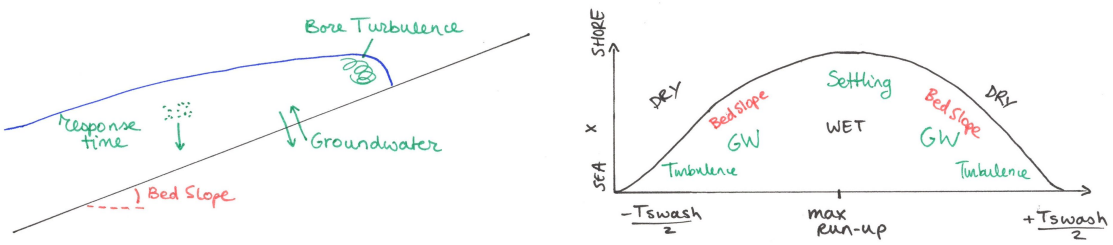

Figure 4.2: Schematic visualisation of the two methods of analysis.

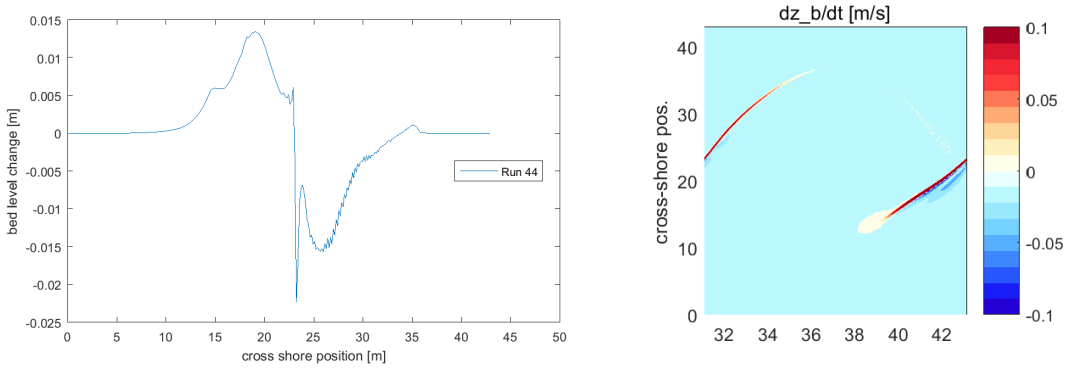

Figure 4.3: Reference case bed level change after one swash event (left) and x,t diagram for rate of bed level change during that swash event.

To analyze the contribution to the total bed level change caused by sediment transport, a difference between suspended sediment transport and bed load transport is made. The bed level changes due to suspended sediment transport and bed load transport and the total bed level change are shown in Figure 4.4 for the profile cross shore (left panel) and the x,t diagrams (right two panels). Remarkable in the modeled sediment transport is the small contribution of the bed load transport to the total morphological change. Suspended transport is expected to be dominant in the uprush, but bed load transport is expected to be in the same order of magnitude and even dominate during backwash which is not observed in the model results.

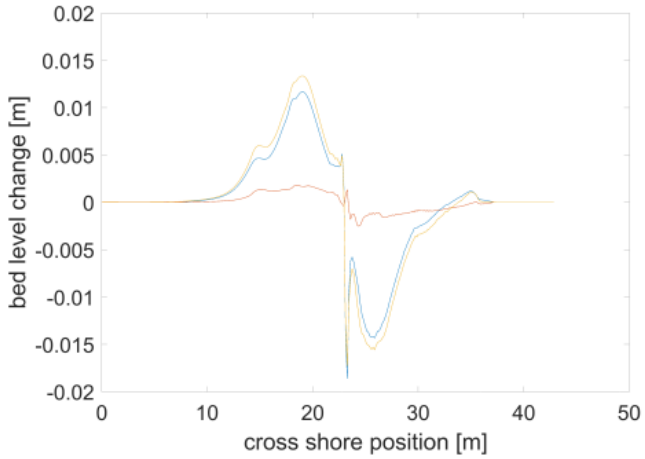

Figure 4.4: Reference case bed level change (yellow line) after one swash event divided in bed load (red line) and suspended transport (blue line) contributions

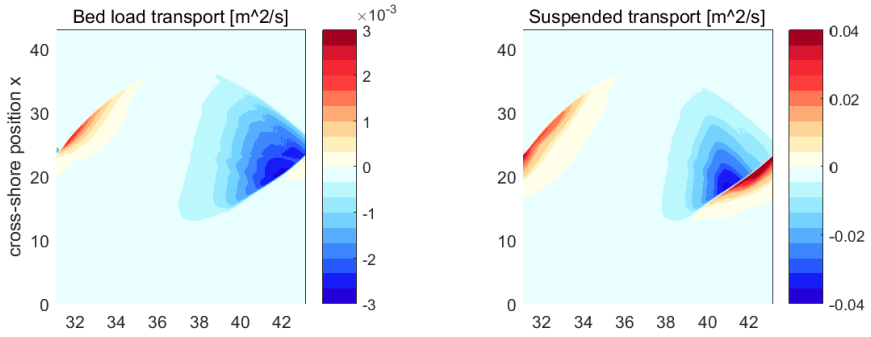

Figure 4.5: x,t diagram for bed load transport(left) and suspended transport(right)

Conclusions Reference Case Figure 4.1 clearly shows that, as was expected for the reference case, without any onshore enhancing processes included in XBeach, the beach will erode under conditions that expected to generate accretion. The suspended sediment transport is much stronger then the bed load transport and the majority of the bed level change occurs under the bore. In the next four sections the influence of bed slope effects, groundwater effects, sediment response time and bore generated turbulence on the morphological response and sediment transport processes will be discussed.

4.3. GROUNDWATER

Introduction In Section 2.2 is explained how the primary groundwater effects influences (mostly) run down velocity and therefore the balance between uprush and backwash sediment transport. The expected effect is that the backwash velocity reduces compared to the uprush velocity and therefore onshore transport is enhanced. In that same section, the equations regarding infiltration of swash water in the beach are explained and the results are shown here. In nature, but also in XBeach, it takes time before the groundwater adjusts to the waves. As shown in Section 2.2, sufficient equilibrium is reached after 2500 s which will be the start time of the groundwater modeling on the planar beach. The groundwater tables of every studied hydraulic conductivity is shown in Figure 4.6.

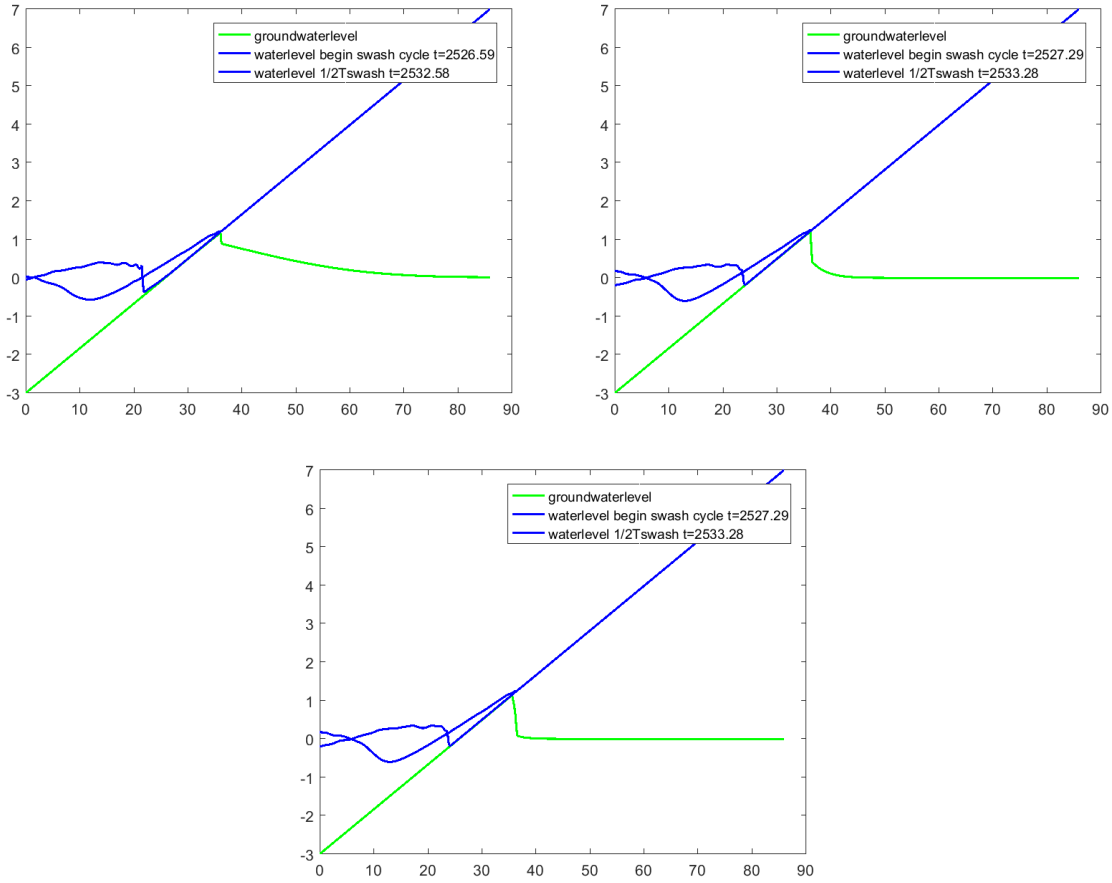

Figure 4.6: groundwater development after 2500 seconds for $K_x = 0.01, 0.0003, 0.00005 m/s$, for scale imagination, the water levels of the start and half swash cycle are plotted in blue.

Total morphological response The expected morphological response of the beach to groundwater infiltration is not very visible in the total morphological response shown in Figure 4.7. The expected values of the hydraulic conductivity for D50=0.42 are around 10^{-4}. For those range of hydraulic conductivity XBeach calculates no real change in the bed level. Taking an extremely permeable value $K_x = 0.01$ (run 59) which is a value close to gravel conductivity, there is a strong effect on the morphological response resulting in strong accretion in the upper swash.

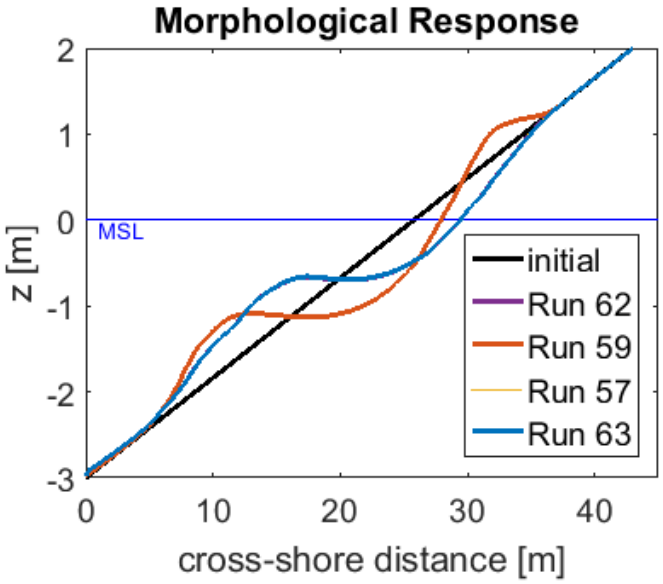

Figure 4.7: Comparison of the morphological response of the planar beach between K = 0.01 (run 59), K = 0.0003 (run 57) and K = 0.00005 (run 62) with reference case (no groundwater in- or exfiltration, run 63) for 1000 waves jonswap.

Intra-swash analysis The difference in sediment transport due to the primary groundwater effects is due to reduced water levels in the backwash due to infiltration of groundwater during the uprush. This lower water level causes smaller backwash velocity to occur and therefore less sediment will be eroded from the bed. The x,t diagrams of the water level and the velocity for the different values of hydraulic conductivity and the reference case without groundwater infiltration are presented in Figure 4.9. For the extreme hydraulic conductivity K_x = 0.01, the water levels and velocity in the backwash decrease as a result of the infiltration, which is shown for the three cases (for the reference case, the infiltration is non-existing and therefore this result is not shown) in Figure 4.8 where increased exchange between sea and groundwater is observed for increasing hydraulic conductivity.

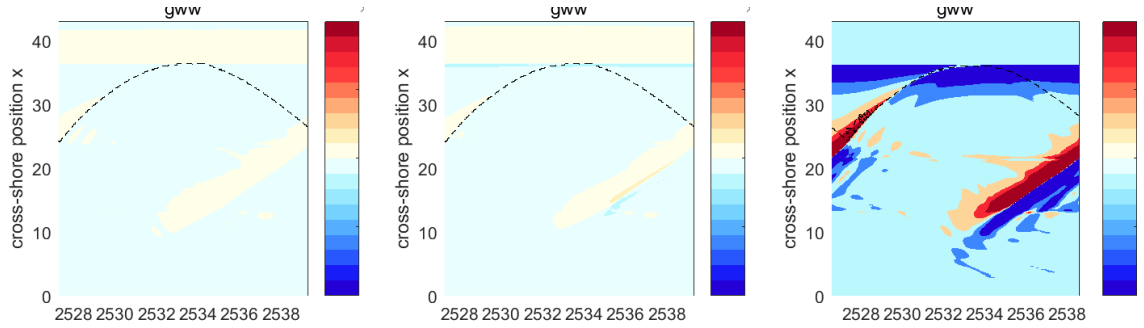

Figure 4.8: x,t diagram of vertical groundwater velocity (interaction between surface and groundwater) from left to right for K = 0.00005, K = 0.0003 and K = 0.01

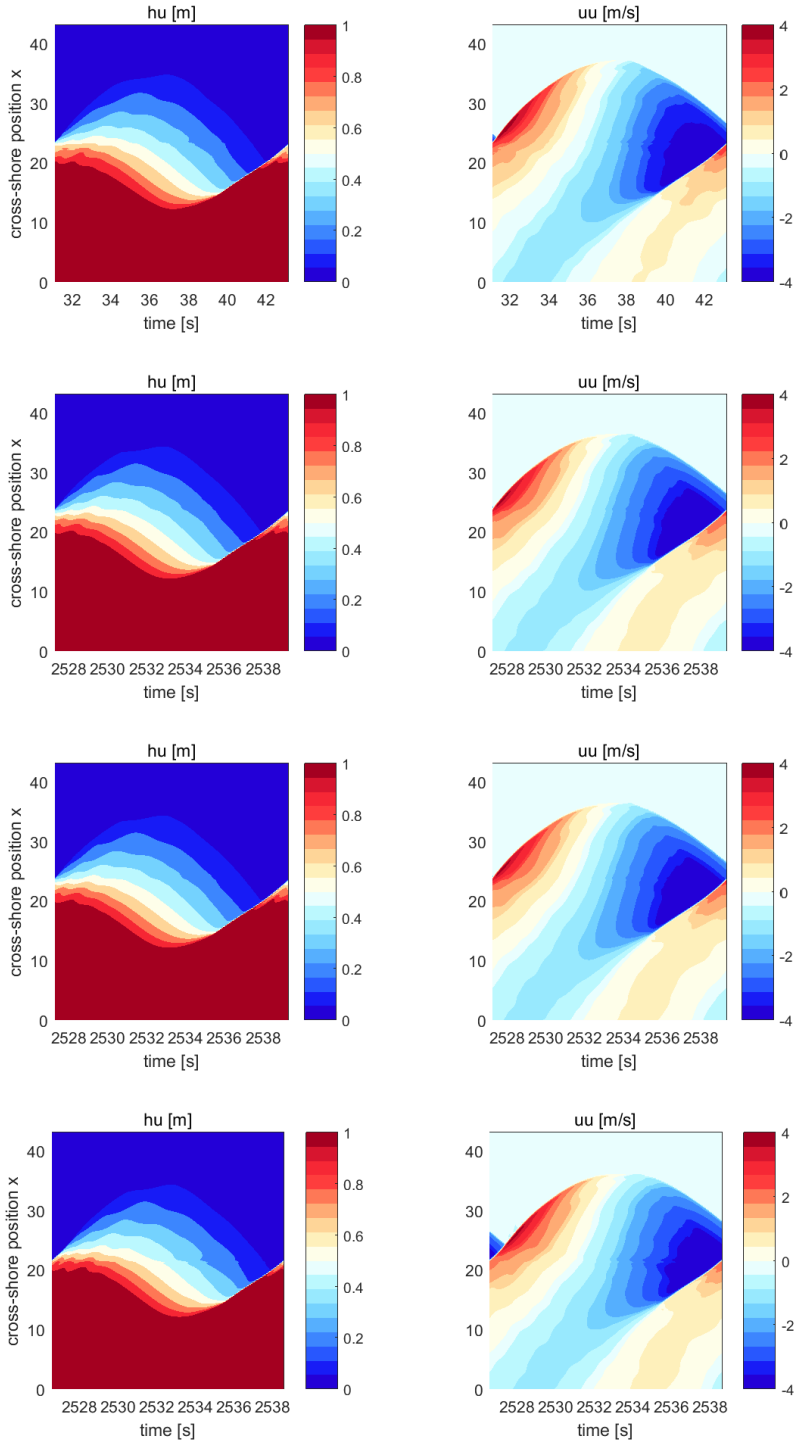

Figure 4.9: x,t diagram of water levels and velocity from top to bottom for Reference case, $K = 0.00005$, $K = 0.0003$ and $K = 0.01$

Conclusions groundwater The effect of groundwater infiltration on the total morphological response is quite small, but for extreme values (comparable to values for gravel) of the hydraulic conductivity, accretion in the upper swash can be achieved. Hydraulic conductivity has large spatial variation and is difficult to determine precisely. However, the values that are needed to make XBeach create accretion in the upper swash are very likely physically not matching the actual hydraulic conductivity of sand with a D50 of 420mu. The velocities are hardly influenced by the groundwater infiltrations neither are the water levels. Only with some imagination and only for extreme value of the hydraulic conductivity in Figure 4.9 a difference in the velocity and water levels can be observed.

4.4. SEDIMENT RESPONSE TIME

Introduction As explained in Chapter 2, a forced lower boundary on the sediment response time prevents the right hand side of the advection-diffusion equation to blow up causing numerical instabilities. This lower boundary depends on the water depth, which (for very shallow water) is expected to influence the sediment response time and therefore the sediment transport and bed level change in regions where shallow water occurs (upper swash).

Total morphological response The total effect on the bed level change is shown in Figure 4.10. The higher the sediment response time, the longer the sediment stays in the water column so for high minimum sediment response time, less erosion is expected for regions where this minimal sediment response time is active, mostly in the upper swash. The figure shows this behavior. For sediment response time very small, the erosion in the upper swash is stronger whereas for an extremely high response time ($T_s = 10s$) the erosion is much less because the whole domain is forced into this 'minimum' T_s.

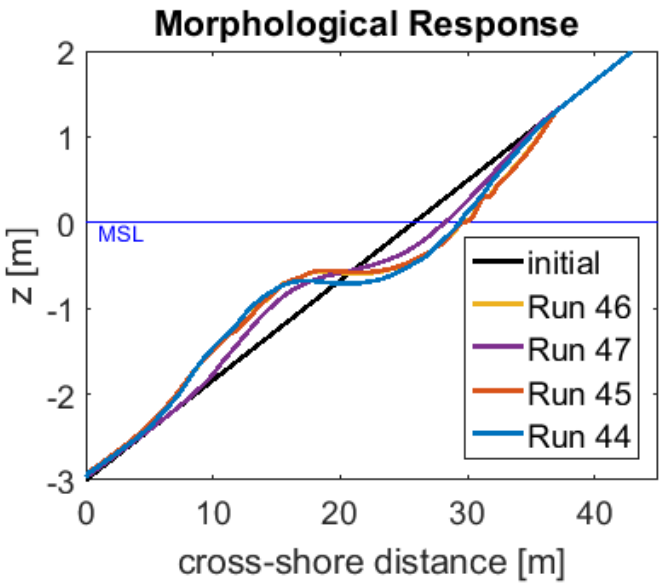

Figure 4.10: Comparison $T_{s,min}$ = 0.01(run 45), $T_{s,min}$ = 0.1(run 46) and $T_{s,min}$ = 10 (run 47) with reference case ($T_{s,min}$ = 0.5) (run 44) for 1000 waves jonswap.

Intra-swash analysis The exact position on the domain where the minimum sediment response time is active is very clear if visualizing in the x,t diagrams. Figure 4.11 shows the region where minimal sediment response time is active (i.e. the calculated sediment response time is lower then the minimum value therefore the minimum value is used in calculations).

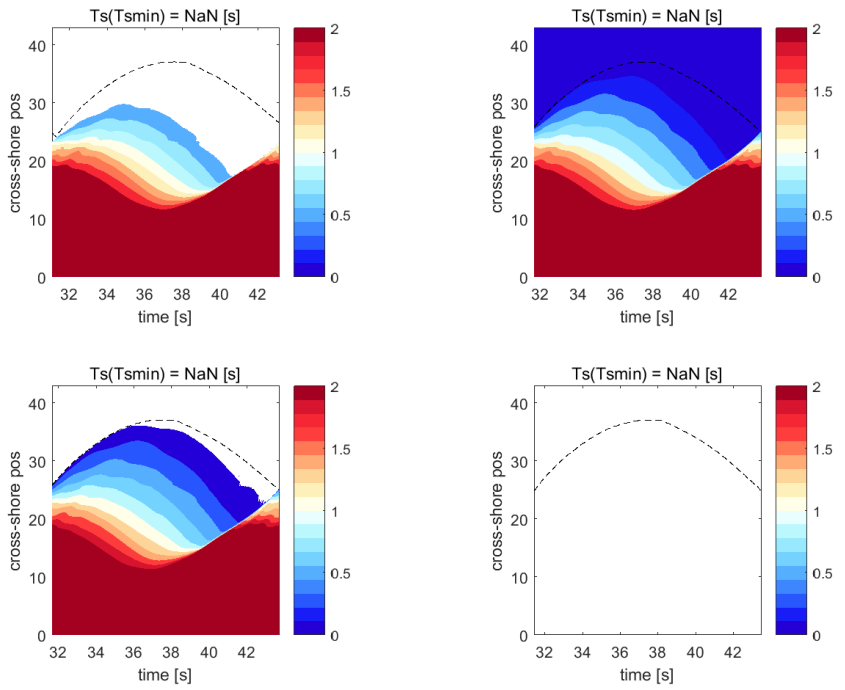

Figure 4.11: Domain where $T_{s,min}$ is active is shown in white, dotted line marks the run up level from upper left to bottom right for the reference case ($T_{s,min} = 0.5$), $T_{s,min} = 0.01$, $T_{s,min} = 0.1$ and $T_{s,min} = 10$.

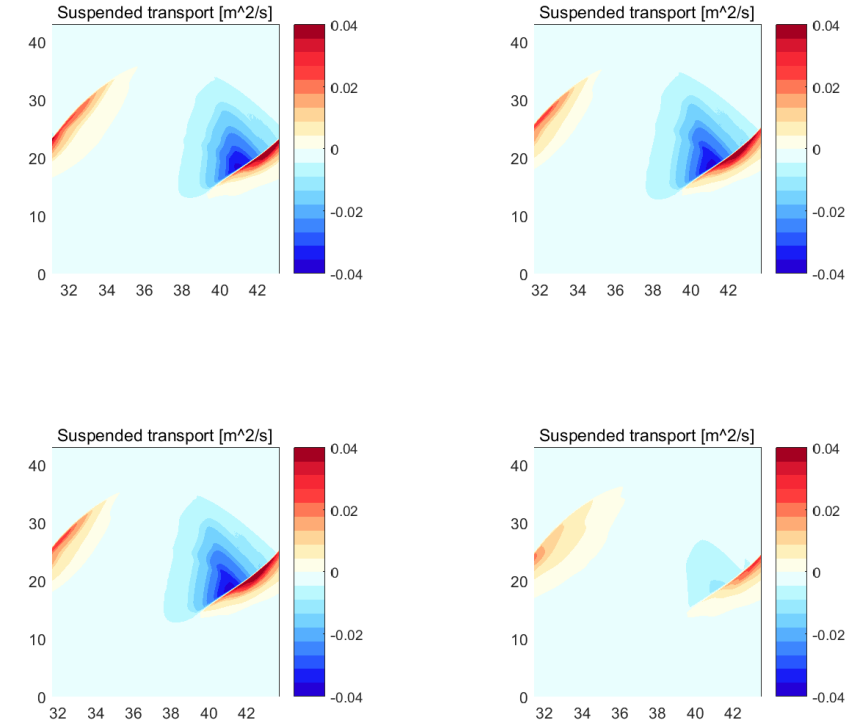

Figure 4.12: Suspended sediment transport influenced by a changed $T_{s,min}$ shown in Figure 4.11, from upper left to bottom right for the reference case ($T_{s,min} = 0.5$), $T_{s,min} = 0.01$, $T_{s,min} = 0.1$ and $T_{s,min} = 10$.

In the reference case, which uses the XBeach default value for $T_{s,min}$, for almost the complete swash domain the calculated value of T_s is smaller then $T_{s,min}$. This means that the whole swash domain is effected by the choice of a parameter originally intended just to guarantee numerical stability. For $T_{s,min} = 0.1s$, the swash domain is covered almost fully, only the last few meters of water remaining on the beach in the very end of the swash just before the new bore arrives is too shallow. On the other end of the influence spectrum, when $T_{s,min}$ is set to be 10 s, the complete x,t domain is using this value for the settling of sediments. This extreme value is used to test the sensitivity of the model to a very large value of T_s in its influence on the suspended transport. As can be seen in Figure 4.12, for this extreme settling response time there is almost no suspended transport and therefore also the bed level change, as determined in Figure 4.10, is small.

As discussed in Section 2.2, Alsina et al. (2009) observed sand to be fully settled after uprush, and no sediment to be transported in the water column at the flow reversal. This means that the water around flow reversal should be clean and no suspended sediment concentrations should be observed in the model either. This is briefly tested for the extreme value of $T_{s,min}$ and the results of this are shown in Figure 4.13. In the left panel the suspended concentrations on a fixed cross shore position in time, in the right panel the same but with a high $T_{s,min}$. Although from Figure 4.11 we concluded that the default value is too high, this value does give the sediment still time to settle completely before flow reversal (the concentration value going close to or zero between uprush peak and backwash peak). The extreme value for sediment response time results in a substantial amount of sediment still in suspension during flow reverse.

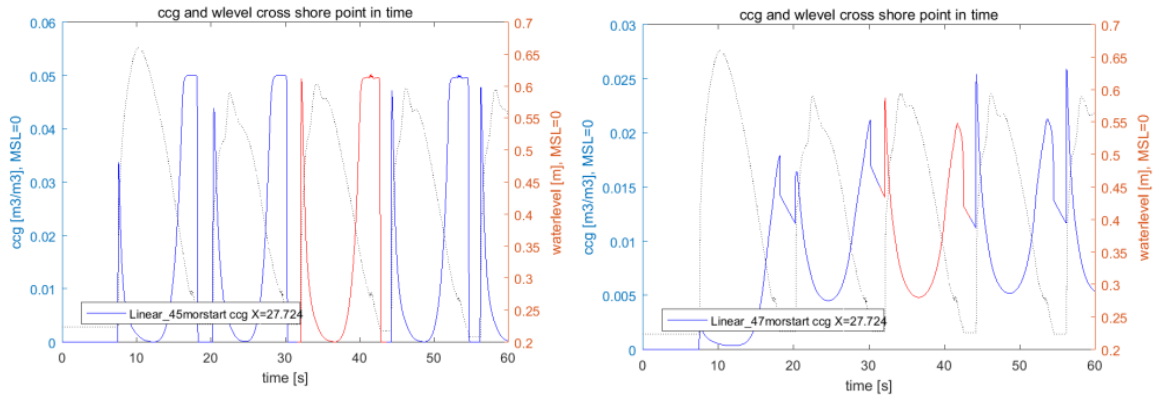

Figure 4.13: Suspended sediment concentrations for one cross shore point in time, low ($T_{s,min} = 0.01$, left panel) value and high $T_{s,min}$ value ($T_{s,min} = 10$, right panel). Water levels are plotted in the background to mark the swash cycle.

Conclusions sediment response time The default value for $T_{s,min}$ does prevent the correct value for the sediment response time to be calculated for very shallow water. With the current settings of $T_{s,min} = 0.5s$ and the conditions used for these modeling cases, this minimum value is used in the whole swash domain. Only a small adaptation of $T_{s,min} = 0.1s$, without changing the numerical stability, almost the whole swash domain is covered in the calculations. A very high value for $T_{s,min}$ causes offshore transport still to dominate, but it does reduce the erosion significantly. However, this high value of the sediment response time does prevent sediment to fully settle during uprush which is not correct if compared to literature.

4.5. BED SLOPE EFFECTS

Introduction In XBeach, the bed slope effects work on the whole swash domain equally strong (assuming constant bottom slope) and are applied after the calculations of the transport. Therefore it is expected that the difference between applying bed slope effects on the bed load transport only is very different to applying the effects on the total (bed load + suspended) transport.

Total morphological response If applied to the total transport as shown in Figure 4.14, the bed slope effects influence the morphology much more then applied to the bed load transport only. The bed load effects get stronger when the beach is steeper, and since the suspended transport dominates both uprush and backwash transport, this effect is strong for more reflective beaches.

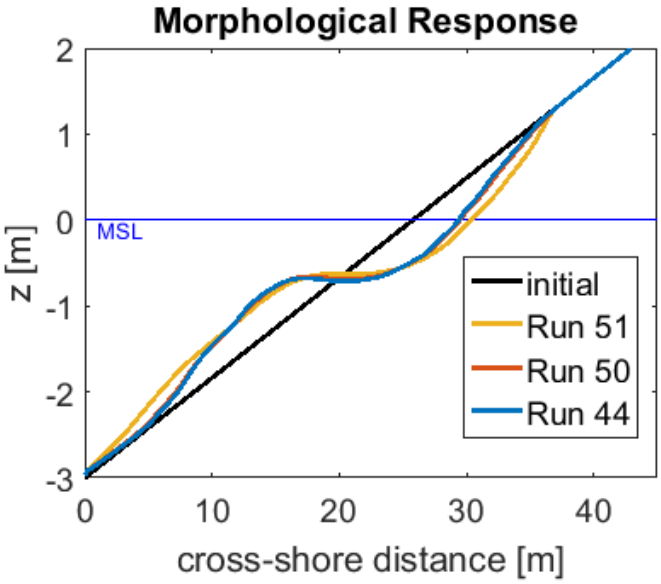

Figure 4.14: Comparison Reference case (no bed slope effects), 'roelvinktotal' and 'roelvinkbed' for 1000 waves JONSWAP.

This division between the influence of the -total and -bed options in bed slope effects become even more clear when the difference in bed load and suspended load transport, as shown in Figure 4.15. In the middle panel, the transport due to bed load transport increased slightly, but in the right panel the total morphologic response after one swash event changed significantly under influence of the bed slope effects.

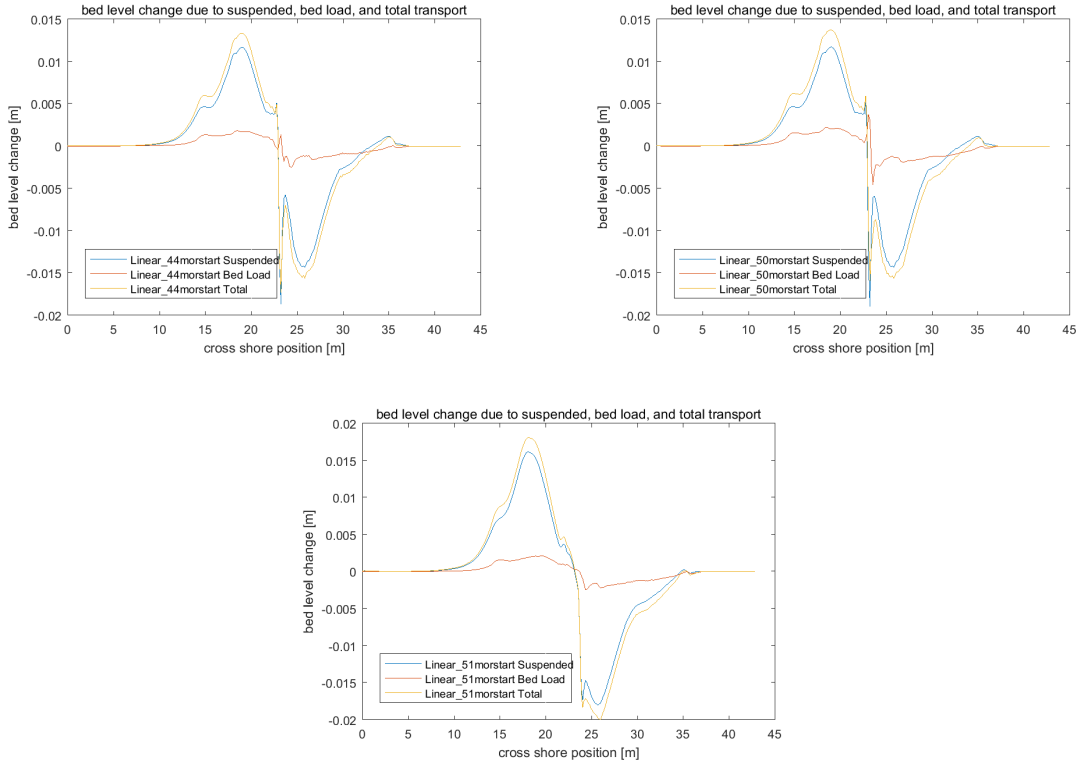

Figure 4.15: The bedslope effect on the bed level change due to suspended/bed load transport from left to right Reference case, 'roelvinkbed' and 'roelvinktotal'.

Intra-swash analysis If looking in the x,t diagram, the bed load transport increases for both the -bed and the -total modules. The suspended sediment transport is similar to the reference case for the -bed module, but indeed as seen in the total morphological response, there is a strong increase in offshore transport and a decrease in onshore transport which is the cause for the erosion in the upper swash and accretion offshore.

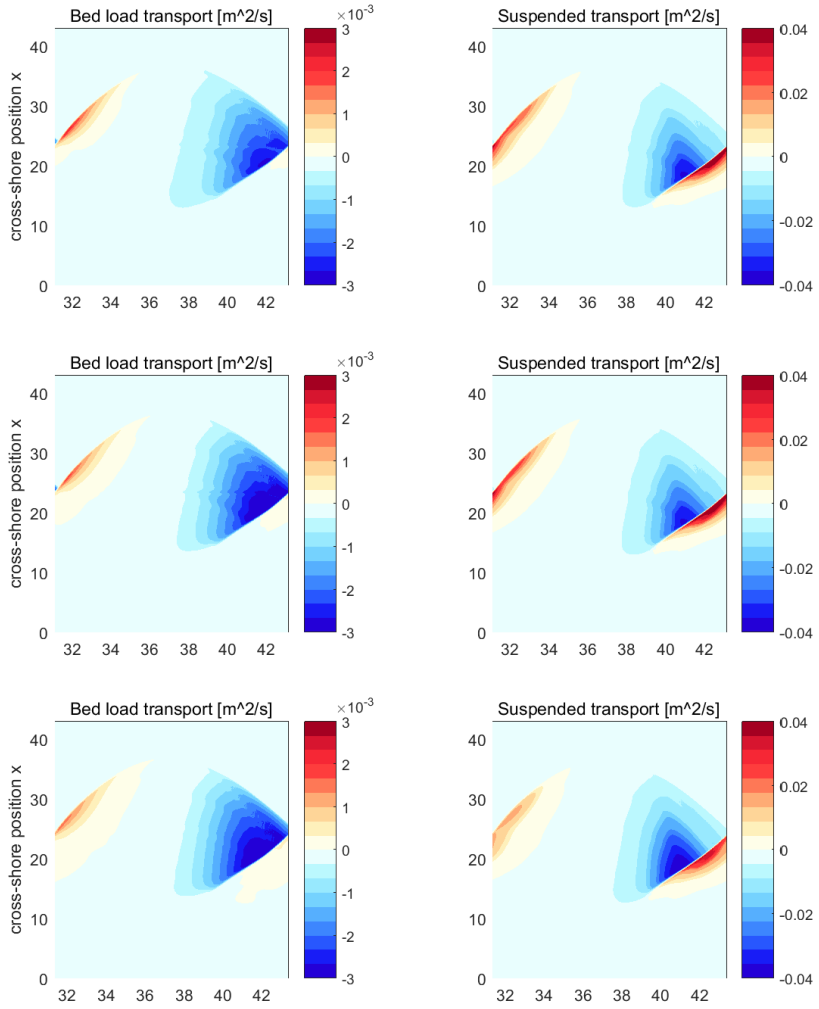

Figure 4.16: Bed load transport (left) and suspended transport (right) for the reference case (upper), 'roelvinkbed' (middle) and 'roelvink-total' (lower).

Conclusions bed slope effects As expected the bed slope effect results in more erosion in the upper swash zone. The amount is very dependent on the choice of adjusting the bed load transport only, or the total transport. There is no physical reason why the bed slope effect should be included in the suspended sediment transport (a particle in suspension does not 'feel' the slope of the bed below) but this has been calibrated previously for dissipative beaches. If the beach gets more reflective/steeper, the effect of bed slope gets stronger and therefore it is very likely that for intermediate reflective beaches the morphological response to addition of the bed slope effect also to the suspended transport is not valid anymore.

4.6. BORE GENERATED TURBULENCE

Introduction So far in the modeling studies on the planar beach, it is observed that almost all sediment transport and significant bed level change occurs under the incoming bore. In Section 2.2 is explained how bore generated turbulence can be calculated and how that effects the sediment concentrations (and therefore the transport-bed level change). In Chapter 3 a new way of enhancing turbulence in XBeach is shortly described, the results of the influence of enhanced bore turbulence on morphological response is shown in this section.

Total morphological response To start with the total response of the beach, it is clear from Figure 4.17 that enhanced bore turbulence effects the morphology quite significant. The net onshore enhancement of the sediment transport is already visible for k_{gain}=10 and when an extremely enhanced turbulence is analysed

the profile shows the opposite behaviour as the reference case: accretion in upper swash and erosion offshore.

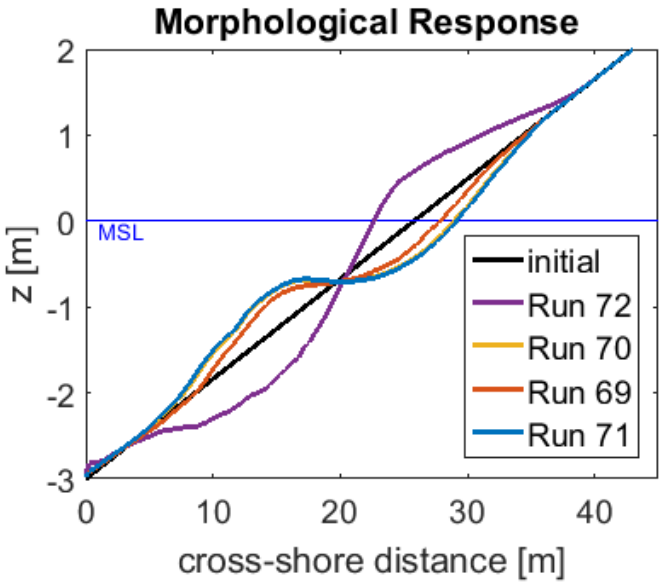

Figure 4.17: Comparison bed level changes for $k_{gain}s$ = 1(run 71),$k_{gain}s$ = 2(run 70), $k_{gain}s$ = 10(run 69), $k_{gain}s$ = 100(run 72), for 1000 waves JONSWAP.

Intra-swash analysis The turbulent kinetic energy has been enhanced by the created variable k_{gain}, as explained in Section 3.1.6. As explained in 2, the turbulent kinetic energy influences the equilibrium sediment concentration which on its turn affects the transport. At one cross shore position the turbulent kinetic energy which is bore induced, and therefore only present when the bore passes, and the suspended sediment concentration are plotted in Figure 4.18. As can be seen in this figure, the influence on the equilibrium concentration is much smaller then the actual increase in k_{turb}. The total spatial and temporal region of influence of the turbulent kinetic energy on the sediment transport, is shown in the x,t diagrams in Figure 4.19

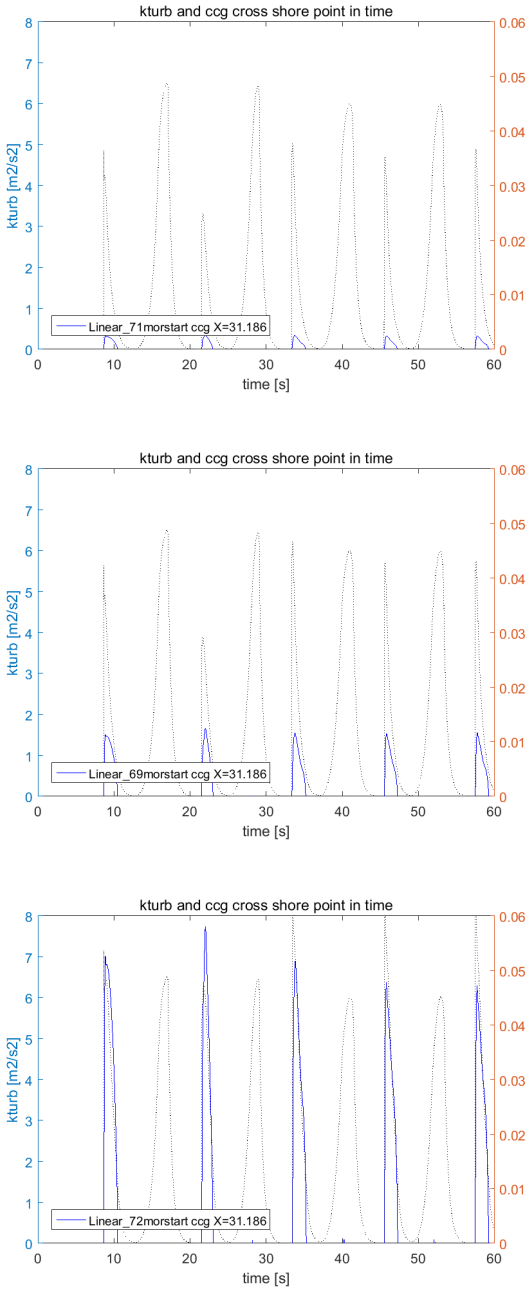

Figure 4.18: Turbulent kinetic energy k_{turb} on fixed cross shore position (left axis) and suspended sediment concentration (right axis) from top to bottom for $k_{gain} = 1$, $k_{gain} = 10$ and $k_{gain} = 100$

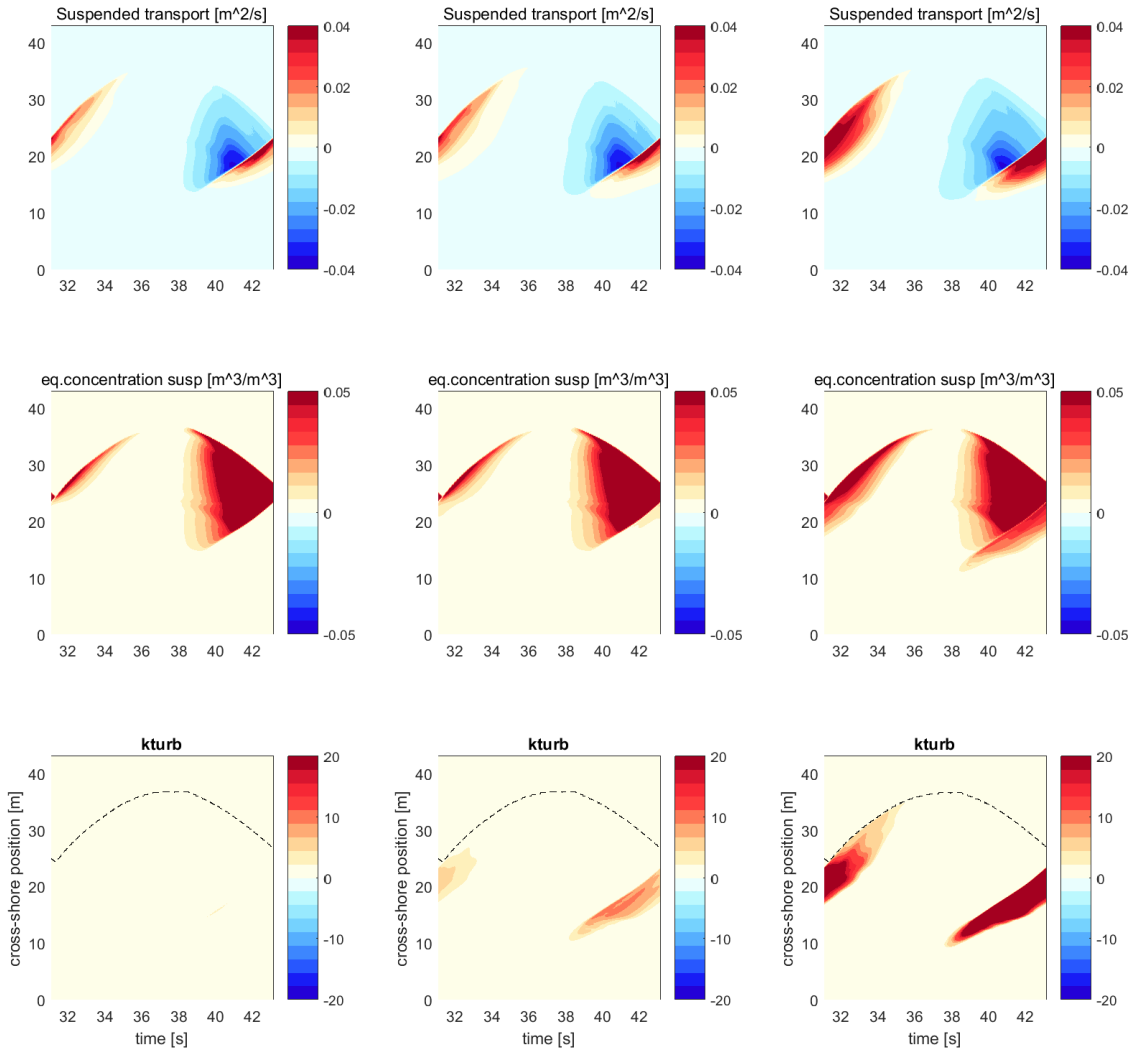

Figure 4.19: Suspended transport (upper panels), equilibrium suspended sediment concentration (middle panels) and turbulent kinetic energy (lower panels) from left to right for $k_{gain} = 1$, $k_{gain} = 10$ and $k_{gain} = 100$

Conclusions turbulence As already discovered in the Literature study and during development of the modeling methodology, turbulence is not very well parametrized in the current non-hydrostatic extension of XBeach. The assumptions made for the surf-beat version are not suitable for the non-hydrostatic extension, and therefore some rough changes have been made to the model before able to test the influence of turbulence. The results of this are very promising, bore generated turbulence is able to enhance accretion in the upper swash and therefore more analysis on the parametrization of turbulence is likely to improve the overall performance of XBeach non-hydrostatic. The turbulent kinetic energy values obtained with an enhancement with a factor 100 seems quite unlikely to be a proper representation of the real turbulent kinetic energy, but as mentioned the parametrization needs to be studied in more detail before conclusions on this can be drawn.

4.7. CONCLUSIONS XBEACH

In general, accretion is quite hard to achieve on a planar beach forced by waves that have in literature shown to induce accretive conditions on the 1:8.6 sloped beach of our modeling study. Based on this qualitative modeling approach, the most promising processes to help represent beach recovery (accretion) in morphodynamic modeling in a better way are turbulence, and to lesser extend groundwater effects. For turbulence, the challenge is to parametrize in such a way that the sediment concentrations and transport under the bore are a good representation of measured values in the field or experiments. For groundwater the 'positive' results from this qualitative modeling study need an unphysical high value for the hydraulic conductivity K_x. To

verify this, infiltration rates and swash volume decreases in the backwash should be compared to measurements in order to analyze the discrepancy between measured hydraulic conductivity and the conductivity needed to create accretion in the upper swash. Obviously, the answer will be in a combination of a better parametrization of mainly bore generated turbulence, and possibly enhancement of the groundwater effects dependent on the hydraulic conductivity.

5

RESULTS COMPARISON TO BARDEX II OBSERVATIONS

5.1. INTRODUCTION

In Chapter 4 the sediment transport formulations of XBeach were assessed and the influence of four processes on swash morphodynamics of intermediate reflective beaches was analyzed. In this chapter, the XBeach morphodynamical predictions of the swash zone are compared to observations made during an erosive (A4) and an accretive (A8) Bardex II experiment. The first part (Section 5.2) focuses on the comparison between the measured and modeled morphological response of the beach. The second part (Section 5.3) focuses on the comparison between the measured and modeled intra-swash processes. The conclusions from Section 5.2 and Section 5.3 form an answer on research question 3: *How do the numerical results perform compared to to experimental results Bardex II (erosive and accretive) and do we need new processes/improvements of current physics?*

5.2. TOTAL MORPHOLOGICAL RESPONSE

5.2.1. INTRODUCTION

In Section 3.2.2, the measured morphological response during Bardex II experiment A4 and A8 is shown (Figure 3.3). In this section the results of the modeled morphological response with XBeach are compared to the observed morphological response during Bardex II. Two modeling cases were set-up and will be compared to Bardex II in this section: the reference case and the XBeach default case (see Table 3.6).

5.2.2. RESULTS

The total bed level change after A4 and A8 and the difference with the measured bed level in Bardex II is shown in Figure 5.1. The profile development using the Bardex II bathymetry compared to the planar beach approach in Chapter 4 is similar. Erosion occurs above the water line and the sediment is deposited offshore. The biggest difference between the XBeach default case and the reference case is that the default case takes into account groundwater in/exfiltration and bore induced turbulence. The influence of these processes, as can be seen in Figure 5.1 is only visible in the upper swash and only in experiment A8. The rest of the profile in the XBeach default case behaves similar as the reference case. Both modeling cases perform very poor compared to the measured response, errors of up to 0.5 m were observed.

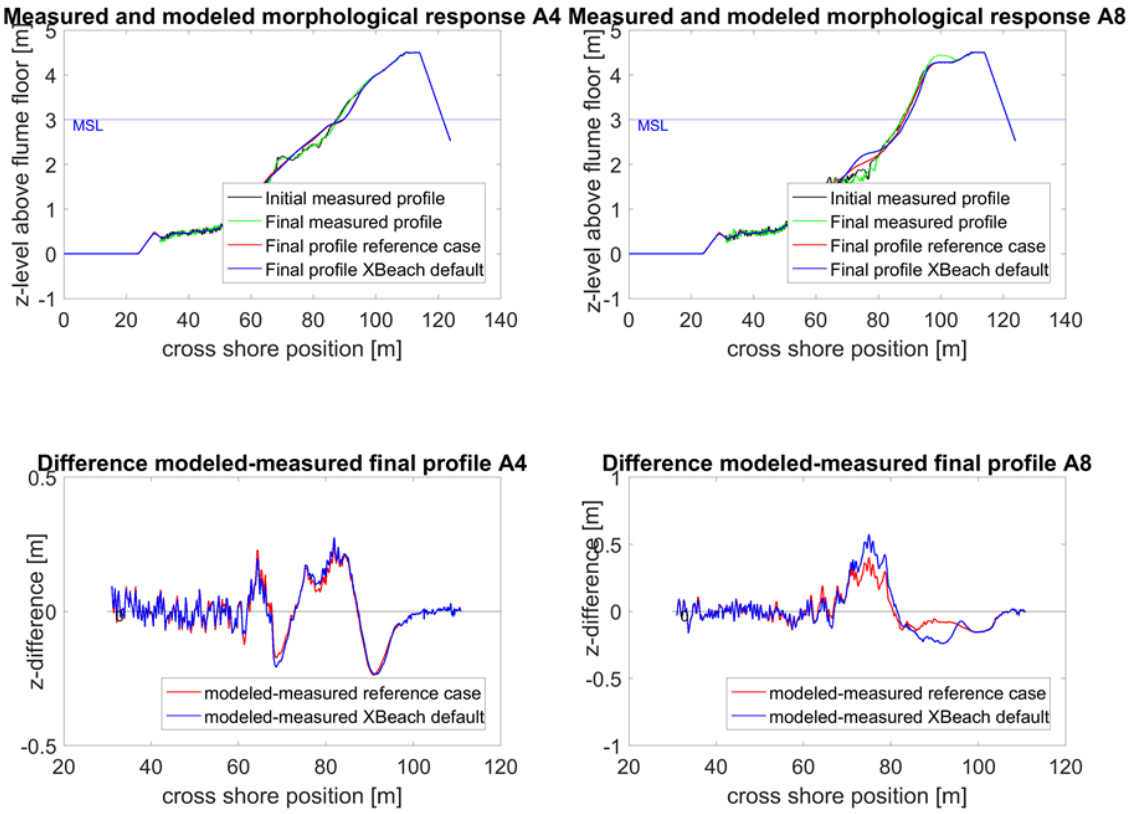

Figure 5.1: modeled and measured morphological response during erosive (A4) and accretive (A8) wave conditions, upper two panels and the difference with the initial profile, lower two panels.

To determine the cause of the error between the morphological response of the XBeach default case compared to the measured morphological response, the evolution of the modeled bed level at several cross-shore positions (between x=80 and x=110) during experiment A4 and A8. Ruessink et al. (2016) performed similar measurements on during the Bardex II experiments which were used to compare the performance of XBeach. The positions on the cross-shore domain where output is generated of the time series of the bed level evolution are shown in Figure 5.2. The lower three panels of Figure 5.2 show the modeled evolution of the bed level in time for three cross-shore positions, one in the lower swash, one around the mean sea level and one in the upper swash.

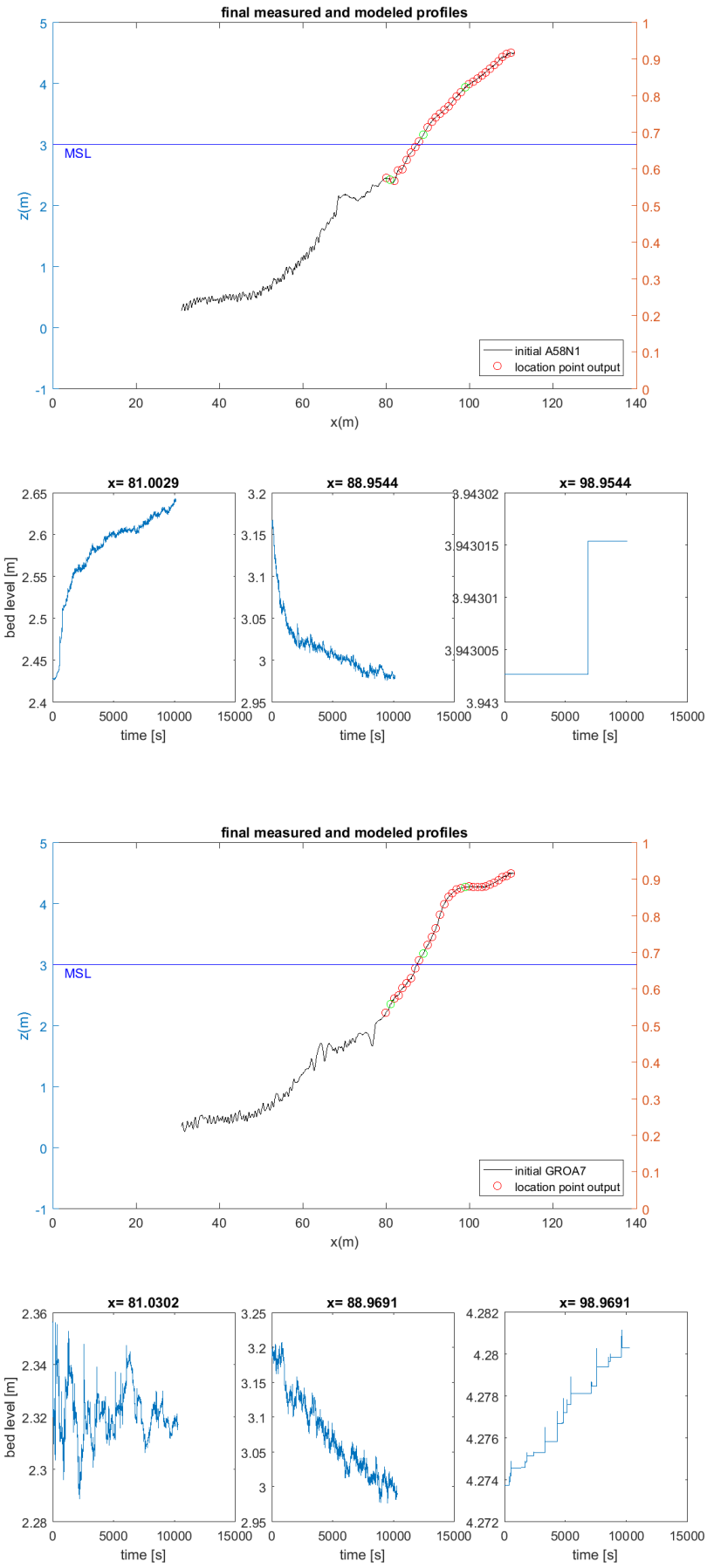

Figure 5.2: The large panels show the initial bathymetry of the XBeach default case for A4 (top) and A8 (bottom) with in red circles the locations along the cross-shore domain where time series of bed level change are generated. The small panels show three time series of modeled bed level change for A4 (top) and A8 (bottom). For both experiments the modeled bed level evolution in the lower swash (left), bed level evolution around the water line (middle) and bed level evolution in the upper swash (right) are shown.

Ruessink et al. (2016) measured the vertical position of the bed above the flume floor at the moment that the bed becomes dry after a swash event. In the model, continuous time series of the bed level change can be made, as shown in the bottom three panels of Figure 5.2. Therefore the time series of the model output have been post-processed in the same way as the observations, where the bed level position is measured after the bed becomes dry. An example of this for the upper swash and lower swash of experiment A4 is shown in Figure 5.3.

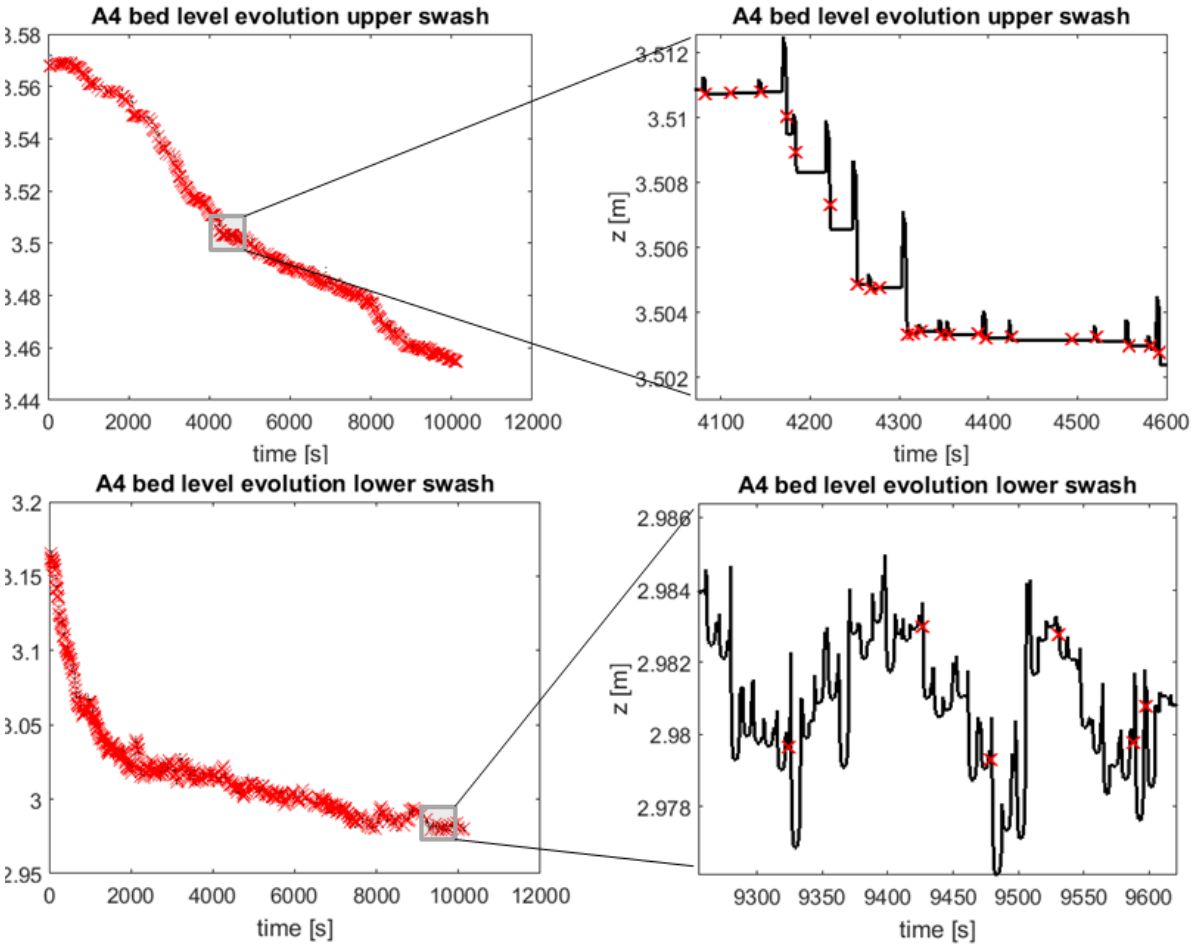

Figure 5.3: Experiment A4: bed level evolution in upper swash (top) and lower swash (bottom). The right panels show a zoomed-in time series of the bed level change.

In the upper swash the bed becomes dry after every swash event. In the lower swash, as shown in the zoomed-in bed level evolution in Figure 5.3, the bed becomes dry not so often resulting in fewer counted swash events. Outside the swash zone, the bed was always wet and no events were counted. Land-ward of the maximum run up measured in the experiment, the bed was always dry and also no events were counted. This resulted in a total count of events per cross-shore output point (Figure 5.4) for experiment A4 and A8. The total number of waves was around 1500 during A4 and around 1000 during A8. This amount of events is only observed in the middle of the swash domain. The number of measured events very quickly reduces towards lower swash and towards upper swash.

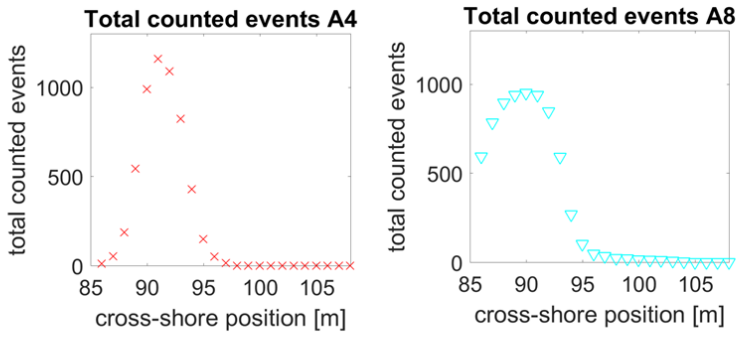

Figure 5.4: total count of modeled swash events for every point output for XBeach default case experiment A4 (left) and A8(right)

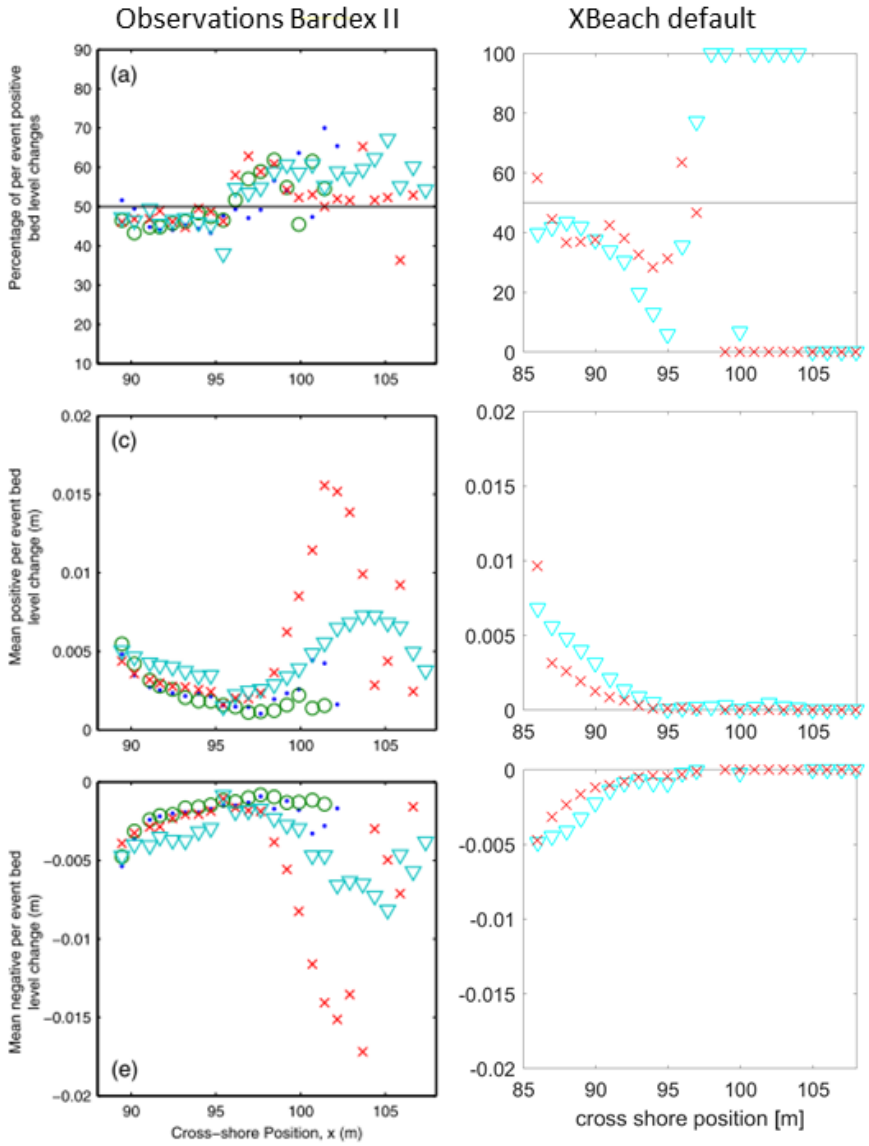

Figure 5.5: Bardex II observations (left) and modeled results (right) of the percentage of positive bed level change (upper panels), total net bed level change per positive (middle panels) and negative (lower panels) event. Blue triangles A8 and red crosses for A4 (other symbols represent other experiments from the A-series). Left panel from Ruessink et al. (2016), right panel XBeach results.

As mentioned, Ruessink et al. (2016) observed the bed level change in the cross-shore domain. The same analysis of bed level change in the cross-shore domain was done for the XBeach default case. The results of this are shown in Figure 5.5. The left three panels show the observations from Ruessink et al. (2016), right three panels show the result from the XBeach A4 and A8 experiment, respectively. The top three panels show the percentage of 'positive' events (an event for which the bed level at a dry moment was measured higher than the bed level measured at the previous dry moment). The observations show a higher percentage of negative events up to 90 m cross-shore position and predominantly positive events in the upper swash. The higher percentage of positive events in the upper swash does not necessarily mean that there was accretion in the upper swash. The amount of bed level change per event needs to determined to obtain the total bed level change. This has been shown in the middle and bottom panels (average net change per positive event and average net change per negative event). For the lower swash, the modeled bed level elevation per event and the ratio of positive and negative events corresponds quite well to the observations in Bardex II. In the upper swash, the behavior as observed by Ruessink et al. (2016) is not represented by the XBeach default case. As mentioned, the number of observed swash events in the upper swash is unknown (although the maximum run-up is observed at x=105m) so the run-up levels can not be compared. The number of swash events that were counted in the XBeach default case reduce quickly in the upper swash (see Figure 5.4). Therefore it is difficult to make a comparison between the measured and modeled upper swash.

5.2.3. CONCLUSIONS MORPHOLOGICAL RESPONSE

The modeled morphological response was compared to the observed morphological response. The observed behavior by Ruessink et al. (2016) is represented by XBeach in the lower swash, but the upper swash could not be compared due to the lack of sufficient swash events. A possible reason for this is that XBeach predicts lower run-up levels than the Bardex II observations. The total morphological response of XBeach, as shown in Figure 5.1 shows erosion in the upper swash and deposition of the sediments further offshore for both the reference case and the XBeach default case.

5.3. INTRA-SWASH HYDRODYNAMICS AND SEDIMENT CONCENTRATIONS

5.3.1. INTRODUCTION

To be able to analyze the sediment concentrations and hydrodynamics on an intra-swash level of detail, a smaller domain with the measured water level and velocity time series at cross-shore position x=72.5 m were used to force XBeach. The modeled water level, velocity and suspended sediment concentration at cross-shore position x=89.6 m were compared to Bardex II observations at the same cross shore point. Figure 3.7 in Section 3.2.3 shows the model domain and cross-shore position of the measurement instruments. First the intra-swash analysis of the XBeach default case will be presented after which the influence of enhanced groundwater effects and enhanced turbulence shortly will be discussed.

5.3.2. XBEACH DEFAULT CASE

Comparison modeled and measured water depth The measured and modeled water depth for Bardex II experiment A4 and A8 are shown in Figure 5.6. The water depth measurement positions, obtained from water level (PT) sensors, were fixed in cross-shore and vertical position for both A4 and A8. For experiment A8, the timing of the water depth and the magnitude corresponds well (the fragment of the time series that shown here suggests lower modeled water levels but over the complete time series modeled water levels closely match the measured values). The forcing of XBeach for the intra-swash analysis is close to the point where this water depths are observed and therefore a good comparison was expected. The large offset between the measured and modeled results for experiment A4 suggest that the sensor changed position and the measured water depth of experiment A4 were therefore not used in the further analysis.

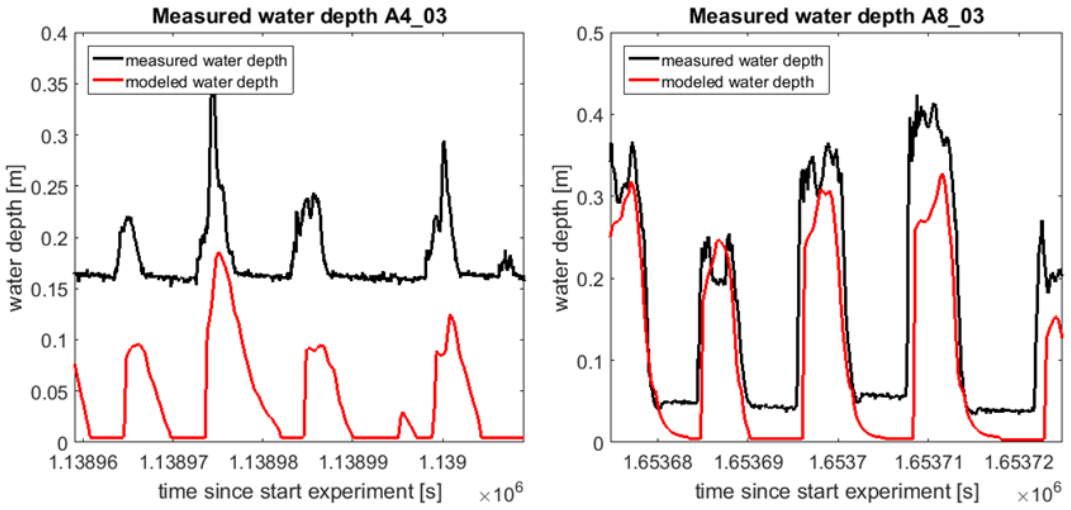

Figure 5.6: measured (red lines) and modeled (black lines) water depths for A4 (left) and A8(right)

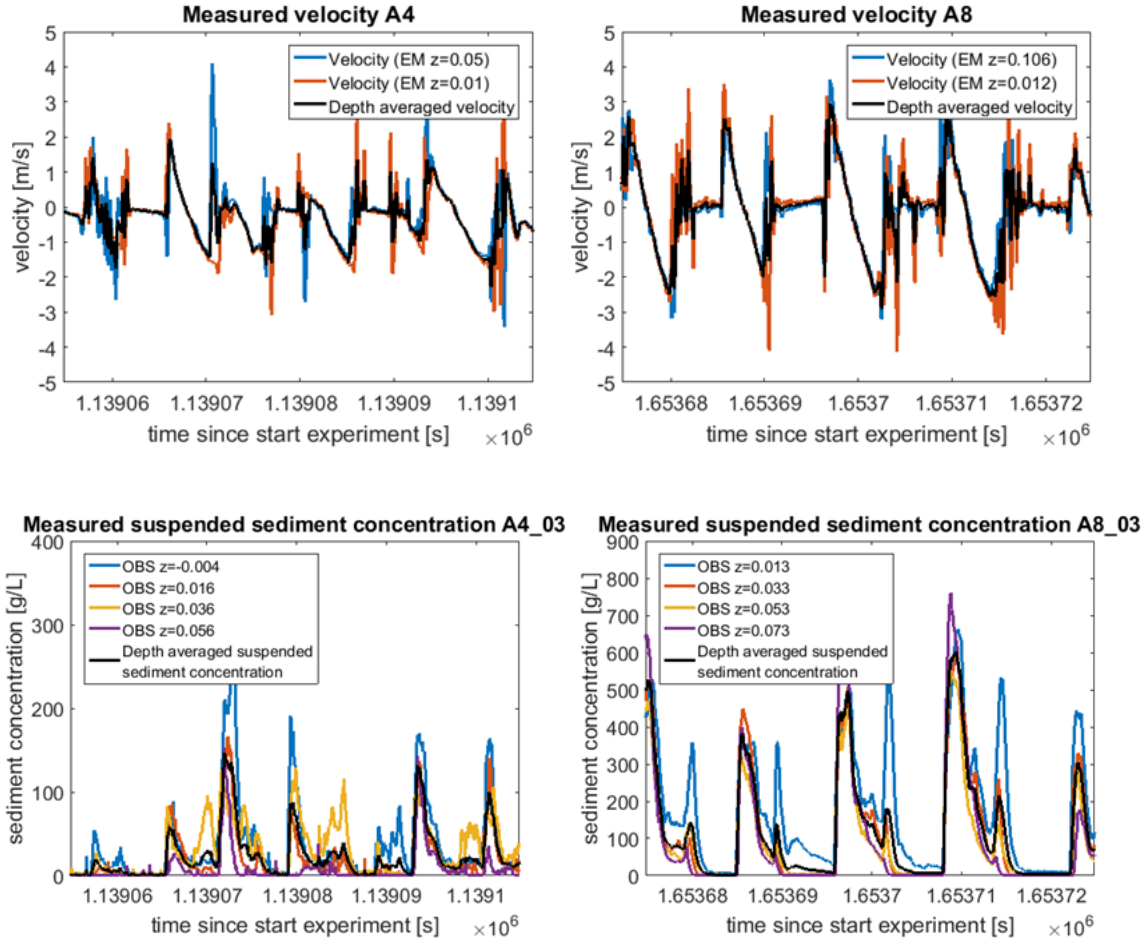

Figure 5.7: Measured velocity (top panels) from two EM sensors and depth average velocity for A4 (left) and A8 (right). Measured suspended sediment concentration (bottom panels) from four OBS sensors and depth average concentration for A4 (left) and A8 (right).

measured velocity and sediment concentration The velocity and suspended sediment concentrations were measured with multiple sensors at different elevations above the bed and were adapted in between every experiment (hence the different in elevations of the sensors above the bed for A8 and A4). Because swash flows are so shallow and intermittent, a constant velocity and sediment concentration profile over the water depth was assumed. Based on this assumption, the depth averaged velocity and sediment concentration is the mean value of the measurements. The measured and depth averaged velocity and the measured and depth averaged suspended sediment concentration are shown in Figure 5.7.

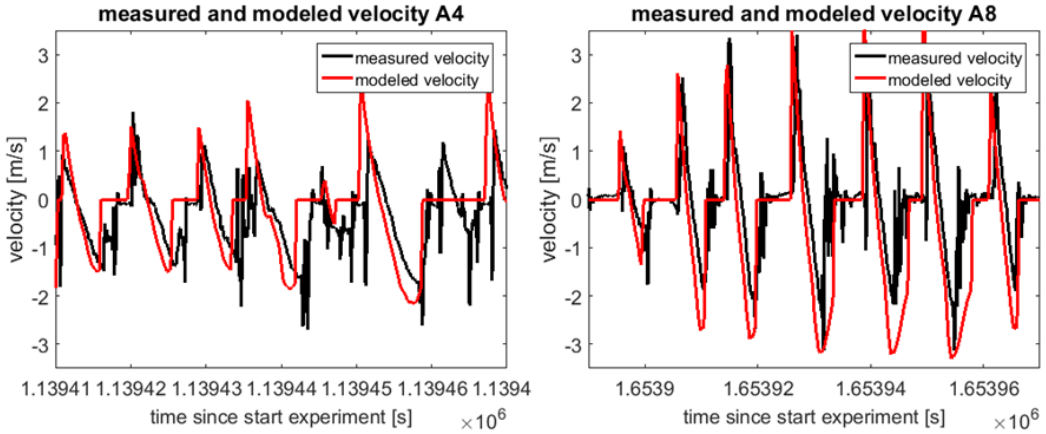

Figure 5.8: measured and modeled velocity time series random swash event for A4 (upper) and A8(lower)

Comparison with XBeach default case Measured and modeled velocity at x= 89.6 m are shown in Figure 5.8. Both the modeled uprush (positive) and backwash (negative) velocities were slightly larger in magnitude then the measured velocity for both experiment A4 and A8. The measured uprush and backwash velocity in A8 was around a factor 2 higher then the measured velocities in A4. This results in higher measured suspended sediment concentrations in experiment A8, as shown in Figure 5.9. In the uprush, the measured sediment concentrations were much higher then in the backwash. This is likely to be caused by the stirring up of sediment by the breaking of waves. The modeled concentrations in the backwash were also higher for experiment A8 than for experiment A4, however the modeled backwash concentrations for both A4 and A8 are higher than the measured values. This suggest that the effect of groundwater in/exfiltration was not strong enough in the XBeach default case. The measured uprush concentrations were higher for A8 than for A4. The modeled uprush concentrations however, were predicted to have similar value for the uprush of A4 as for the uprush of A8. This suggested that wave breaking induced turbulence was not represented correctly by the default XBeach case. In Figure 5.10 the measured sediment concentration profile during one typical swash event from the 4 OBS sensors at different elevations above the bed is compared with the modeled depth-averaged sediment concentration. Similar results as for the time series of sediment concentrations can be seen in the profiles as well, the average uprush sediment concentration was larger for the measured, and the average backwash sediment concentration for the modeled results for both experiment A4 and A8.

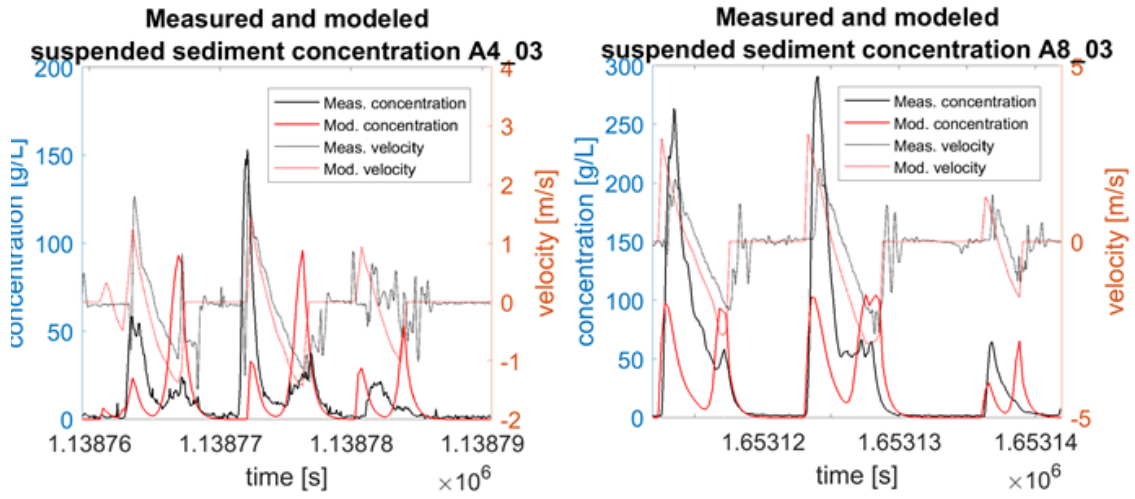

Figure 5.9: The measured and modeled 'best we do now' sediment concentration and velocity for A4 (left) and A8(right)

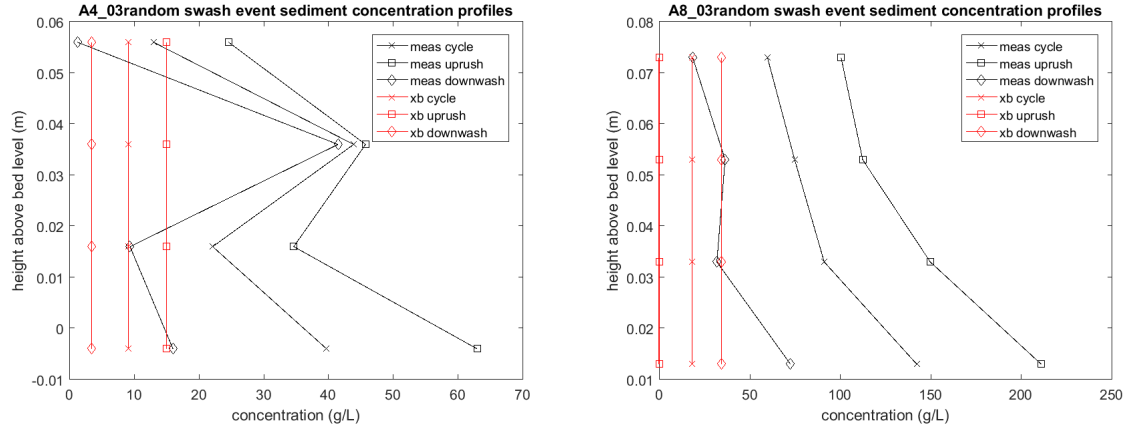

Figure 5.10: Measured (red lines) and modeled (black lines) sediment concentration profile for one typical swash event. Three lines represent average sediment concentratin during uprush (positive velocity), during backwash (negative velocity) and averaged over total swash cycle (between two dry sensor measurements) for experiment A4 (left) and experiment A8 (right).

Conclusion intraswash analysis XBeach default case The measured sediment concentrations in both Bardex II experiment A4 and A8 were not represented by the XBeach default case. The uprush concentrations were under-predicted while the backwash concentrations were over-predicted. Therefore, two model cases will be compared with the measured sediment concentrations in the next two sub-sections. The first case uses enhanced groundwater effects to decrease the backwash velocity and therefore the backwash sediment concentrations. The second case uses enhanced wave breaking induced turbulence to increase the sediment concentrations in the uprush.

5.3.3. ENHANCED GROUNDWATER INFILTRATION

The backwash sediment concentrations were over-predicted in the XBeach default case. Enhanced groundwater infiltration has showed on the planar beach to reduce the erosion in the upper swash which is associated with this. A modeling case is performed on the Bardex II intra-swash bathymetry (see Figure 3.7) with a hydraulic conductivity of K=0.01m/s to enhance infiltration (see Table 3.8). The results of this case are shown in 5.11. Compared to the XBeach default case, the width of the backwash peak is slightly smaller, caused by the stronger groundwater infiltration during the backwash. The total backwash concentration however, is still over-predicted even with a very high (gravel-like) hydraulic conductivity both for experiment A4 and A8.

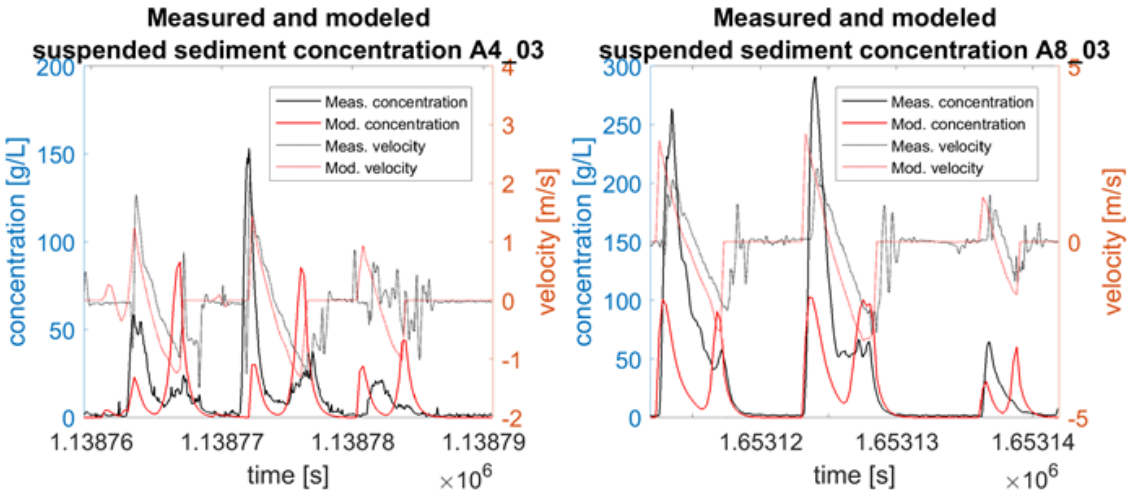

Figure 5.11: The influence of a higher hydraulic conductivity (easier infiltration/exfiltration) on modeled sediment concentration and velocity for A4 (left) and A8(right)

5.3.4. ENHANCED TURBULENCE

The uprush sediment concentrations were under-predicted in the XBeach default case. Enhanced wave breaking induced turbulence has showed on the planar beach to increase suspended sediment concentrations in the uprush (see Figure 4.18). A modeling case is performed on the Bardex II intra-swash bathymetry (see Figure 3.7) with a turbulent kinetic energy enhancement factor k_{gain}=50 (see Table 3.8). For experiment A4 this resulted in significantly higher predicted uprush concentrations. For experiment A8 also a higher uprush concentration was measured but the difference with the measured concentration was still large. The waves in A4 are shorter and steeper, which could be an explanation why wave breaking had more influence on the results of experiment A4.

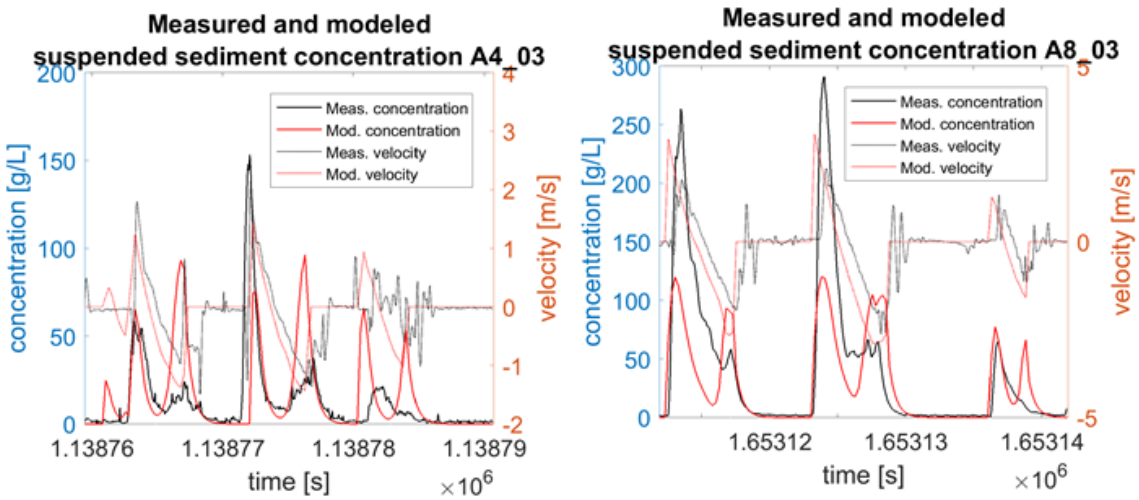

Figure 5.12: The influence of enhanced turbulence on modeled sediment concentration and velocity for A4 (left) and A8(right)

5.3.5. CONCLUSIONS INTRA-SWASH ANALYSIS

In this section, by means of an intra-swash time scale analysis The water levels, velocity and sediment concentrations have been looked at on an intra-swash timescale. The modeled water depth, velocity and sediment concentrations for the XBeach reference case, a case with enhanced groundwater effects and a case with enhanced turbulence have been compared to Bardex II measurements. The measured water depth for A4 could not be used but the measured water depth of A8 was represented well by the modeled water depth. This was expected since the forcing signal was close to the point of interest on the modeling domain. The

velocity for both uprush and backwash was slightly over-predicted by all modeling cases. Uprush sediment concentrations in the XBeach default case were under-predicted. Enhancing wave breaking induced turbulence did improve the results however the modeled concentrations did still not correspond to the observed values in Bardex II. The backwash sediment concentrations were over-predicted by the XBeach default case. Enhancing groundwater infiltration led to very small improvement but the backwash sediment concentrations did still not correspond to the observed values in Bardex II.

6

RESULTS MATLAB 1D SEDIMENT TRANSPORT MODEL

6.1. INTRODUCTION

In this chapter the results of three cases using a 1D Matlab model to calculate sediment transport are presented. The conclusion from the results of the planar beach approach in Chapter 4 were that wave breaking induced turbulence is an important process in onshore enhancement of sediment transport. The conclusions of the comparison to Bardex II observations in Chapter 5 were that the modeled velocity was slightly over-predicted by XBeach compared to Bardex II both for uprush and backwash phase. However the predicted suspended sediment concentrations did not correspond to the Bardex II observations. The uprush sediment concentrations were strongly under-predicted and the backwash concentrations strongly over-predicted.

The approach using XBeach and force at an offshore boundary the measured water levels and velocity leaves multiple conclusions open for the cause of the observed mismatch between measured and modeled sediment concentrations at x = 89.6m. Since the transport formulations as in Equation 2.1 are dependent on the local velocity and water depth, either the mismatch between the modeled and measured velocity and water depth is the cause for wrongly predicted sediment concentrations, or the transport equation is wrong (or both). Figure 6.1 shows a method to distinguish between those two potential causes of the erroneous prediction of sediment concentrations and a modeling approach that lead to conclusions about the cause of the wrongly predicted sediment concentrations and about the possible solutions.

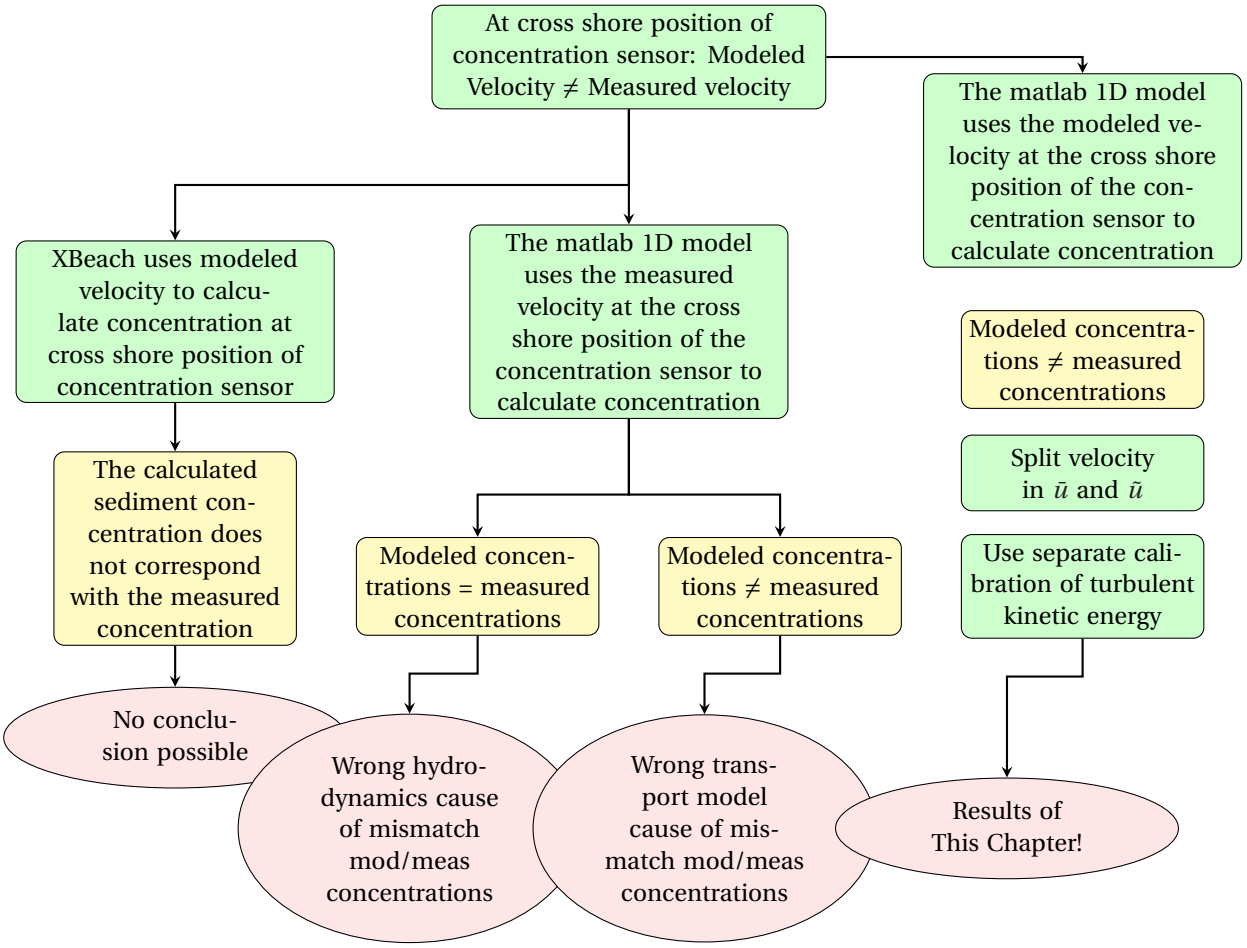

Figure 6.1: Schematic visualization of the modeling approach performed with XBeach and in the right two branches the approach with the Matlab model and their paths to the possible conclusions.

6.2. RESULTS MEASURED VERSUS MODELED HYDRODYNAMICAL FORCING

In this part, the modeled hydrodynamical forcing was replaced by measured water level and velocity at cross-shore position x=89.6m. In Section 3.3 the preparation of the measured and modeled datasets for this comparison was explained. Figure 6.2 shows the cumulative sediment transport measured during the Bardex II experiment A8. The difference between the calculated transports (either with the measured or with the modeled forcing) is large. The difference between using measured or modeled velocity and water depth for the calculation of the sediment concentrations is very small and therefore it can be concluded that the wrongly predicted sediment concentrations are not due to a wrongly predicted velocity and/or water depth but due to incorrect sediment transport formulations.

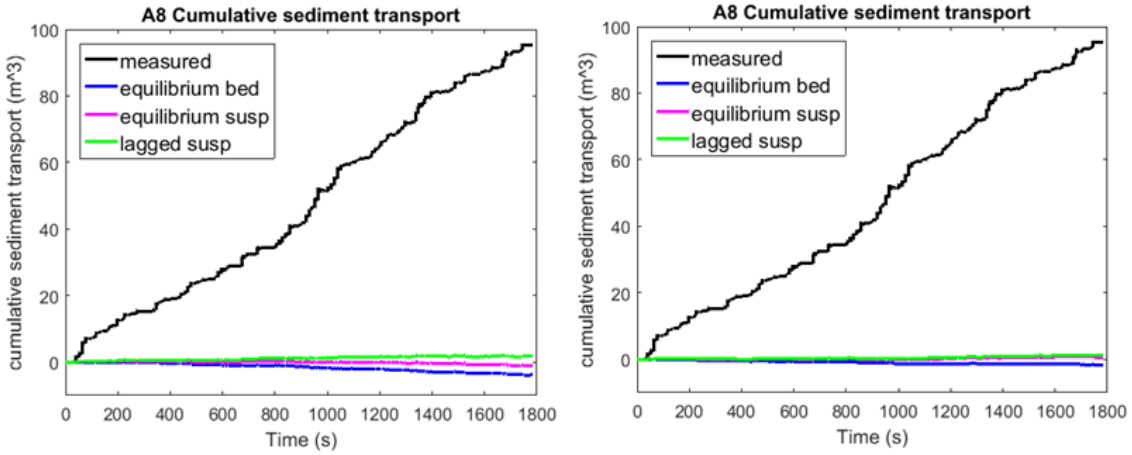

Figure 6.2: Cumulative suspended sediment transport at cross-shore position x=89.6m using XBeach modeled (left) or Bardex II measured (right) water level and velocity at x=89.6m

6.3. RESULTS OF THE DECOMPOSITION OF MEAN AND FLUCTUATING PART OF VELOCITY IN TRANSPORT FORMULATIONS

As explained in Section 3.3 the velocity in the non-hydrostatic version of XBeach is not the long wave (mean) velocity. The short wave velocity is included in this velocity and therefore the first step was to replace the $\tilde{u}$ term in Equation 2.3 with the non-hydrostatic total velocity. The sediment concentrations are then calculated with Equation 3.3 and the result of this calculation (in the form of the cumulative sediment transport during experiment A8) is shown in Figure 6.4. The second step was taken because it is the closest to how the transport equations were developed, with a mean velocity in the first term, and a fluctuating velocity part in the second velocity term as is given by Equation 3.5 and explained in Section 3.3. The result of the decomposition of the velocity is shown in Figure 6.3 for the XBeach modeled and Bardex II measured velocity signals. The mean and fluctuating part are applied in the transport formulation via Equation 3.5 resulting in a cumulative sediment transport as shown in Figure 6.4.

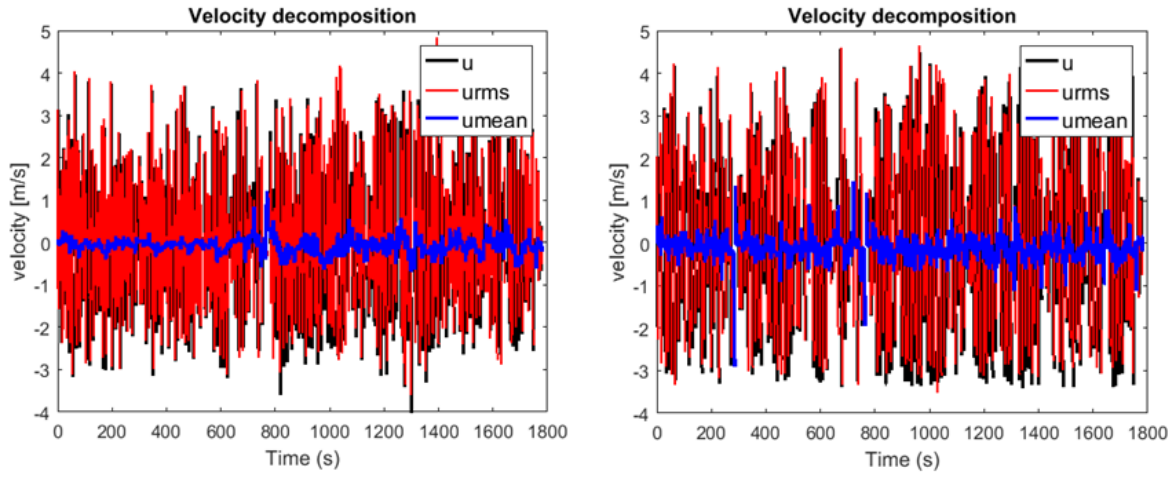

Figure 6.3: Velocity decomposition of the signal modeled by XBeach (left) and measured in Bardex II (right) in u, $\bar{u}$, and $\tilde{u}$.

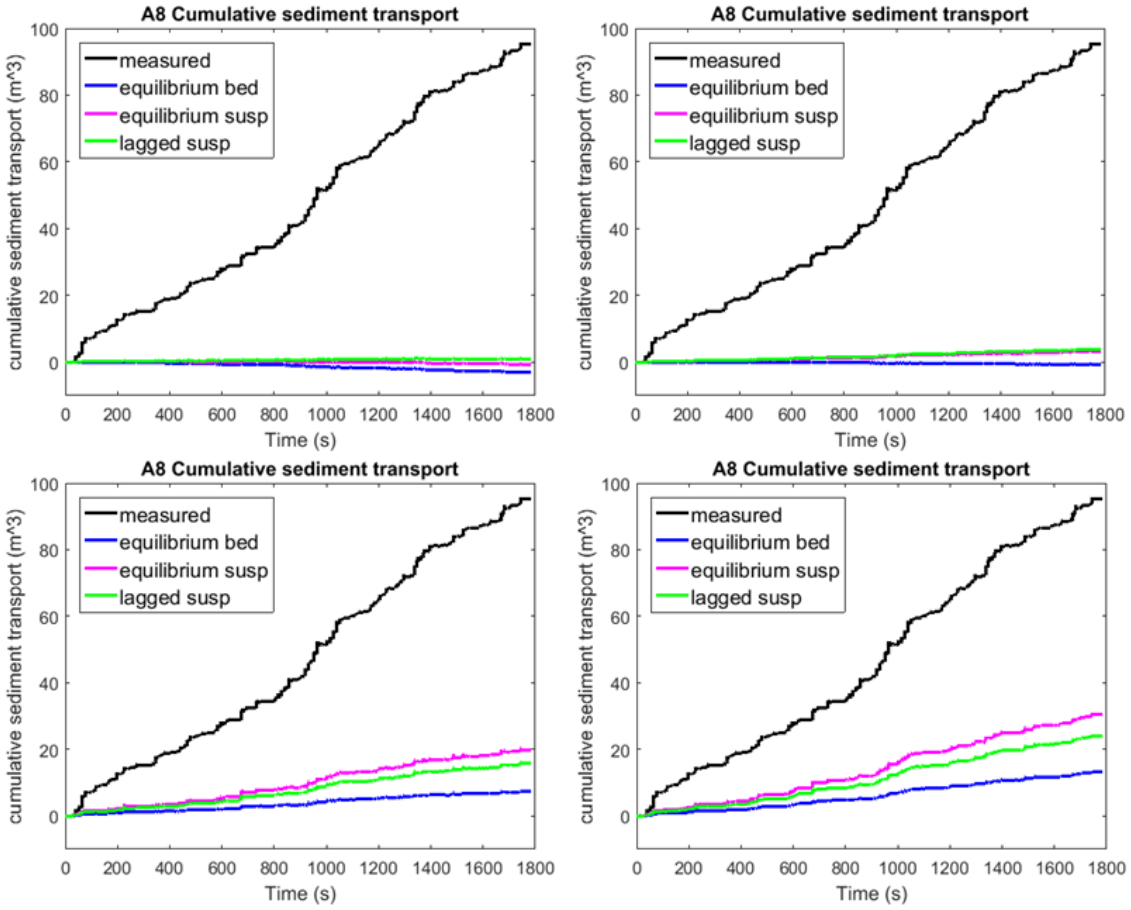

Figure 6.4: Cumulative suspended sediment transport at cross-shore position x=89.6m using total non-hydrostatic velocity as $\tilde{u}$ (left) or using decomposition of the non-hydrostatic velocity in $\bar{u}$ and $\tilde{u}$ (right) in the calculation of sediment concentrations at x=89.6m. Top panels show the results for the van Thiel-van Rijn sediment transport formulation, bottom panels for Soulsby-van Rijn.

For the sediment formulations of van Thiel-van Rijn the repositioning of the total non-hydrostatic velocity term to the $\tilde{u}$ term has very little influence on the total cumulative transport. The velocity decomposition has a small positive influence but the results are still very different from the Bardex II observed cumulative transport for experiment A8. Therefore the other sediment transport formulation of XBeach (Soulsby-van Rijn) is assessed as well. In the lower two panels of Figure 6.4 it is shown that for this formulation the decomposition of the velocity leads to a significant improvement of the sediment transport prediction at cross shore position x=89.6 using XBeach modeled hydrodynamic forcing.

6.4. RESULTS OF THE SEPARATE CALIBRATION OF TURBULENT KINETIC ENERGY

The previous results in this thesis have shown that wave breaking induced turbulence plays a big role in the enhancement of onshore sediment transport. Therefore the turbulent kinetic energy has been separated from the fluctuating part of the velocity and a calibration factor k_{gain} is attached to it, see Equation 3.6. The results of the sediment concentration calculations with k_{gain}=50 are shown in Figure 6.5.

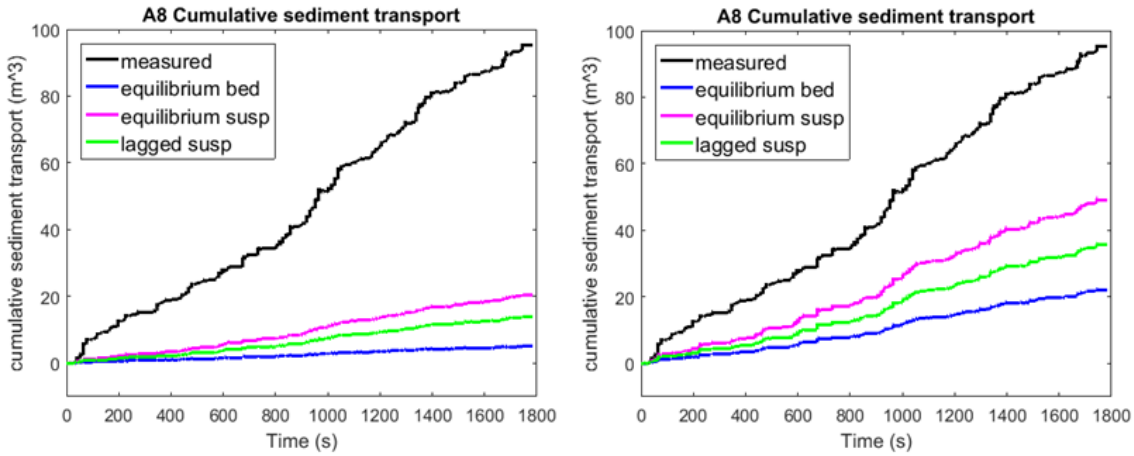

Figure 6.5: Cumulative suspended sediment transport at cross-shore position x=89.6m with separately enhanced turbulence using k_{gain}=55 for van Thiel-van Rijn (left) and Soulsby-van Rijn (right) sediment transport formulations. XBeach modeled water level and velocity were used to calculate the sediment concentrations at x=89.6m

Figure 6.5 shows clearly that enhancing the wave breaking induced turbulence improves the prediction of the sediment transport at cross-shore position x=89.6m for both transport formulations. However, to be able to predict the observed cumulative sediment transport, enhancement factors of k_{gain}=100 for Soulsby-van Rijn and k_{gain}=200 for van Thiel-van Rijn were needed.

6.5. CONCLUSIONS MATLAB MODEL

The Matlab model helped to understand where the cause of the mismatch between measured and modeled sediment concentrations originated. Three different hypothesis were tested. The first one, making use of the measured hydrodynamics at the cross-shore position x = 89.6 to calculate the sediment concentrations did not lead to different results. Therefore, if following the Flowchart in Figure 6.1 the calculation of the hydrodynamics in XBeach non-hydrostatic are not the cause of the underprediction of the onshore directed cumulative sediment transport. Two changes to the transport formulations have been tested for both Soulsby-van Rijn and van Thiel-van Rijn. The decomposition of the velocity did not improve the predictions made with van Thiel-van Rijn significantly. For Soulsby-van Rijn the velocity composition led to a significantly improved cumulative transport prediction. The last assessed part was the separate calibration of turbulent kinetic energy. For both sediment transport equations this led to a significant improvement of the cumulative transport predictions. Despite this improvement, the predicted values still do not correspond to the observed transport during Bardex II experiment A8.

7

DISCUSSION

This thesis has four main parts each answering one of the research questions. The first part was a literature study of swash morphodynamics to determine relevant processes for intermediate-reflective beaches. The second a qualitative modeling study on a planar beach to assess the sediment transport formulations in XBeach and the parameterization of four relevant processes. The third part compares the performance of XBeach to the Bardex II measurements. The last part assesses two adaptations to the sediment transport formulations with a 1D Matlab model. The results will be discussed in this chapter.

7.1. RESULTS PLANAR BEACH

The sediment response time as it is implemented now only is applied outside of the swash zone. Inside the swash zone the threshold value $T_{s,min}$ is applied almost everywhere. Whether the current parametrization works for the swash zone is assessed by choosing a very low threshold value $T_{s,min}$=0.01 to still guarantee numerical stability of the advection diffusion equation but including a depth- and fall velocity dependent T_s

The non-hydrostatic groundwater model as implemented in XBeach is able to reproduce the infiltration in the swash zone, leading to an observed smaller water depth and velocity and decreased offshore transport in the top of the swash during backwash. However, to make a significant change in the total morphological response, extremely high values for the hydraulic conductivity (in the scale of values used for gravel) have to be chosen. The secondary effects as described in the literature study are not implemented in XBeach although Turner & Masselink (1998) suggests that the secondary effects could have an effect on the accretion under certain conditions.

Most of the processes regarding morphodynamics in XBeach have been parametrized with the constraint that long waves could be resolved and only the short wave energy could be used for the velocity and water levels, since most of them have been developed for the XBeach surfbeat model. The new non-hydrostatic extension, by solving short waves and therefore have a more realistic representation of water level and velocity increased the amount of possibilities regarding parametrization of processes in the swash. However, most processes are still unchanged since the switch from surfbeat to non-hydrostatic and therefore in quite some parameterizations the original ideas behind them are violated by just swapping the old 'long wave velocity' by the non-hydrostatic 'total velocity' which includes orbital velocity as well.

The bed slope effects as implemented in XBeach works equally over the whole cross-shore domain (given equal slope) enhancing sediment transport in the offshore direction. The idea behind the bed slope effects is that they account for many processes all caused by the bed not being flat. An easier rolling down of grains due to gravity being the most important one. For dissipative beaches, the bed slope has always been applied to the bed load and suspended load transport. The idea behind this that also processes that effect the suspended sediment transport (like for example a compensation for the shortest distance to the bed not being vertically downward) were taken into account. For steeper beaches, the bed slope effects become stronger and since the dominance of suspended sediment transport is present in the model (not necessarily correct) the risk of overprediction of offshore transport due to the overprediction of bed slope effects is present.

Similar as for the transport equation, the turbulence is calculated assuming a long wave resolving and short wave addition though energy balance. In this routine, roller dissipation and short wave energy parameters are used. These terms are zero, leading to a wrong turbulence calculation in the non-hydrostatic extension. For this reason the k_{gain} turbulence enhancement factor has been added. In the current parametrization of bore turbulence, the depth average value is applied to induce stirring of sediment. The actual force stirring the sediment is caused by the highest velocities in the turbulent eddies generated by the bore. The velocity differences within these eddies are large and therefore it might be valid to enhance the depth average value of the kinetic energy by quite a large factor when used for stirring of sediment.

7.2. RESULTS COMPARISON WITH BARDEX II

This thesis has focused on the current prediction skill of the non-hydrostatic extension of XBeach and physical processes have been examined that could lead to better prediction of swash morphodynamics on intermediate reflective beaches. Turbulence and groundwater effects were concluded to improve the predictions, but only one type of beach has been studied. The effect of the steepness of the beach, the sediment properties and the wave conditions (storm conditions, recovering conditions) can be added to study the influence on the swash morphodynamic predictions. However, the wronly predicted sediment concentrations that resulted from the intra-swash analysis seem to be more fundamental than just the beach type or wave condition. The expectation is that similar analysis as done in this thesis, but for more general beaches under more general conditions would come to the same conclusions that the sediment concentrations in the uprush are underpredicted and in de backwash overpredicted leading to net overprediction of erosion, and creating difficulties modeling (accretion during) beach recovery.

7.3. RESULTS MATLAB MODEL

A Matlab 1D model was written to allow for flexibility in the input time series. Several assumptions have been made but the underlying thought of the model was to calculate the sediment transport similar as XBeach, and from that point start improving the transport formulations. Only one point in the cross-shore position was analyzed. This means that advection of sediment and turbulence can not be taken into account. Bed level change could not be calculated with the Matlabl mode because spatial gradients would be needed to do that. Therefore the cumulative sediment transport was taken as a proxy to compare the prediction with observations. Bakhtyar et al. (2009) suggested that for plunging breakers advection is dominant in the propagation of turbulent kinetic energy and this energy is onshore ward, whereas in spilling breakers the distribution is mostly caused by diffusion and offshore ward. Therefore for intermediate reflective beaches if accretion is wanted advection should be taken into account.

The mean velocity was obtained by taking an average value both forward and backwards in time. In XBeach (and other models) in predictions no information about the future is available. This will introduce a time lag in the mean velocity if only the past is taken into account.

In order to improve these parameterizations in XBeach non hydrostatic, the most influential parametrization are the sediment transport Equations 2.2 and 2.1. These equations for bed load and suspended sediment transport originate from a current only, and adapted for waves and currents situation (Van Thiel De Vries 2009). They are wave average equations, working well for the surf-beat model which resolved long waves but used short wave energy balance to create the short wave (orbital) part of the velocity. Orbital velocity and turbulent fluctuations have been calibrated as one 'fluctuation' to the long wave velocity. The way transport is calculated from fluid dynamics and grain properties has been studied elaborately over the last decade, however there is no well-established transport formula that takes into account all the different factors that control sediment transport. A complete formula should quantify bed load and suspended load, describe random waves as well as the effects of wave breaking, and include transport in the swash zone. In a study by Bayram, different transport formulas have been tested on a dataset of DUCK beach, and the van Rijn transport formula has been proven to perform te best calculating the total rate and distribution of longshore sand transport (Bayram et al. 2001). In the current non hydrostatic model, short waves are resolved and therefore there is need for an appropriate transport parametrization. In the current source code, without adapting the formulation, the $\tilde{u}$ term was zero due to the absence of the short wave energy balance. The long wave part

of the velocity is now substituted for all short and long wave velocity since XBeach non-hydrostatic does not differ between it. This debalances the original transport equation and needs to be looked into mainly to find out whether the calibration on the short wave energy and turbulent kinetic energy is still valid. In deeper water, where bore turbulence is not present at the bed, sediment transport in the current 'use a wave averaged equation intra wave'- method works. In shallower water as shown in this study this approach does not work very well. If no good way can be found for adapting the Soulsby-van Rijn equation to short wave resolving models, different transport parameterizations (e.g. Nielsen & Callaghan (2003)) should be considered.

8

CONCLUSIONS AND OUTLOOK

8.1. CONLUSIONS

RQ[1]: What are relevant physical processes for the morphodynamics in the swash zone on intermediate-reflective beaches?

In a literature study swash processes have been studied. Four relevant processes have been determined to be relevant in the prediction of swash morphodynamics.

- Groundwater effects: Due to infiltration during the uprush, the volume of water that is available for the backwash is reduced. This leads to lower velocities during the backwash leading to less offshore transport hence less erosion. Secondary groundwater effects include the thinning of the boundary layer due to infiltration and the loosening of grains on the bed due to exfiltration.
- Bed slope effects: The bed slope effects enhance offshore transport and several processes, for example that grains roll downwards easier than upwards, are included.
- Bore generated turbulence: The turbulent swash bore is higher during uprush than during the backwash. Therefore sediment concentrations due to upstirring of sediment by the turbulent eddies that reach the bottom will be higher in uprush than in backwash. This will lead to onshore enhancement of the sediment transport.
- Sediment response time: The time lag of sediment settling is determined by the sediment response time. It is dependent on the fall velocity. The fall velocity and therefore the sediment response time varies over the swash domain. All sediment is observed to be settled during flow reversal, therefore when more sediment is stirred up in the uprush than in the backwash onshore transport is enhanced.

RQ[2]: How are these processes represented by XBeach non-hydrostatic?

- Groundwater effects: Only the primary effect of groundwater is implemented in XBeach where less backwash volume due to infiltrations leads to lower velocity. The results of the Planar beach showed very little effect on the morphology for the hydraulic conductivity as measured for D_{50} = 0.42 mm (K=0.0008 m/s) but for very high conductivity (K=0.01) accretion in the upper swash was achieved.
- Bed slope effects: The bed slope effect is by default in XBeach applied on the total transport. Changing the bed slope effect to only apply for the bed load transport reduces erosion significantly. The 'bedslopeffdir' option was assesed separately because it turned out an error in the source code caused an accretion enhancing effect on the modeled results. This is further discussed in Appendix A.
- Sediment response time: In XBeach, the threshold value $T_{s,min}$ of the sediment response time was met throughout the whole swash domain because the threshold is connected to a minimum water depth. The results of changing this threshold value were assessed on the Planar beach. The conclusion is that the influence of a minimum sediment response time threshold does not influence the morphology significantly.

- Bore generated turbulence: The turbulence was parameterized for the surf-beat version of XBeach. Bore generated turbulence was not implemented correctly in the code of the non-hydrostatic version. After some changes in the source code (see Section 3.1) the effect of bore generated turbulence was assesed. A parameter enhancing directly the turbulent kinetic energy at the bottom k_{gain} was introduced and the results of the planar beach show that for strongly enhanced turbulence, accretion in the swash can be achieved.

The methodology as used in this thesis starting with a qualitative modeling study on a planar beach has been useful to get more insight in the parametrization and effect of several physical processes on the morphodynamic response on a planar beach without the influence of complex geometries (i.e. offshore bars). The conclusions about the influence of the processes helped in the analysis of the Bardex II model case and the comparison with the observed morphological change.

RQ[3]: How do the numerical results perform compared to the experimental results from Bardex II(erosive and accretive) and do we need new processes/improvements of current physics?

Two modeling time scales have been analyzed: Total experiment (200 minutes) A4 and A8 and the intra-swash timescale of one swash period (O(10s)). The total morphodynamic response for both (measured) accretive and erosive conditions representing experiment A4 and A8 does not correspond to this behavior. Although in the upper swash less erosion is modeled for accretive conditions then in the upper swash for erosive conditions, no significant difference in the profile is developed by XBeach non hydrostatic in the 'best we do now' approach. This suggest that the inclusion of groundwater and long wave turbulence as it is now in XBeach is not enough for the profile to recover enough under erosive conditions but also erodes too much during accretive conditions.

RQ[4]: How can predictions be improved for swash morphodynamics of intermediate-reflective beaches?
Two methods of improvement have been tested with a 1D Matlab model. Decomposition of the velocity and manually enhanced turbulence were assessed. From the results of the Matlab model it can be concluded that the calculation of the hydrodynamics in XBeach non-hydrostatic are not the cause of the underprediction of the onshore directed cumulative sediment transport. Two changes to the transport formulations have been tested for both Soulsby-van Rijn and van Thiel-van Rijn transport formulations. The decomposition of the velocity did not improve the predictions made with van Thiel-van Rijn significantly. For Soulsby-van Rijn the velocity composition led to a significantly improved cumulative transport prediction. The last assessed part was the separate calibration of turbulent kinetic energy. For both sediment transport equations this led to a significant improvement of the cumulative transport predictions. Despite this improvement, the predicted values still do not correspond to the observed transport during Bardex II experiment A8.

8.2. OUTLOOK

The most important conclusion is that even with inclusion of processes that are based on literature likely to enhance onshore transport, the expected accretion under mild conditions as used on the planar beach is hard to achieve without introducing extreme values for enhancing factors. The sediment concentrations, gradients and transport and therefore the bed level change is in the model the highest exactly at the cross shore position under the bore, and to a lesser extent in the end of the backwash when negative velocities are high. Apart from whether that is observed in nature as well, all other parts of the swash region in the model will undergo hardly any morphological change. This is emphasizing the expectation that a better representation of turbulence will improve the morphodynamic predictions in the swash zone on intermediate-reflective beaches.

A similar approach as for the turbulence in the surfbeat model (based on Reniers et al. (2013)) can be used in the non-hydrostatic extension (already partly implemented) based on the steepness of the wave, the roller thickness and the exponential decay of turbulence to the bed. Blenkinsopp et al. (2016) found that the vertical run-up excursion of each swash was also correlated strongly with the height of the bore at collapse and could be predicted based on the assumption of a conversion of potential to kinetic energy at bore collapse.

The bed slope effects enhance offshore transport in the whole swash domain. For steep beaches the influence of the inclusion of suspended transport to the bed slope effects becomes high. Therefore to improve

the predictions the bed slope effect should only be applied to the bed load transport, possibly helping the under-predicted contribution of bed load transport in the backwash compared to measurements.

The matlab model showed promising results for the decomposition of the non-hydrostatic velocity in a mean and a fluctuating part. However, only one cross-shore position was assessed just above the mean sea level. The comparison of modeled sediment transport with Bardex II observations at different positions throughout the upper and lower swash zone is needed to give a full validation of the proposed adaptations to the transport formulations.

A

Bed Slope Direction Effect

Bed Slope direction effects Daly et al. (2017) showed that the bed slope direction module can positively influence the reproduction of accretion on intermediate reflective beaches in the recovery period after a storm A.1. They found that the RMSE (root mean squared error) reduced with a factor 4 through applying this module. First the way this bed slope direction effect is calculated in XBeach is explained, after that the results from Daly are reproduced and compared to the reference case and conclusions about this effect discussed.

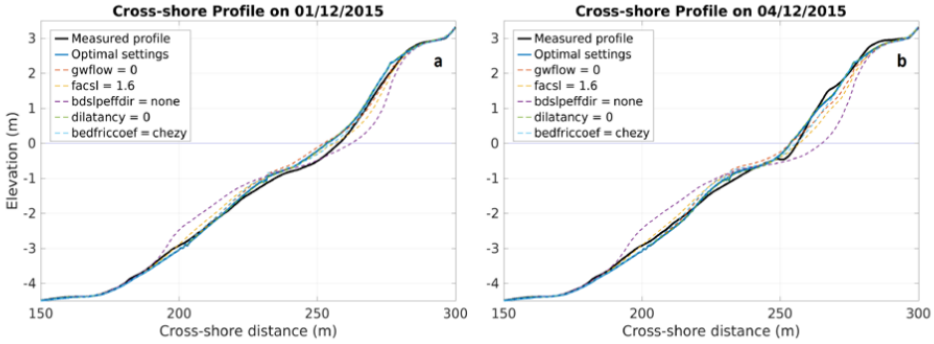

Figure A.1: Measured and predicted bed levels halfway and at the end of the recovery period, dashed lines show the effect of different model settings. Clearly the bedslpeffdir=none (purple dashed) has a negative effect on the accretion during recovery. Figure from Daly et al. (2017)

The bdlspeffdir = talmon module has been developed to correct the bed load transport for 2D effects in the bed slope (as seen e.g. in cusp systems or during breaching events). First, the angle of the velocity vector with the cross shore direction is determined. If the the x-component of the velocity is onshore, this angle is

$$\alpha_\Psi = tan^{-1}\left(\frac{u}{u}\right) \tag{A.1}$$

and if the x-component of the velocity is offshore the angle is

$$\alpha_\Psi = tan^{-1}\left(\frac{u}{u}\right) + \pi \tag{A.2}$$

The total transport direction is adjusted by the theory of Talmon Roelvink et al. (2015)

$$\alpha_{\Psi\,new} = \tan^{-1}\left(\frac{\sin(\alpha_\Psi) - f(\theta)\frac{dz_b}{dy}}{\cos(\alpha_\Psi) - f(\theta)\frac{dz_b}{dy}}\right) \tag{A.3}$$

with the Shields parameter θ

$$\theta = \frac{\sqrt{{\tau_x}^2 + {\tau_y}^2}}{\Delta\rho_w} \tag{A.4}$$

and

$$f(\theta) = \frac{1}{9\,(D_{50}/h)^{0.3}\,\theta^{0.5}} \tag{A.5}$$

The magnitude of the total bed transport vector

$$|S_b| = \sqrt{S_{b_x}^2 + S_{b_x}^2} \tag{A.6}$$

is then 'redistributed' as following over the cross shore and alongshore component of the bed load transport, to take into account the effect of the bed slope:

$$S_{bx} = |S_b|\cos(\alpha_\Psi)\, S_{bx} = |S_b|\cos(\alpha_\Psi) \tag{A.7}$$

The results of this bed slope effect is compared to the reference case in Figure A.3. For 1000 cycles the result is shown in Figure A.2. Corresponding to the results of Daly et al. (2017), this bed slope effect enhances onshore transport and therefore has a positive effect on accretion.

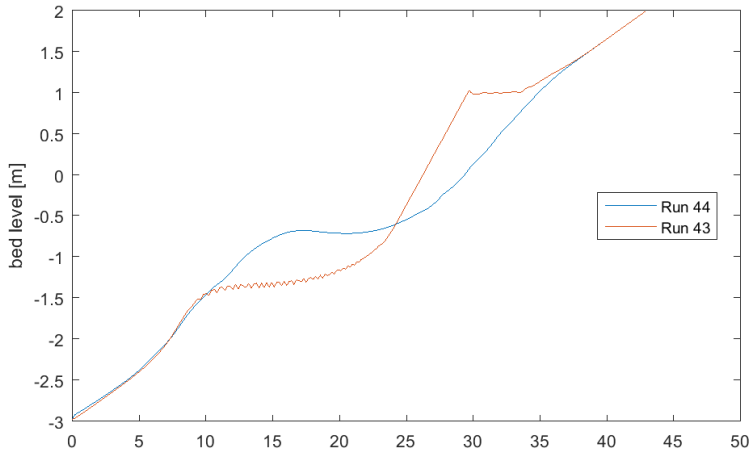

Figure A.2: Comparison bdslpeffdir=talmon with reference case (bdspeffdir=0) for 1000 waves jonswap.

However, this 2D module is designed to account for 2D effect in the bed slope (as seen in cusp systems) and should not influence the transport for 1D calculations as Daly is using. The transport for one cycle is shown in Figure A.3 where, if compared to the reference case clearly the bed level change is different from the expected change. Therefore the results have been analyzed with the x,t diagrams as also used in Section 4.5. The problem with the talmon module is clearly visible in the suspended and bed load transport x,t diagrams in Figure A.4. The bed load transport is always directed up-slope.

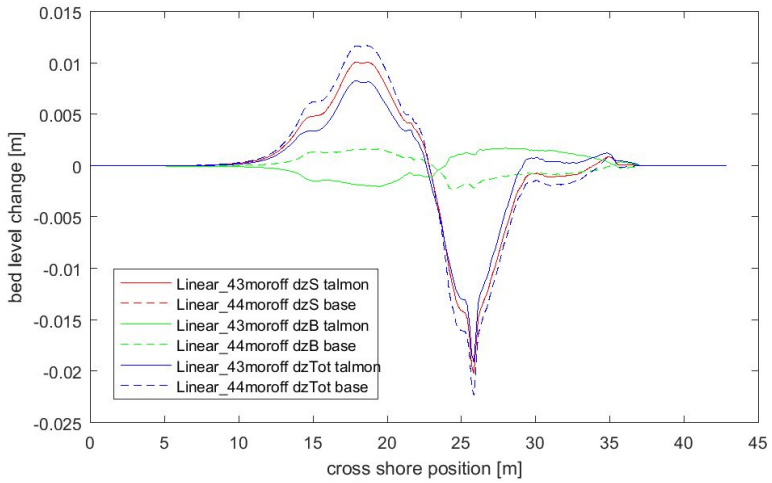

Figure A.3: Bed level change due to suspended and bed load transport with bdslpeffdir=talmon after one swash cycle.

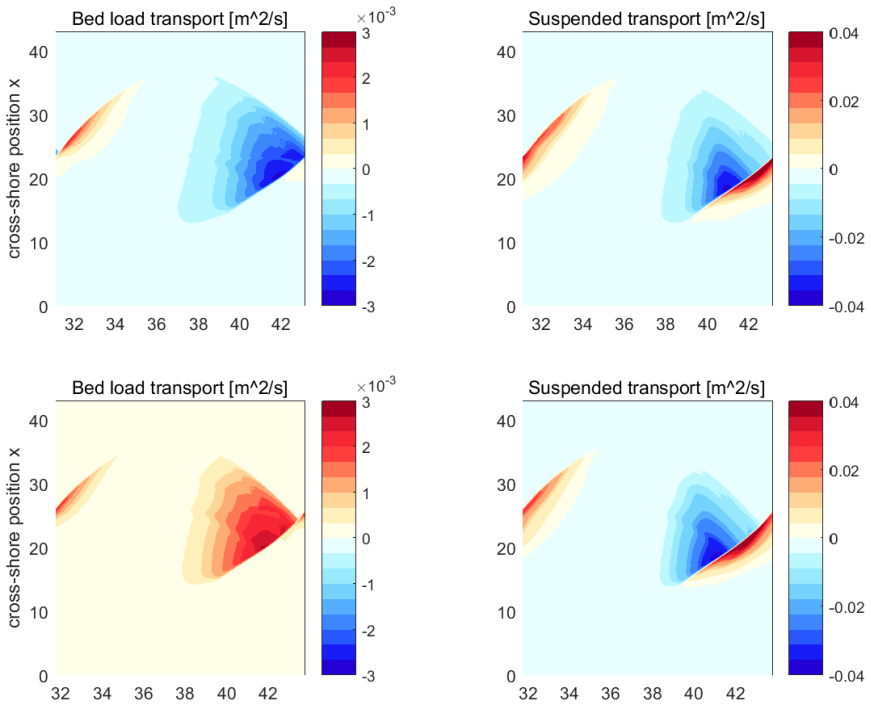

Figure A.4: Bed load (left two panels) and Suspended sediment transport (right two panels) for the reference case (upper panels) and the bedslpeffdir=talmon (lower panels).

Analysing this result and the effect of the bed slope direction over one swash cycle shows that for negative velocity (so during the backwash) the sign of the bed load transport is opposite to the flow velocity. This is due to Equation A.6. For 1D calculations this produces the wrong results, and has been fixed for a 1D case. Work needs to be done in the XBeach source code to fix this bug also for 2D cases. A quick test after the fix gave exactly the same results now for the talmon module in 1D compared to the reference case, and as expected the direction of the bed slope in 1D (which can be only in the grid-direction) does not influence the sediment transport.

BIBLIOGRAPHY

Alsina, J. M., Falchetti, S. & Baldock, T. E. (2009), 'Measurements and modelling of the advection of suspended sediment in the swash zone by solitary waves', *Coastal Engineering* **56**(5-6), 621–631.

Bakhtyar, R., Barry, D. A., Yeganeh-Bakhtiary, A. & Ghaheri, A. (2009), 'Numerical simulation of surf-swash zone motions and turbulent flow', *Advances in Water Resources* **32**(2), 250–263.
URL: *http://dx.doi.org/10.1016/j.advwatres.2008.11.004*

Baldock, T. E. & Hughes, M. G. (2006), 'Field observations of instantaneous water slopes and horizontal pressure gradients in the swash-zone', *Continental Shelf Research* **26**(5), 574–588.

Bayram, A., Larson, M., Miller, H. C. & Kraus, N. C. (2001), 'Cross-shore distribution of longshore sediment transport: Comparison between predictive formulas and field measurements', *Coastal Engineering* **44**(2), 79–99.

Blenkinsopp, C. E., Matias, A., Howe, D., Castelle, B., Marieu, V. & Turner, I. L. (2016), 'Wave runup and overwash on a prototype-scale sand barrier', *Coastal Engineering* **113**(May 2016), 88–103.
URL: *http://dx.doi.org/10.1016/j.coastaleng.2015.08.006*

Blenkinsopp, C. E., Turner, I. L., Masselink, G. & Russell, P. E. (2011), 'Swash zone sediment fluxes: Field observations', *Coastal Engineering* **58**(1), 28–44.
URL: *http://dx.doi.org/10.1016/j.coastaleng.2010.08.002*

Bosboom, J. & Stive, M. J. (2013), *Coastal Dynamics I*, number Delft University of Technology. VSSD.

Briganti, R., Torres-Freyermuth, A., Baldock, T. E., Brocchini, M., Dodd, N., Hsu, T. J., Jiang, Z., Kim, Y., Pintado-Patiño, J. C. & Postacchini, M. (2016), 'Advances in numerical modelling of swash zone dynamics', *Coastal Engineering* **115**, 26–41.

Brocchini, M. & Baldock, T. E. (2008), 'Recent advances in modeling swash zone dynamics: Influence of surf-swash interaction on nearshore hydrodynamics and morphodynamics', *Reviews of Geophysics* **46**(3).

Butt, T. (1999), 'Sediment Transport in the Swash-Zone of Natural Beaches', (September), 280.
URL: *http://hdl.handle.net/10026.1/1784*

Butt, T., Russell, P., Puleo, J., Miles, J. & Masselink, G. (2004), 'The influence of bore turbulence on sediment transport in the swash and inner surf zones', *Continental Shelf Research* **24**(7-8), 757–771.

Chardón-Maldonado, P., Pintado-Patiño, J. C. & Puleo, J. A. (2015), 'Advances in swash-zone research: Small-scale hydrodynamic and sediment transport processes', *Coastal Engineering* .

Daly, C., Floc'h, F., Almeida, L. P. & Almar, R. (2017), 'Modelling accretion at nha trang beach,Vietnam', *Conference Paper* (170).

Deltares (2017), CoMIDAS 2016 : progress report, Technical report.

Dohmen-Janssen, C. M., Kroekenstoel, D. F., Hassan, W. N. & Ribberink, J. S. (2002), 'Phase lags in oscillatory sheet flow : experiments and bed load modelling', *Coastal Engineering* **46**, 61–87.

Galappatti, G. & Vreughenhil, C. B. (1985), 'A depth integrated model for suspended sediment transport', *J. Hydraul. Res.* **23**(4), 359–377.

Guza, R., Thornton, E. B. & ASCE, M. (1985), 'Velocity Moments in Nearshore', *Journal of Waterway, Port, Coastal, and Ocean Engineering* **111**(2), 235–256.

Hughes, M. G., Aagaard, T., Baldock, T. E. & Power, H. E. (2014), 'Spectral signatures for swash on reflective, intermediate and dissipative beaches', *Marine Geology* **355**, 88–97.
URL: *http://dx.doi.org/10.1016/j.margeo.2014.05.015*

Komar, P. & Miller, M. (1975), 'On the comparison between the threshold of sediment motion under waves and unidirectional currents with a discussion of the practical evaluation of the threshold.', *Journal of Sedimentary Research* **45**(1).

Masselink, G., Conley, D. & Ruju, A. (n.d.), Data Storage Report, Technical report, Bardex II.

Masselink, G. & Puleo, J. A. (2006), 'Swash-zone morphodynamics', *Continental Shelf Research* **26**(5), 661–680.

Masselink, G., Ruju, A., Conley, D., Turner, I., Ruessink, G., Matias, A., Thompson, C., Castelle, B., Puleo, J., Citerone, V. & Wolters, G. (2016), 'Large-scale Barrier Dynamics Experiment II (BARDEX II): Experimental design, instrumentation, test program, and data set', *Coastal Engineering* **113**, 3–18.
URL: *http://dx.doi.org/10.1016/j.coastaleng.2015.07.009*

Masselink, G., Turner, I. L., Conley, D., Ruessink, G., Matias, A., Thompson, C., Castelle, B. & Wolters, G. (2013), 'BARDEX II : Bringing the beach to the laboratory – again !', *Journal of Coastal Research* (65), 1545–1550.

Nielsen, P. & Callaghan, D. P. (2003), 'No Title', *Coastal Engineering* **47**(3), 347–354.

Puleo, J. A., Lanckriet, T., Conley, D. & Foster, D. (2016), 'Sediment transport partitioning in the swash zone of a large-scale laboratory beach', *Coastal Engineering* **113**, 73–87.
URL: *http://dx.doi.org/10.1016/j.coastaleng.2015.11.001*

Reniers, A. J. H. M., Gallagher, E. L., MacMahan, J. H., Brown, J. A., Van Rooijen, A. A., Van Thiel De Vries, J. S. M. & Van Prooijen, B. C. (2013), 'Observations and modeling of steep-beach grain-size variability', *Journal of Geophysical Research: Oceans* **118**(2), 577–591.

Roelvink, D., Reniers, A., van Dongeren, A., van Thiel de Vries, J., McCall, R. & Lescinski, J. (2009), 'Modelling storm impacts on beaches, dunes and barrier islands', *Coastal Engineering* **56**(11-12), 1133–1152.

Roelvink, D., van Dongeren, A., McCall, R., Hoonhout, B., van Rooijen, A., van Geer, P., de Vet, L., Nederhoff, K. & Quataert, E. (2015), XBeach Technical Reference : Kingsday Release, Technical report.

Ruessink, B. G., Blenkinsopp, C., Brinkkemper, J. A., Castelle, B., Dubarbier, B., Grasso, F., Puleo, J. A. & Lanckriet, T. (2016), 'Sandbar and beach-face evolution on a prototype coarse sandy barrier', *Coastal Engineering* **113**, 19–32.
URL: *http://dx.doi.org/10.1016/j.coastaleng.2015.11.005*

Ruju, A., Conley, D., Masselink, G. & Puleo, J. (2016), 'Boundary layer dynamics in the swash zone under large-scale laboratory conditions', *Coastal Engineering* **113**, 47–61.
URL: *http://dx.doi.org/10.1016/j.coastaleng.2015.08.001*

Shen, M. C. & Meyer, R. E. (1963), 'Climb of a bore on a beach Part 3. Run-up', *Journal of Fluid Mechanics* **16**(01), 113–125.
URL: *http://www.journals.cambridge.org/abstract_S0022112063000628*

Smit, P. B., Roelvink, J. A., van Thiel de Vries, J. S. M., McCall, R., van Dongeren, A. & Zwinkels, J. R. (2014), 'XBeach: Non-hydrostatic model', p. 69.

Soulsby, R. L. (1997), 'Dynamics of marine sands: a manual for practical applications', *Dynamics of marine sands: a manual for practical applications* pp. —-.

Turner, I. L., Rau, G. C., Austin, M. J. & Andersen, M. S. (2016), 'Groundwater fluxes and flow paths within coastal barriers: Observations from a large-scale laboratory experiment (BARDEX II)', *Coastal Engineering* **113**, 104–116.
URL: *http://dx.doi.org/10.1016/j.coastaleng.2015.08.004*

Turner, I. & Masselink, G. (1998), 'Swash infiltration-exfiltration and sediment transport cal flow rates of net', *Journal of Geophysical Research* **103**(C13), 30813–30824.

van der Zanden, J. (2016), *Sand transport processes in the surf and swash zones*.
URL: *http://doc.utwente.nl/102073/*

van Rijn, L. C., Walstra, D.-J. R. & van Ormondt, M. (2007), 'Unified View of Sediment Transport by Currents and Waves. I: Initiation of Motion, Bed Roughness, and Bed-Load Transport', *Journal of Hydraulic Engineering* **133**(7), 776–793.

Van Thiel De Vries, J. S. M. (2009), *Une erosion during storm surges*.

Walstra, D. J. R., Van Rijn, L. C., Van Ormondt, M., Briere, C. & Talmon, a. M. (2007), 'The effects of bed slope and wave skewness on sediment transport and morphology', *6th International Symposium on Coastal Engineering and Science of Coastal Sediment Processes* pp. —-.

Wright, L. D. & Short, A. D. (1984), 'Morphodynamic variability of surf zones and beaches: A synthesis', *Marine Geology* **56**(1-4), 93–118.

Yates, M. L., Guza, R. T. & O'Reilly, W. C. (2009), 'Equilibrium shoreline response: Observations and modeling', *Journal of Geophysical Research: Oceans* **114**(9), 1–16.